New Radiopharmaceuticals and Expansion of Nuclear Medicine in Brazil

Claudio Tinoco Mesquita, MD, PhD

Professor Associado Departamento de Radiologia – Universidade Federal Fluminense

Pesquisador CNPq e Cientista do Estado do Rio de Janeiro

claudiotinocomesquita@id.uff.br

Agenda

- Perspectivas em traçadores de PET CT cardíaco
- Perspectivas em traçadores de SPECT CT cardíaco
- Perspectivas com novos equipamentos
- Panorama da medicina nuclear brasileira – foco cardiologia

Fornecimento de Geradores de $^{99}Mo/^{99m}Tc$
Distribuição Regional

Sociedade Brasileira de Medicina Nuclear

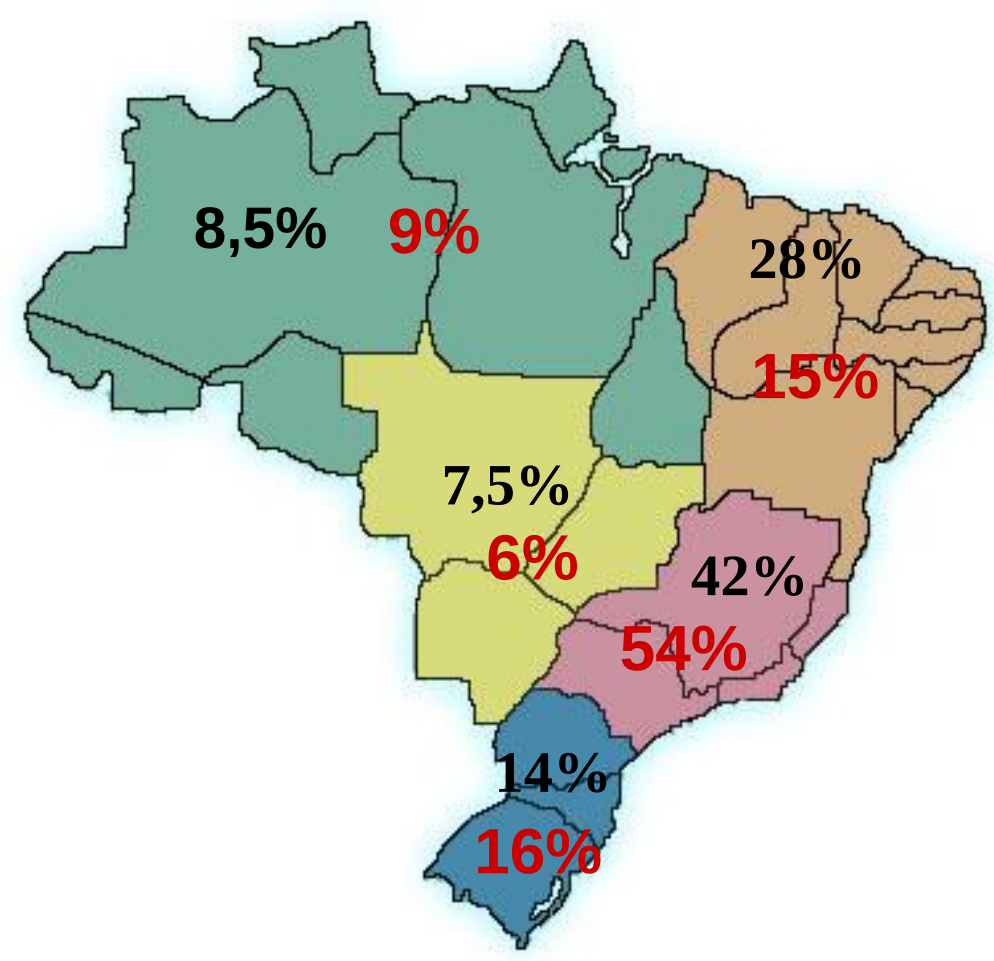

- População da região (%)
- Fornecimento regional (%)
- Total fornecido em 2014: 20.653.500 mCi
- Mais de 430 clínicas
- Uso per capita 2,5 vezes menor que na Argentina e 6 vezes menor que nos EUA.

Sociedade Brasileira de Medicina Nuclear

Produção e Distribuição - Radiofármacos

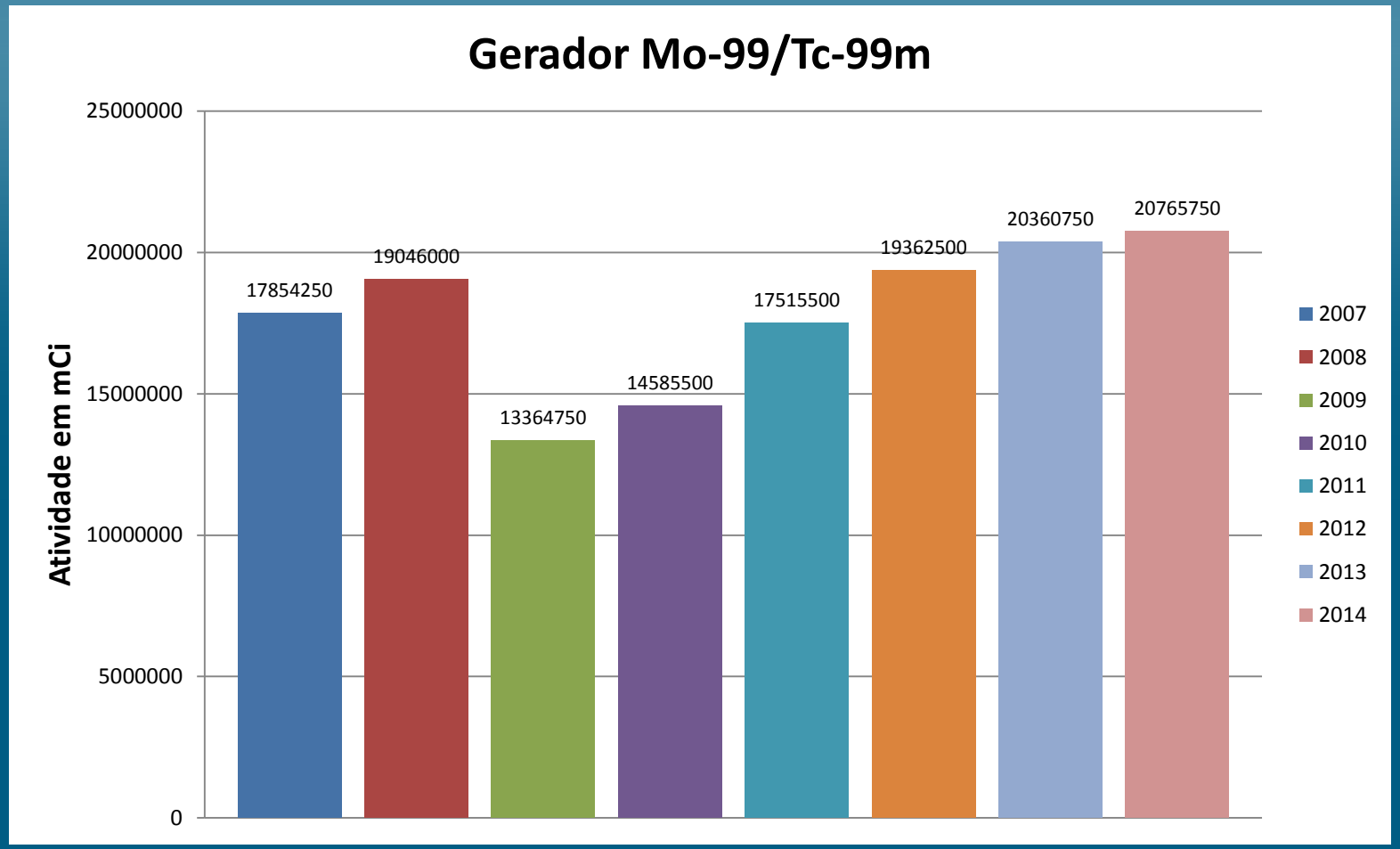

Brasil precisa dobrar oferta de serviços de medicina nuclear para atender população

Publicado em 02/08/2016 Atualizado em 02/08/2016

Através de medicamentos e técnicas diagnósticas que usam radiação, a medicina nuclear consegue prevenir e tratar tipos de câncer e doenças cardiovasculares responsáveis por quase metade de todas as mortes registradas na América Latina e Caribe. Agência Internacional de Energia Atômica (AIEA) tem dado apoio ao Brasil e a países da região para ampliar atendimento à população.

Tomografia pode identificar câncer e doenças do coração. Foto: Ministério da Saúde do Brasil

+ NOTÍCIAS DO BRASIL

Governo e ONU lançam concurso de melhores receitas da merenda no Brasil
17/12/2018

Rede hoteleira se une a aliança da ONU pela saúde sexual e reprodutiva no Brasil
17/12/2018

ONU promove oficina em São Paulo para refugiados e migrantes LGBTI
14/12/2018

ONU apresenta em Milão projeto de produção sustentável do algodão
14/12/2018

Laboratório de universidade do Rio de Janeiro usa hidrogênio como fonte limpa de energia
14/12/2018

✱ RECENTES

Países chegam a consenso na implementação do Acordo de Paris para o clima

O que tem na sua calça jeans?

Dados

- 150 milhões de usuários dependem SUS
- 51 milhões de usuários do Sistema Suplementar de Saúde
- Total de cintilografias miocárdicas em 2013 no SUS: 228.713
- Total de cintilografias miocárdicas estresse em 2013 na Saúde Suplementar: 858.757
- Taxa de crescimento anual de cintilografias miocárdicas no SUS = 4%

Fontes: Datasus e Relatório da Saúde Suplementar

Assimetria do Uso de Medicina Nuclear

- Taxa de uso de cintilografia miocárdica Brasil usuários Saúde Suplementar = 1683 exames/100.000 habitantes/ano
- Taxa de uso de cintilografia miocárdica Brasil usuários SUS = 152 exames/100.000 habitantes/ano

Taxa de Utilização de Cintilografias

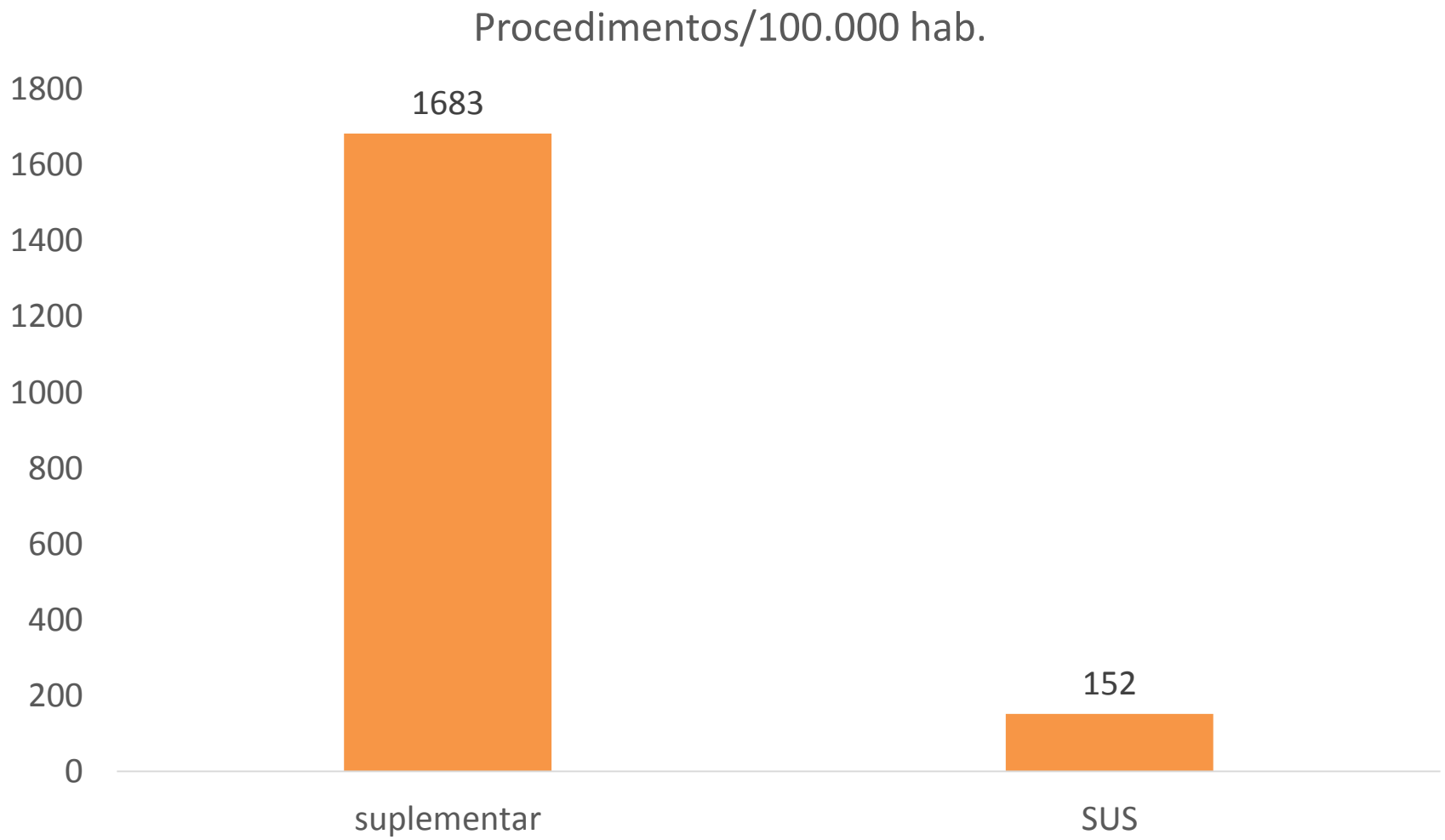

Se nada for feito o SUS só alcançará a taxa de atendimento de cintilografias miocárdicas da Saúde Suplementar em 54 anos, ou seja em **2069**

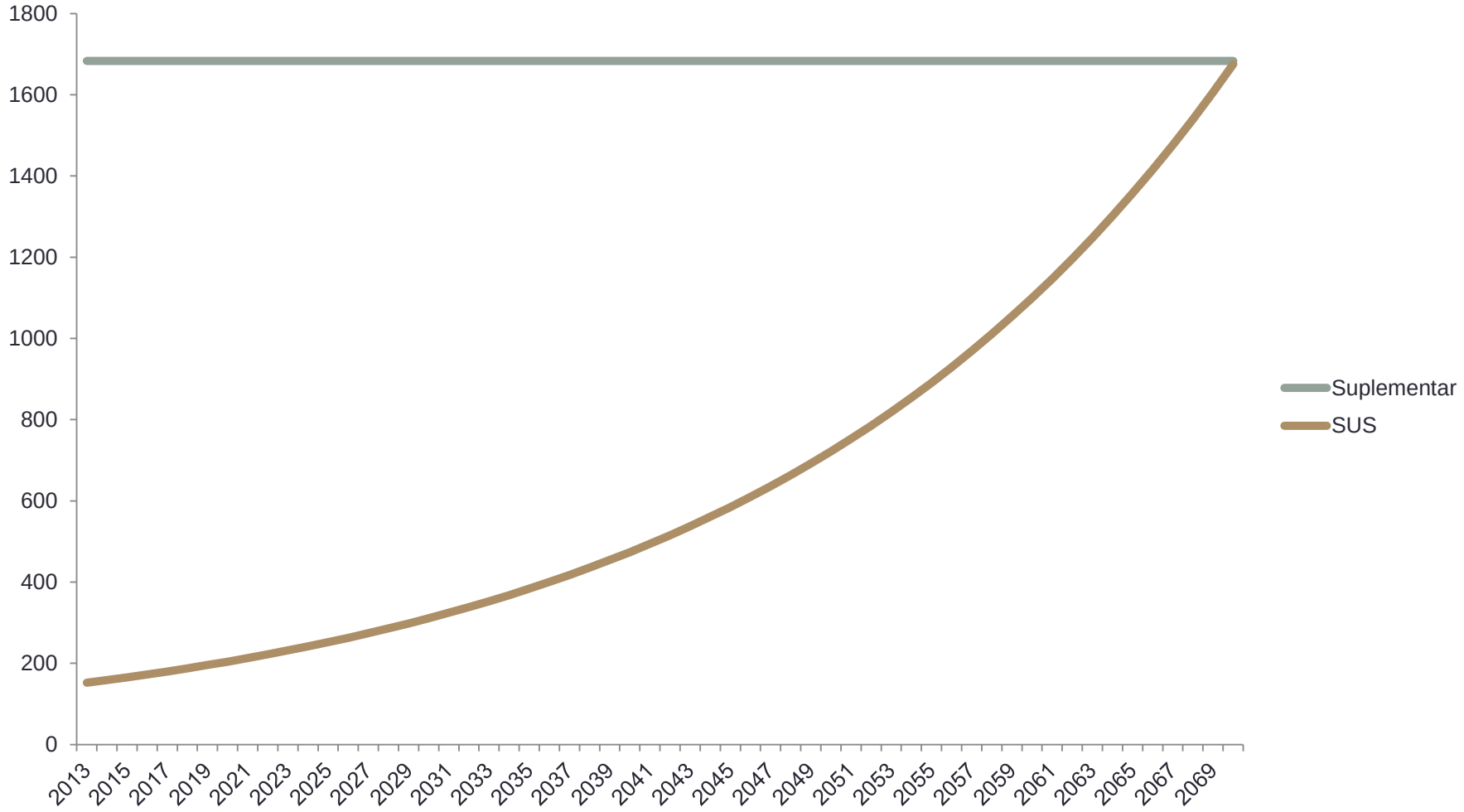

Caso Clínico

- RM, masc, 64 anos, natural Brescia, Itália.

- QP: Assintomático em avaliação de teste ergométrico alterado.

- HDA: Paciente com história de SCA e PTCA com stent em ACDA em 2007. Faz atividades físicas moderadas sem queixas.
- HPP: HAS, Dislipidemia grave, Tx renal em 2002. Passado de FA em uso de propafenona. Em 2015: SPECT miocárdico com dipiridamol normal.
- Medicamentos: sotalol, losartan, aspirina, ezetimiba, atorvastatina, propafenona.
- Exames recentes: creatinina 1,76 mg/dl, LDL 75 mg/dL.

Caso Clínico

- Foi submetido a teste de esforço em cicloergômetro em uso de tratamento cardiológico (sotalol, aas, losartana) (Protocolo utilizado: 30 watts a cada dois minutos) e este foi interrompido em FC submáxima(FC máx 104, 65% da FC orêmica), sem sintomas. O ECG apresentou alterações durante o estresse: depressão do segmento ST de 1mm de caráter horizontal de V4-V6.

- Em 3 de março de 2018 foi encaminhado para realizar SPECT miocárdico de estresse.

ECG BASAL

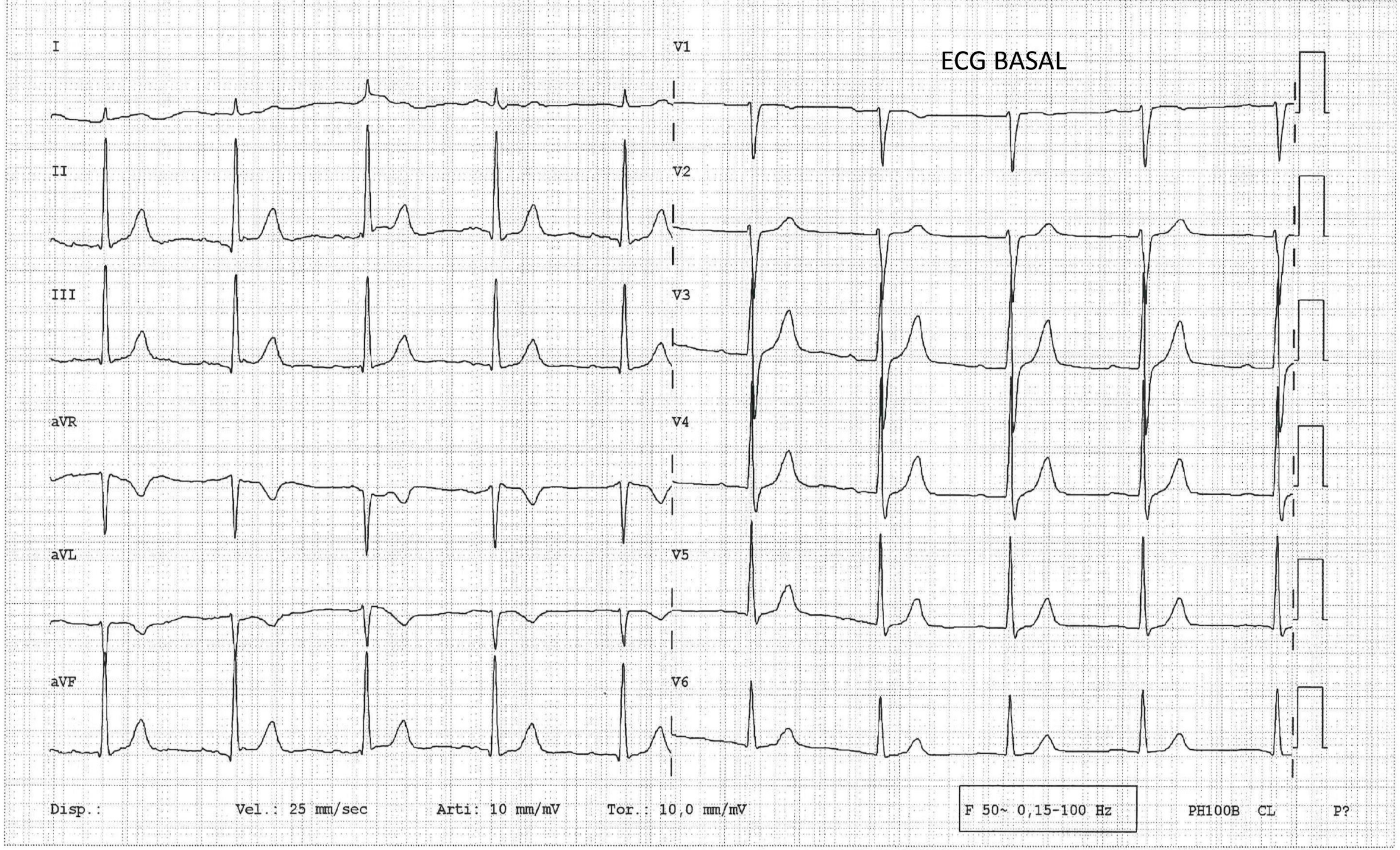
I
II
III
aVR
aVL
aVF
V1
V2
V3
V4
V5
V6
Disp.:
Vel.: 25 mm/sec
Arti: 10 mm/mV
Tor.: 10,0 mm/mV
F 50~ 0,15-100 Hz
PH100B CL
P?

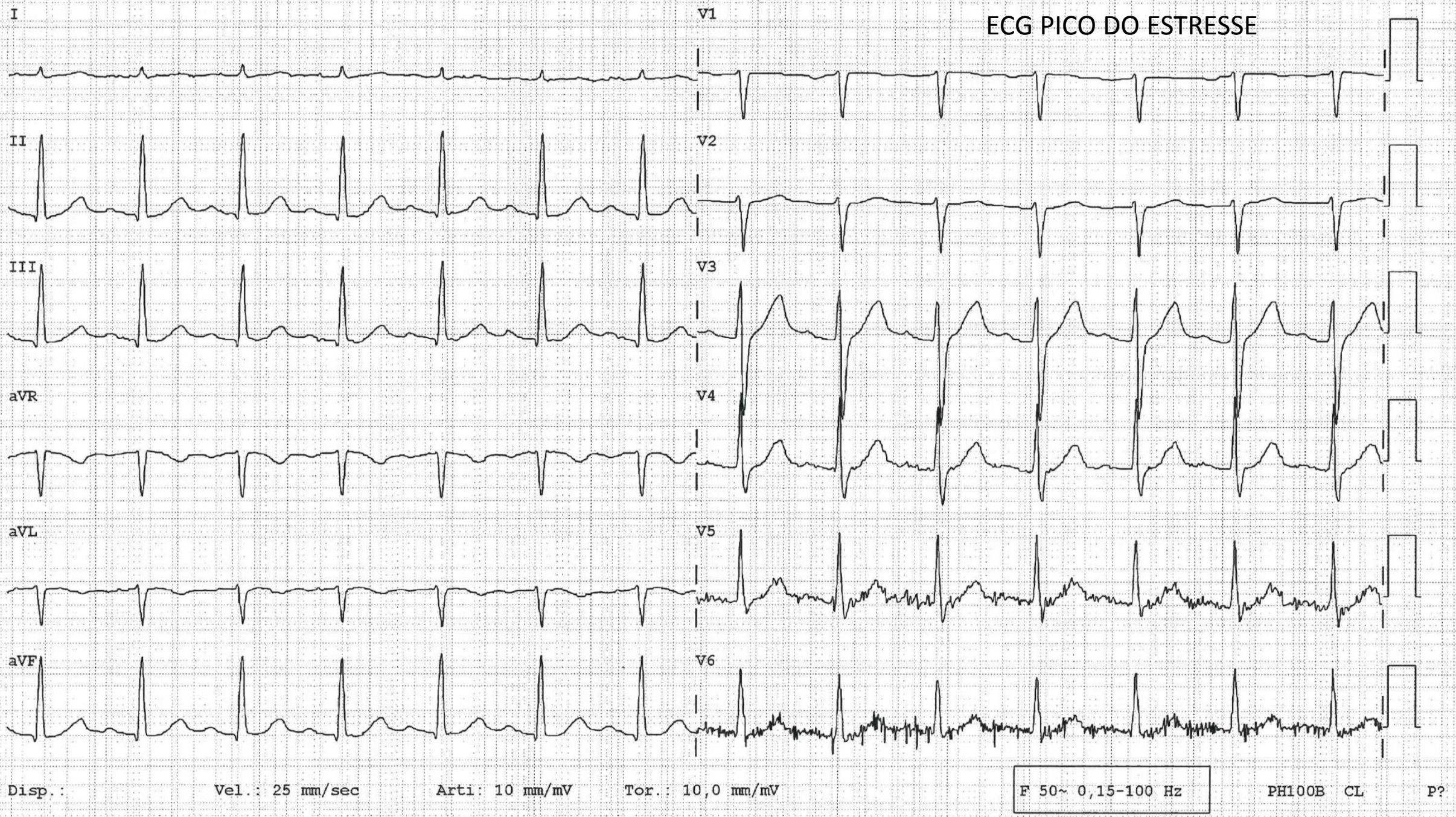
ECG PICO DO ESTRESSE
I
II
III
aVR
aVL
aVF
V1
V2
V3
V4
V5
V6
Disp.:
Vel.: 25 mm/sec
Arti: 10 mm/mV
Tor.: 10,0 mm/mV
F 50~ 0,15-100 Hz
PH100B CL
P?

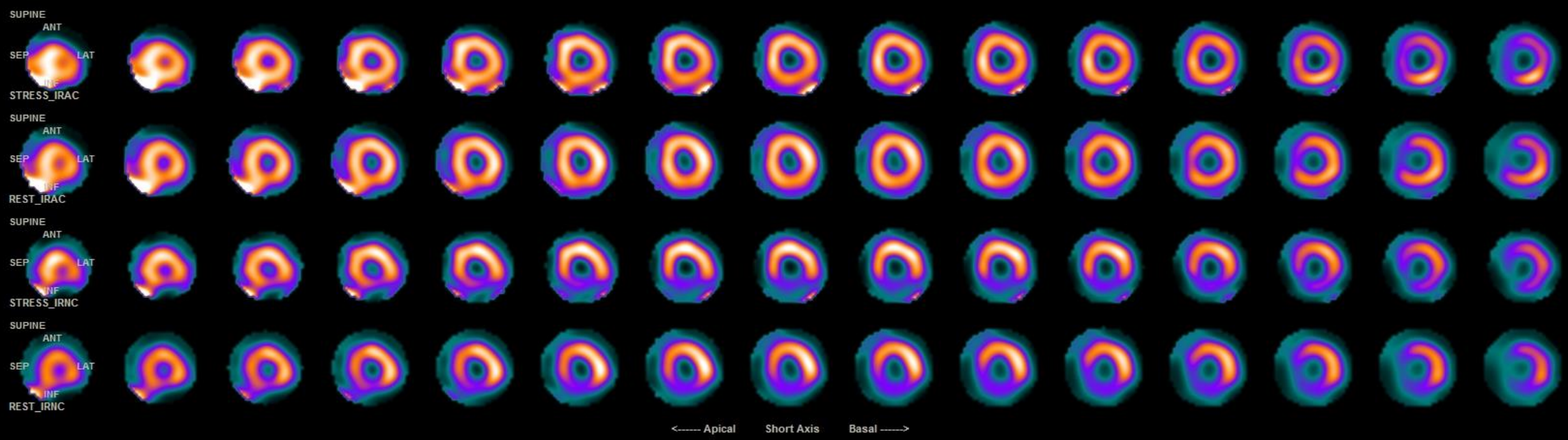

IMAGENS CORRIGIDAS PELA CT E IMAGENS NÃO CORRIGIDAS PELA CT

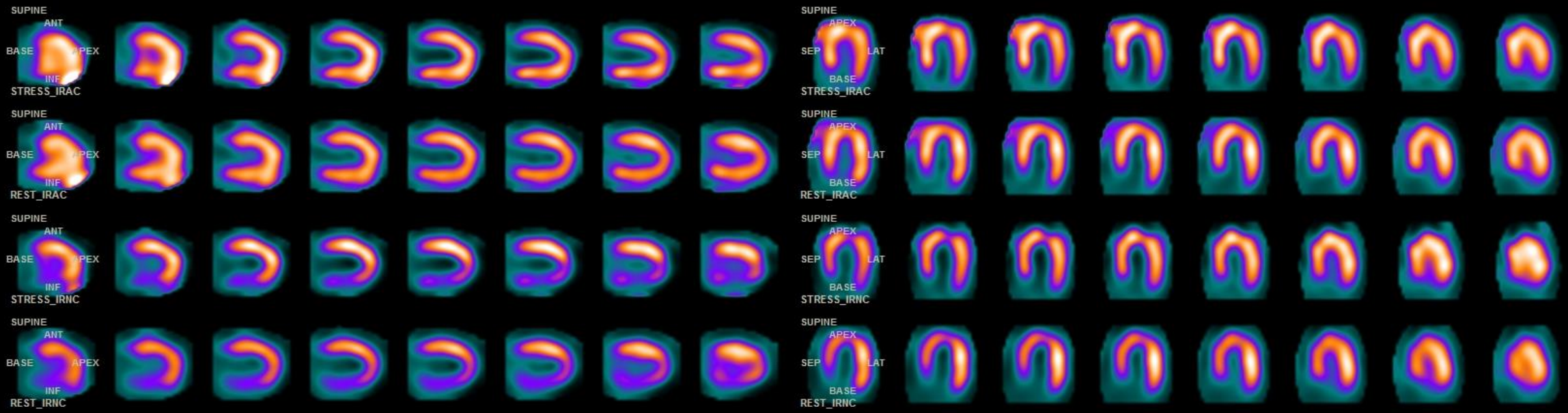

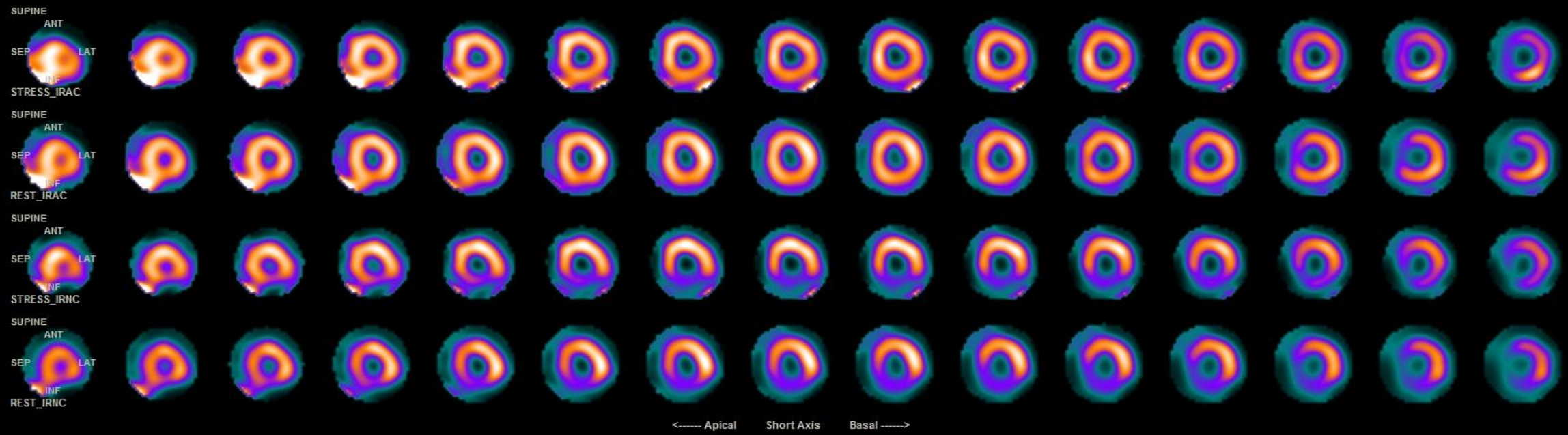

IMAGENS CORRIGIDAS PELA CT E IMAGENS NÃO CORRIGIDAS PELA CT

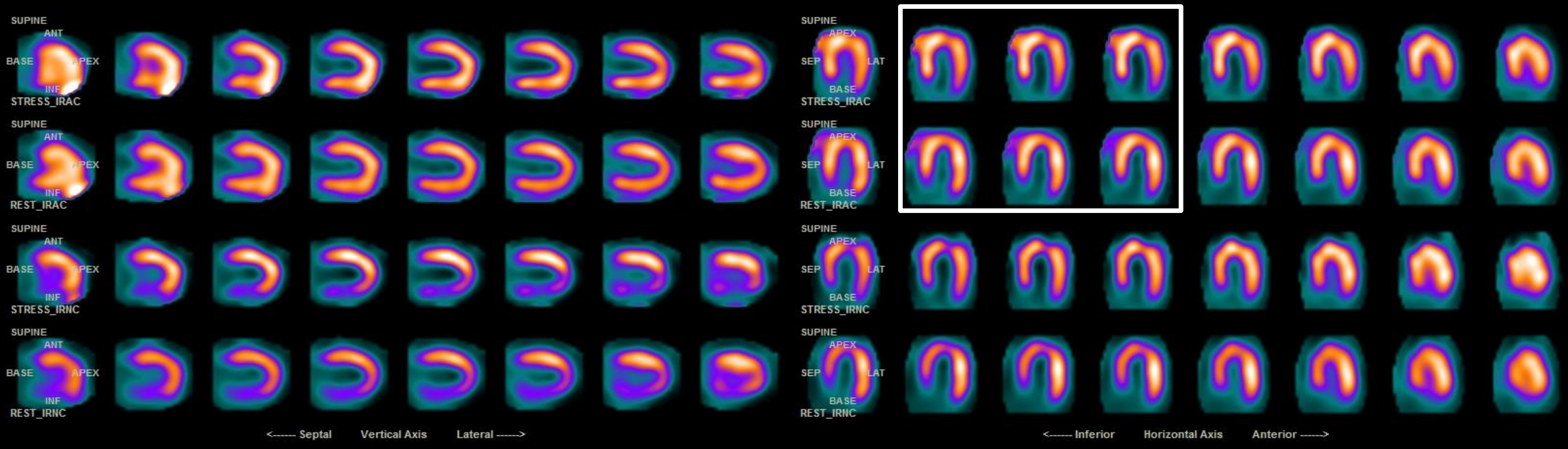

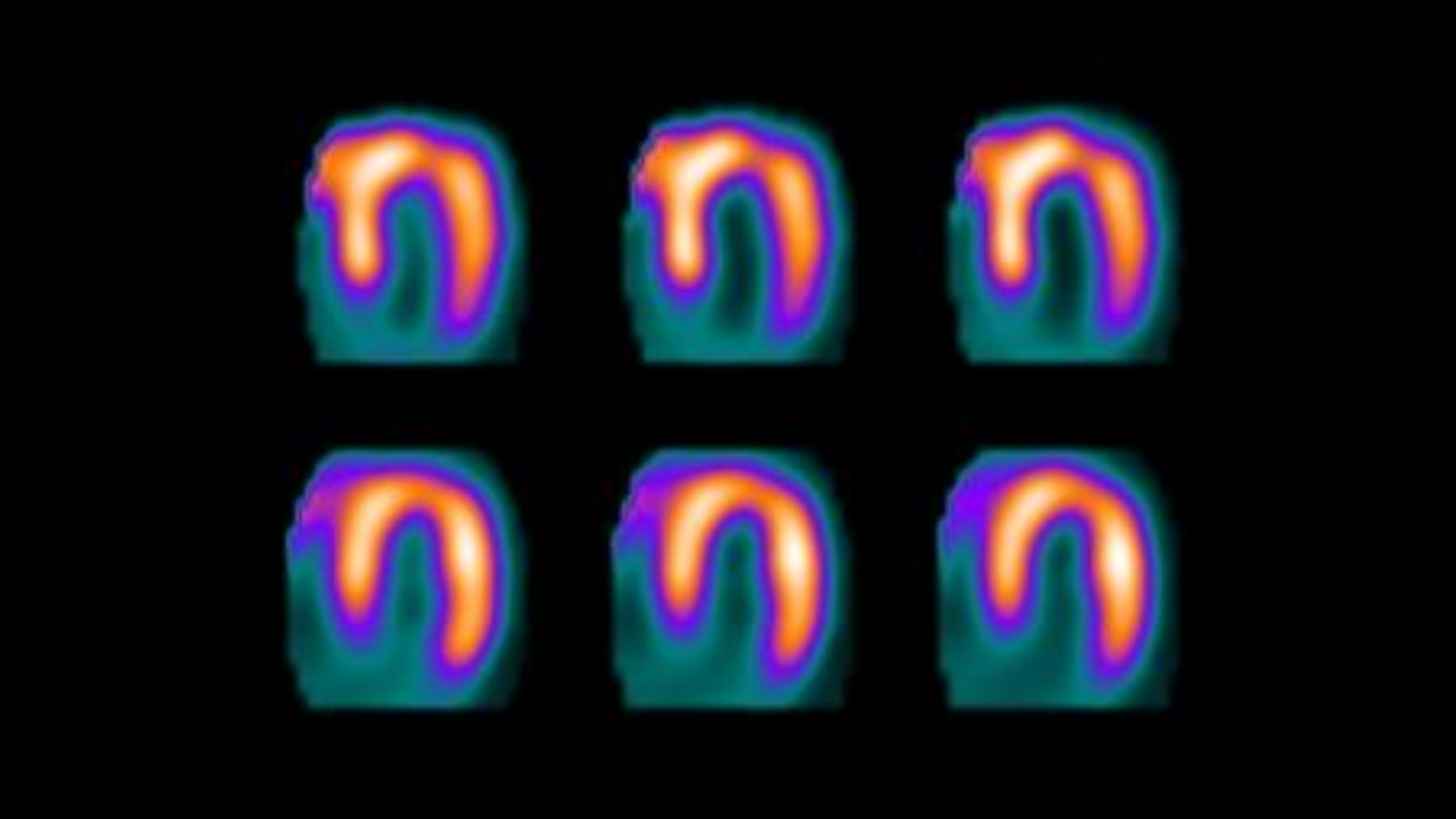

Str

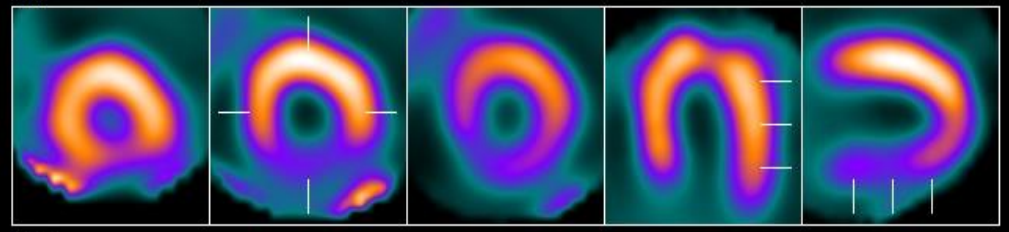

Rst

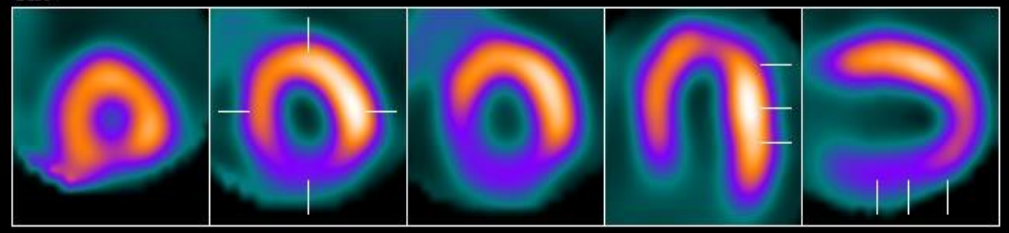

Perfusion-Blackout

STRESS_IRNC_SA

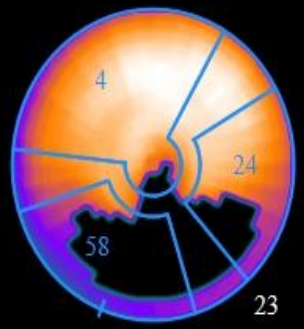

REST_IRNC_SA

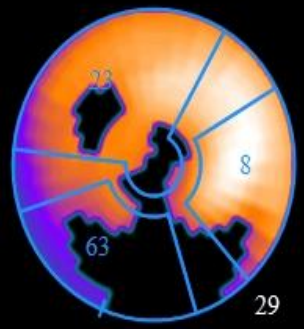

Reversibility

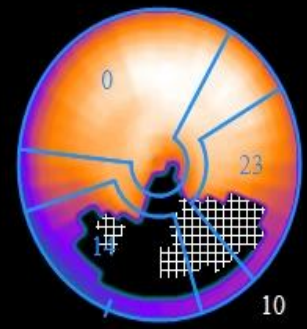

SSS

SRS

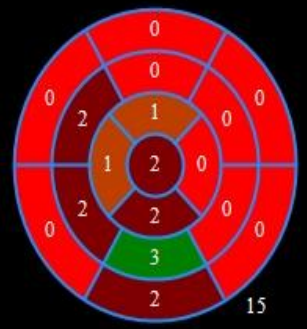

SDS

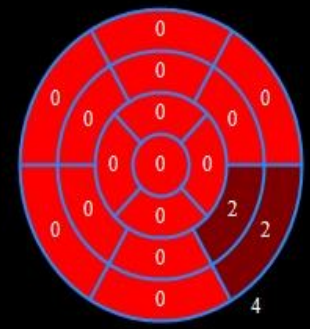

Auto	UNG	None	Ungated	Blackout	Revers	Vascular	None	-

ISQUEMIA LATERAL de 5% do MIOCÁRDIO

Alle immagini dopo Regadenoson: ventricolo sinistro di normali dimensioni, pareti ipertrofiche. Area di lieve ipocaptazione del radiofarmaco in sede laterale ed infero laterale. Ipocaptazione di possibile natura artefattuale da attenuazione in sede inferiore medio-prossimale. Omogenea captazione a livello di tutti i restanti segmenti esplorati.
Alle immagini basali: Normalizzazione della captazione laterale. Invariati i rimanenti reperti.
La valutazione funzionale del ventricolo sinistro, in condizioni di riposo, ottenuta mediante acquisizione Gated-Spect, ha permesso di determinare:

FE%: >65 EDV: 100 ml TID: 0.90 MASSA: 130g

CINETICA REGIONALE: normale cinetica segmentaria.

CONCLUSIONI
In condizioni basali ed regime di abolita riserva coronarica da vasodilatazione massimale evidenza scintigrafica di lieve ipoperfusione miocardica in sede laterale.
Area di persistente ipoperfusione miocardica in sede inferiore medio-prossimale ai limiti della significatività scintigrafica in presenza di attività extracardiaca da verosimile attenuazione diaframmatica, per la quale risulta meritevole un approfondimento diagnostico.

PET CT

Produção da Amônia-N13 no cíclotron

Estresse cardíaco e Administração da N^{13}-NH_3

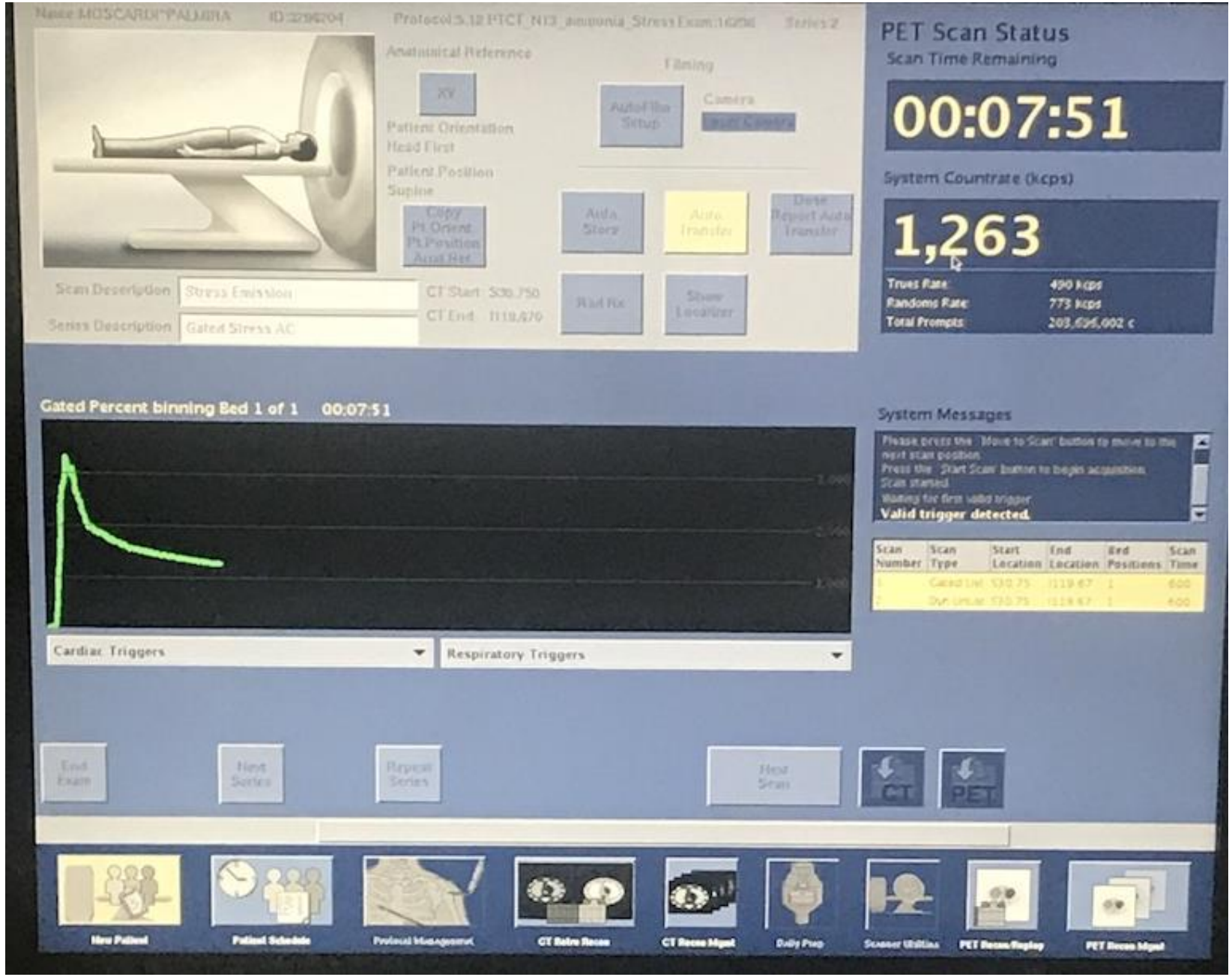
PET Scan Status
Scan Time Remaining
00:07:51
System Countrate (kcps)
1,263
Trues Rate 490 kcps
Randoms Rate 773 kcps
Total Prompts 203,696,002 c
Gated Percent binning Bed 1 of 1 00:07:51
System Messages
Valid trigger detected.
Cardiac Triggers
Respiratory Triggers
CT
PET

+SDYN STRESS ACQ
13-Mar-2018 09:03:23
Ung, Supine, IR:3D:SC:CTAC
N-13 Ammonia
UgVol: 78 ml, TID: 1.13
SSS: 0 SDS: 0
STR/NH3/SC-CTAC/M

+SDYN REST ACQC
13-Mar-2018 10:57:52
Ung, Supine, IR:3D:SC:CTAC
N-13 Ammonia
UgVol: 69 ml, TID: --
SRS: 3
RST/NH3/SC-CTAC/M

SA (Apex→Base)

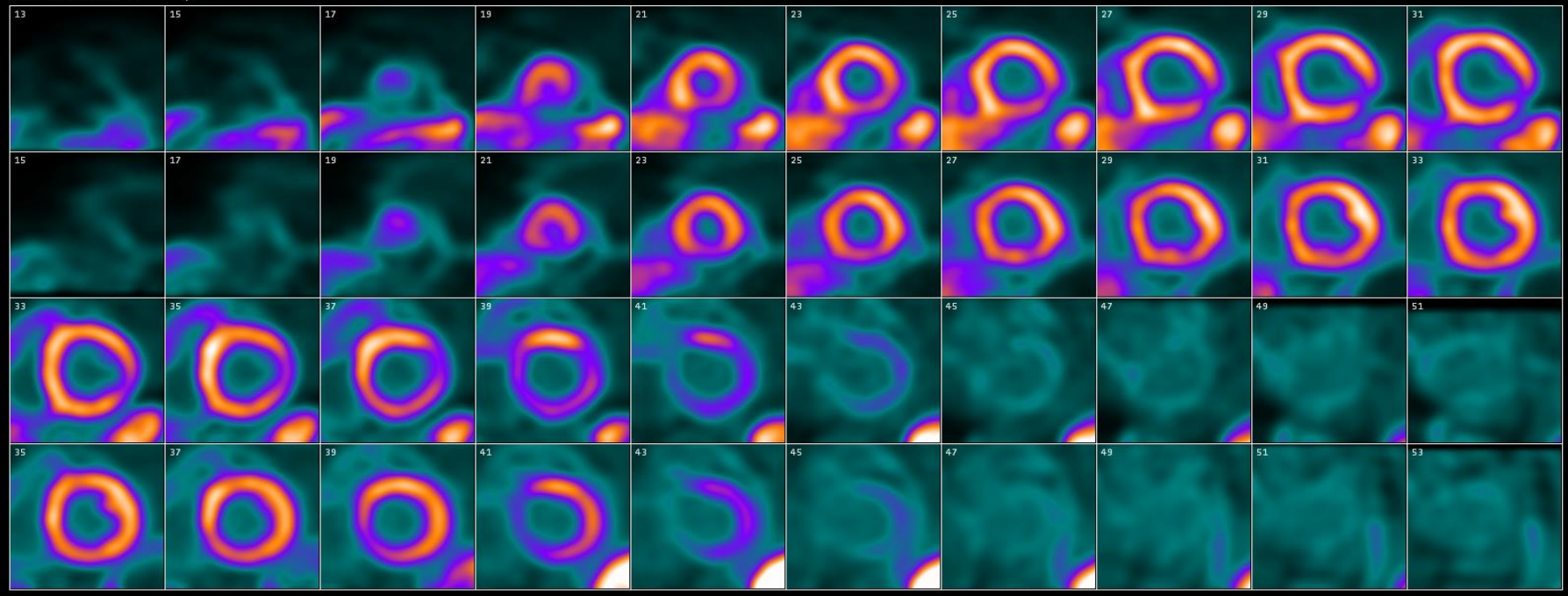

HLA (INF→ANT)

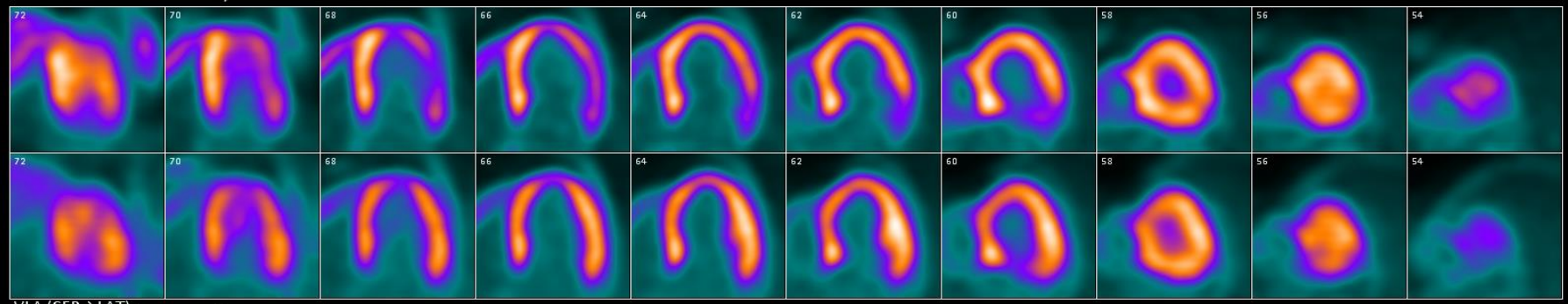

VLA (SEP→LAT)

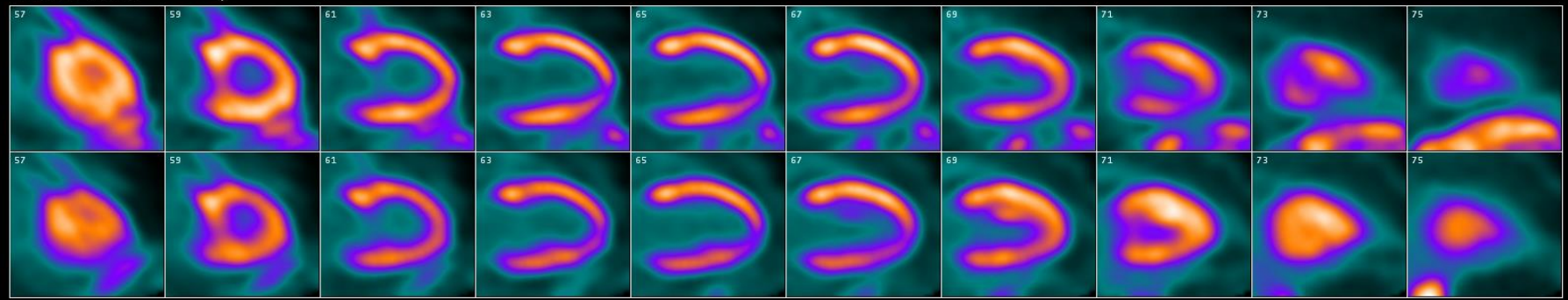

MI Processing
Fusion
Images
Images + Quant
Func + Quant
Reserve
AC Images
AC Images + Quant
AC Func + Quant
Dyssynchrony
MPI Summary
CT Viewer
Ca Scoring
3D Melons
Polar Maps
DB Generator
DB Editor

Patient Info
Export Data
Save
Screen Capture
Help
Preferences
Quit

+SGATED STRESS ACQC
13-Mar-2018 09:03:24
16 Fr, Supine, IR:3D:SC:CTAC
N-13 Ammonia
EDV: 132 ml (72 ml/m²)
ESV: 50 ml (27 ml/m²)
EF: 62 %
Mass: 156 g, CO: --
UgVol: 78 ml, TID: --
SSS: -- SDS: --
STR/NH3/SC-CTAC/M

+SGATED REST ACQC
13-Mar-2018 10:57:53
16 Fr, Supine, IR:3D:SC:CTAC
N-13 Ammonia
EDV: 121 ml (66 ml/m²)
ESV: 41 ml (22 ml/m²)
EF: 66 %
Mass: 150 g, CO: --
UgVol: 66 ml, TID: --
SRS: --
RST/NH3/SC-CTAC/M

GStrCTAC Frame: 11

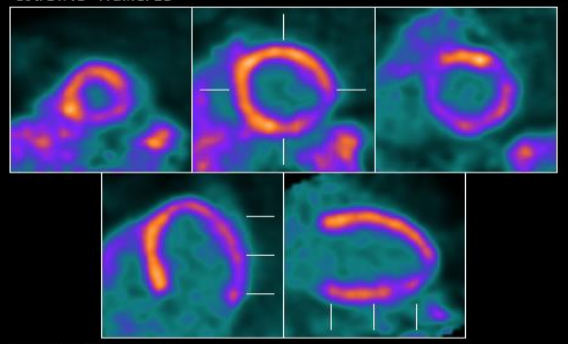

GRstCTAC Frame: 11

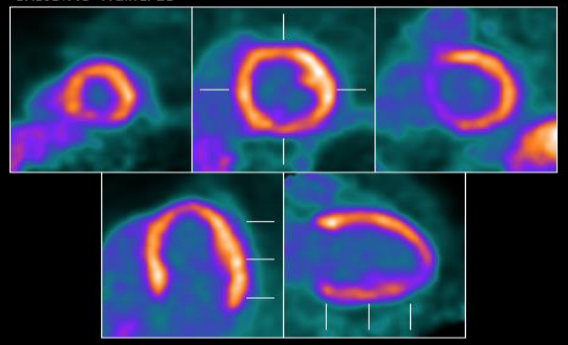

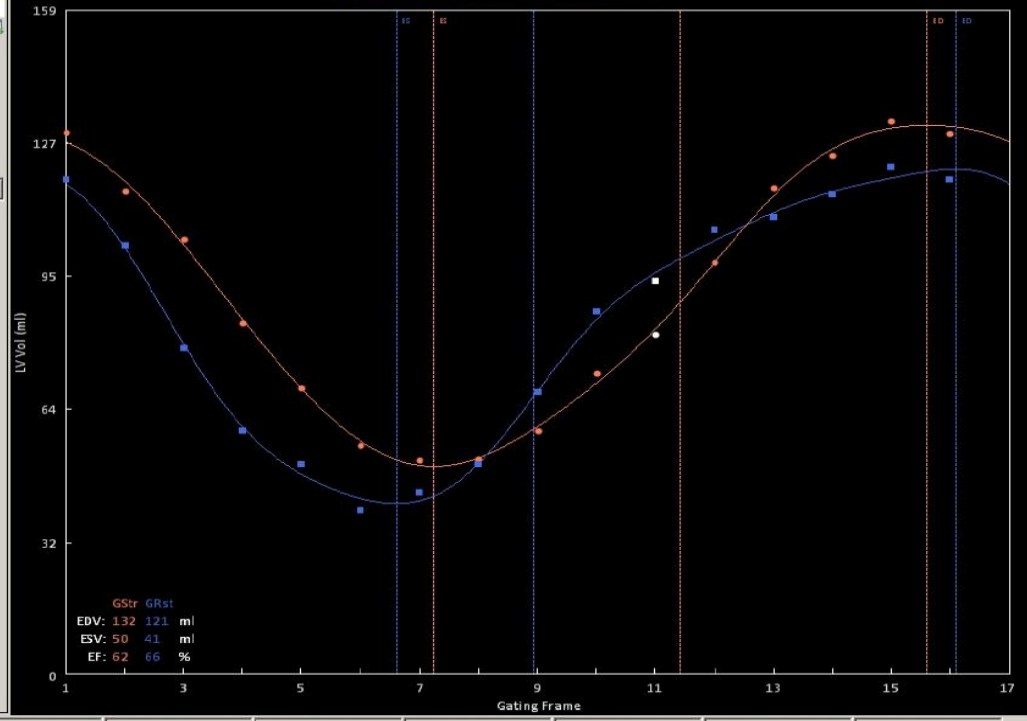

Wall Motion

+SGATED STRESS ACQC

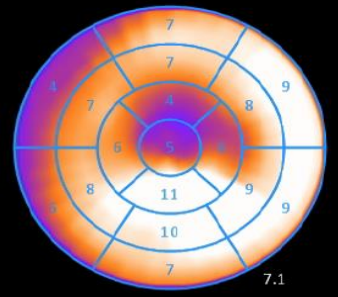

+SGATED REST ACQC

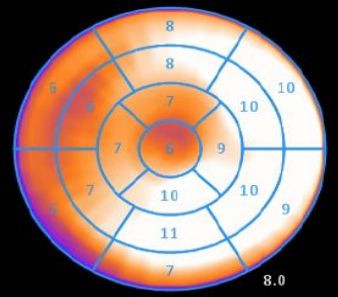

Wall Motion Scores

+SGATED STRESS ACQC

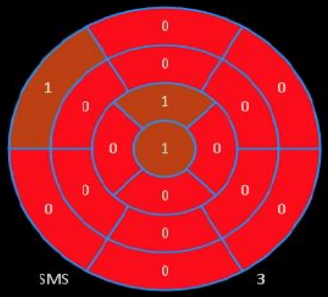

+SGATED REST ACQC

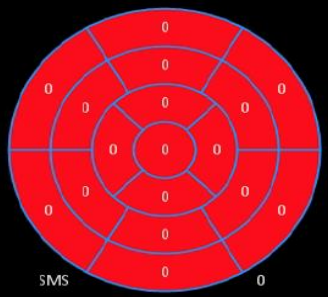

Wall Thickening

+SGATED STRESS ACQC

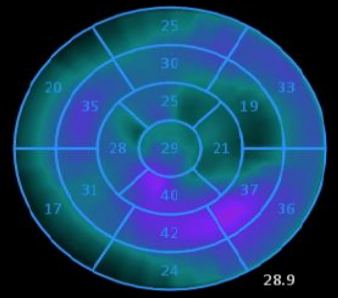

+SGATED REST ACQC

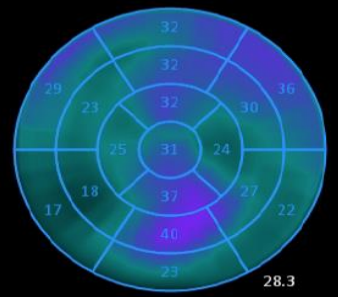

Wall Thickening Scores

+SGATED STRESS ACQC

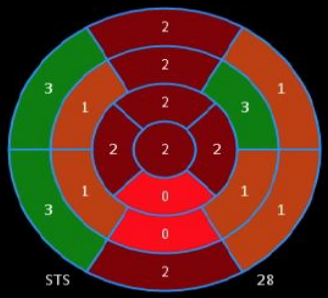

+SGATED REST ACQC

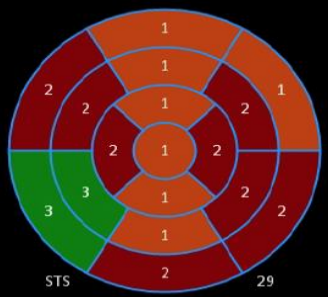

+SDYN STRESS ACQ
13-Mar-2018 09:03:23
Ung, Supine, IR:3D:SC:CTAC
N-13 Ammonia
UgVol: 78 ml, TID: 1.13
SSS: 5 SDS: 5
STR/NH3/SC-CTAC/M

Perfusion
StrCTAC

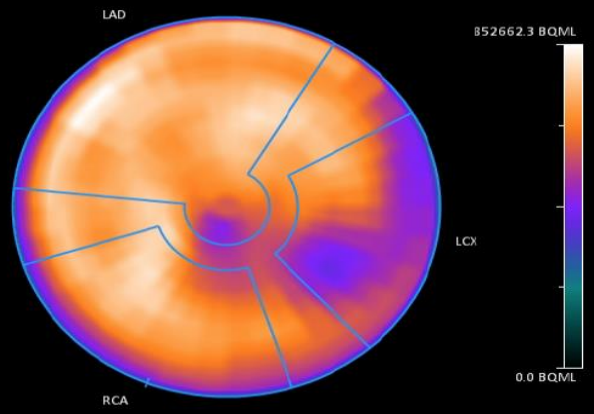

Defect Blackout Map

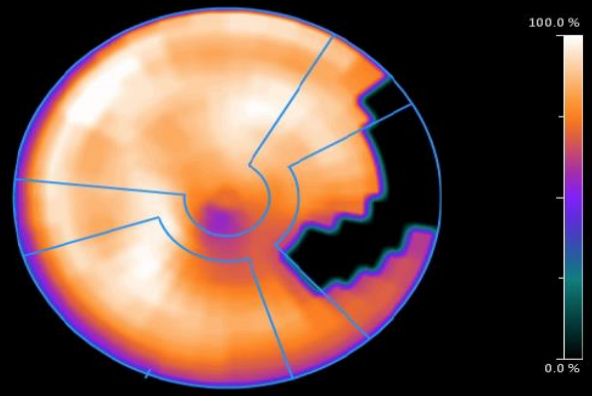

Region	Extent
LAD	0 %
LCX	46 %
RCA	0 %
TOT	9 %

+SDYN REST ACQC
13-Mar-2018 10:57:52
Ung, Supine, IR:3D:SC:CTAC
N-13 Ammonia
UgVol: 69 ml, TID: --
SRS: 3
RST/NH3/SC-CTAC/M

Perfusion
RstCTAC

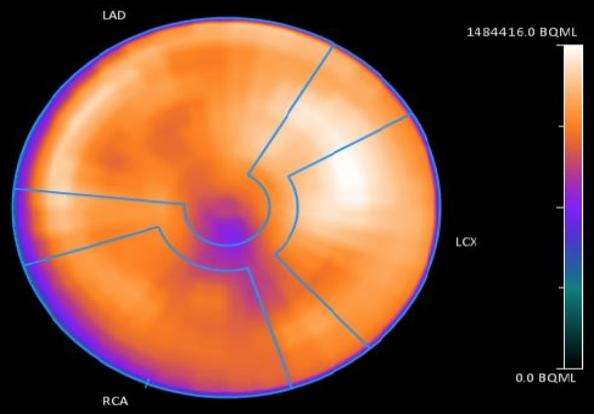

Defect Blackout Map

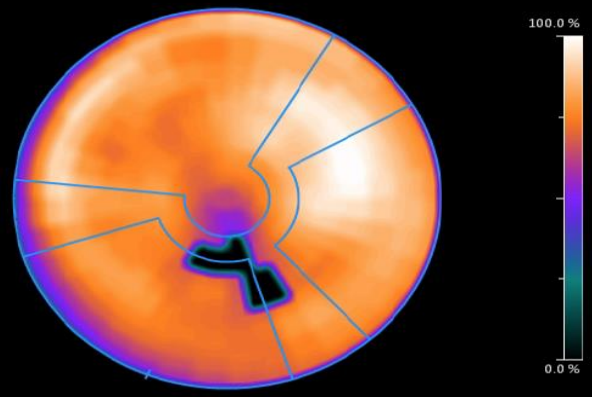

Region	Extent
LAD	0 %
LCX	0 %
RCA	9 %
TOT	4 %

Reversibility
13-Mar-2018 09:03:23
Ung, --
N-13 Ammonia
V-REVER

Reversibility

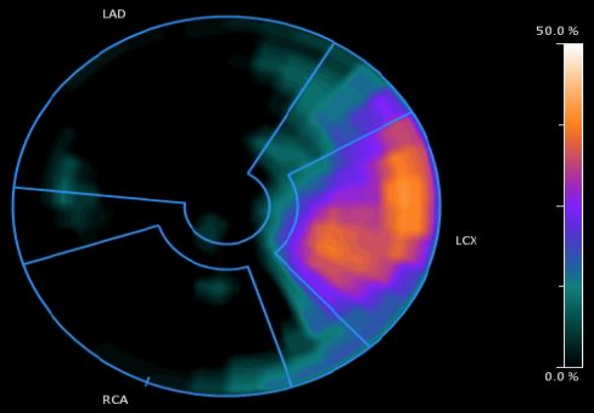

Defect Blackout Map

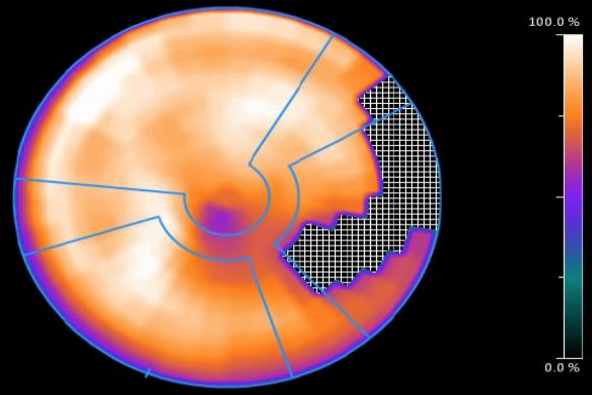

Region	Nml	Fixed	Revers
LAD	100 %	0 %	0 %
LCX	54 %	0 %	46 %
RCA	100 %	0 %	0 %
TOT	91 %	0 %	9 %

Área de isquemia = 9%

PET – Amônio-N13

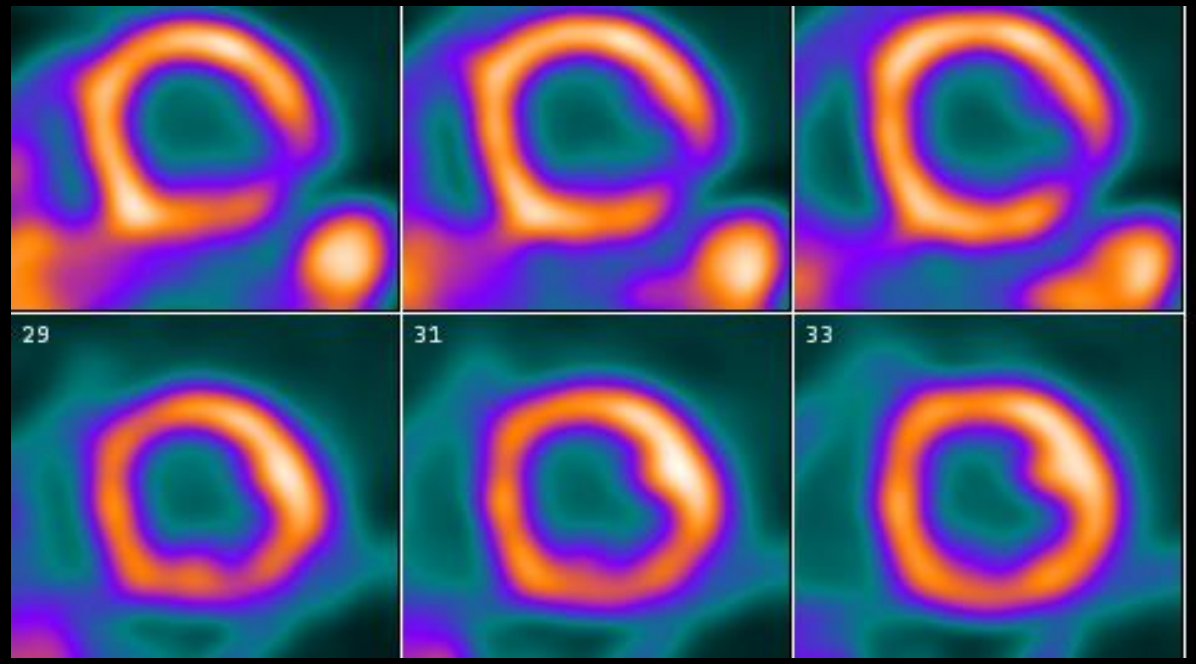

SPECT – TETROFOSMIN-Tc99m

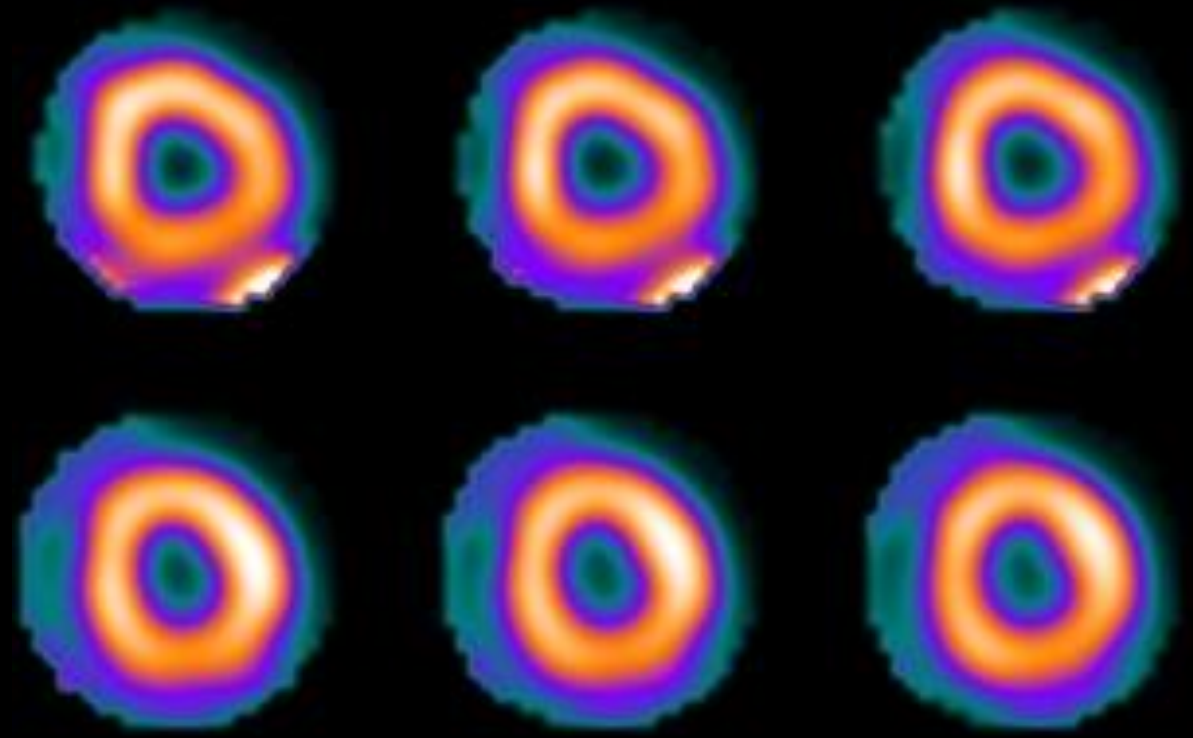

+SDYN STRESS ACQ
13-Mar-2018 09:03:23
Ung, Supine, IR:3D:SC:CTAC
N-13 Ammonia
UgVol: 78 ml, TID: 1.13
SSS: -- SDS: --
STR/NH3/SC-CTAC/M

+SDYN REST ACQC
13-Mar-2018 10:57:52
Ung, Supine, IR:3D:SC:CTAC
N-13 Ammonia
UgVol: 69 ml, TID: --
SRS: --
None

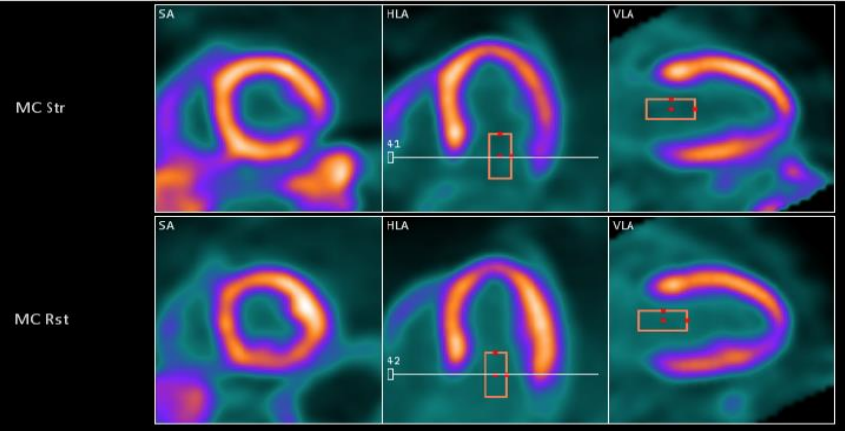

Global Results

Region	Mean MC Str	Mean MC Rst	Flow (ml/min/g) MC Str	Flow (ml/min/g) MC Rst	Reserve
LAD	88 %	79 %	1.69	0.78	2.18
LCX	68 %	87 %	1.31	0.91	1.45
RCA	82 %	72 %	1.66	0.70	2.36
TOT	81 %	79 %	1.57	0.79	2.00

Algorithm (MC Str): INVIA N-13 ROI 1:1
Algorithm (MC Rst): INVIA N-13 ROI 1:1

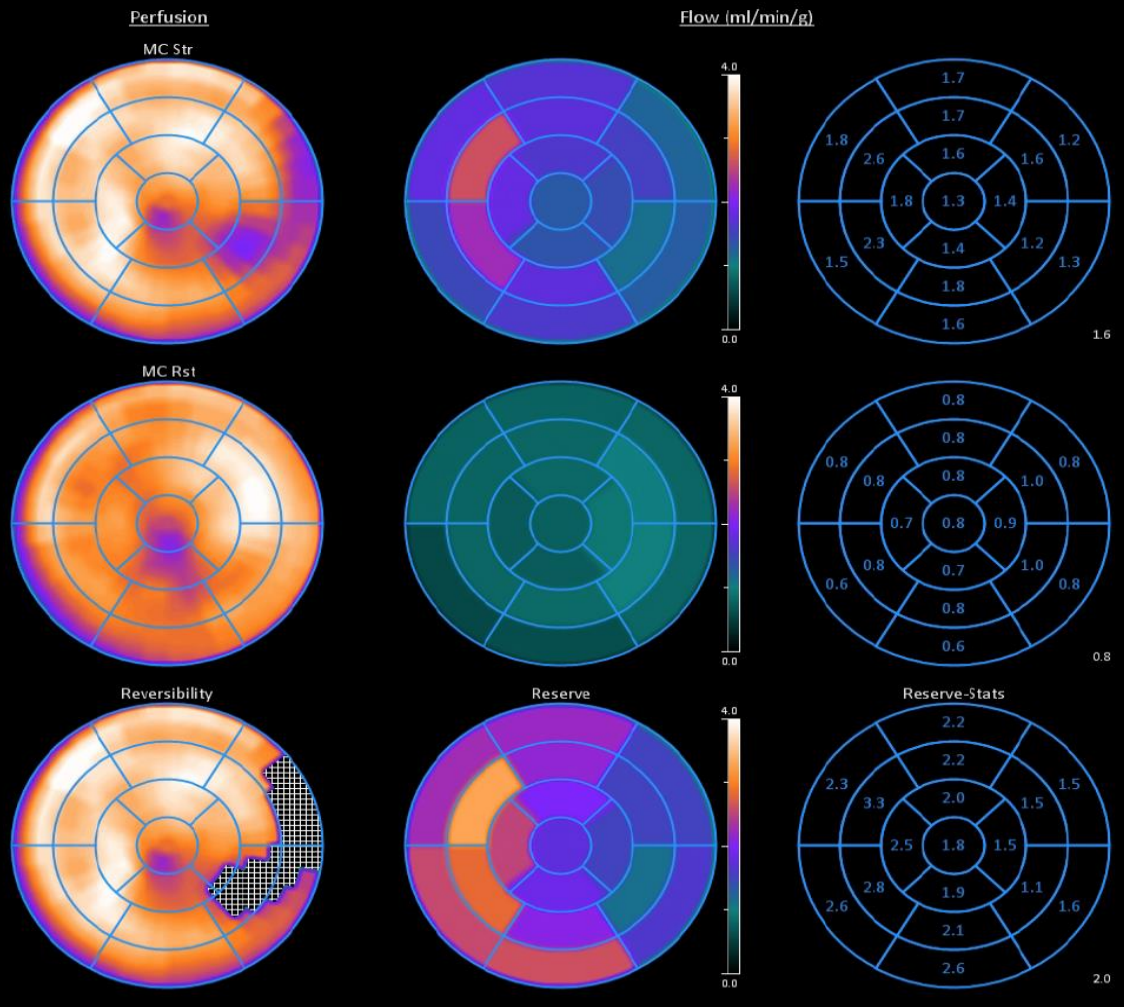

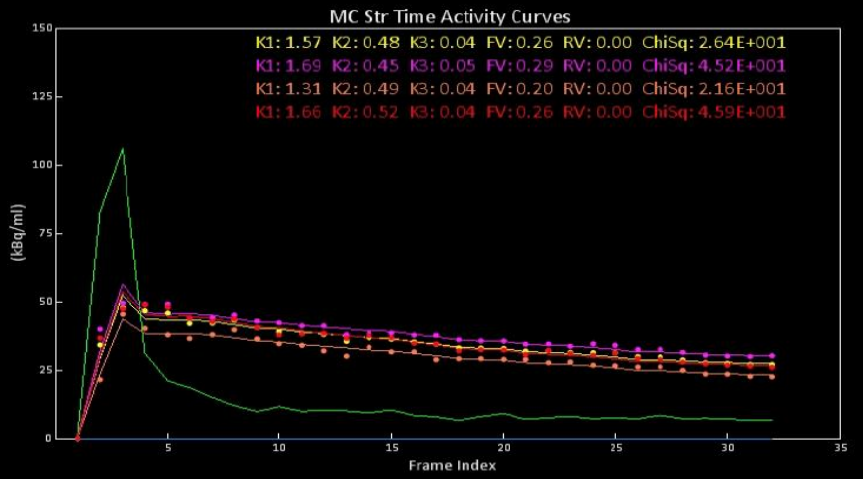

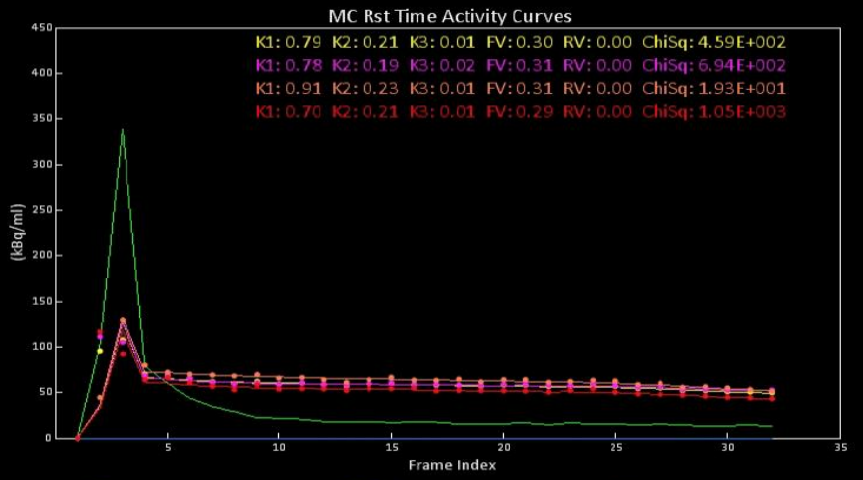

+SDYN STRESS ACQ
13-Mar-2018 09:03:23
Ung, Supine, IR:3D:SC:CTAC
N-13 Ammonia
UgVol: 78 ml, TID: 1.13
SSS: -- SDS: --
STR/NH3/SC-CTAC/M

+SDYN REST ACQC
13-Mar-2018 10:57:52
Ung, Supine, IR:3D:SC:CTAC
N-13 Ammonia
UgVol: 69 ml, TID: --
SRS: --
None

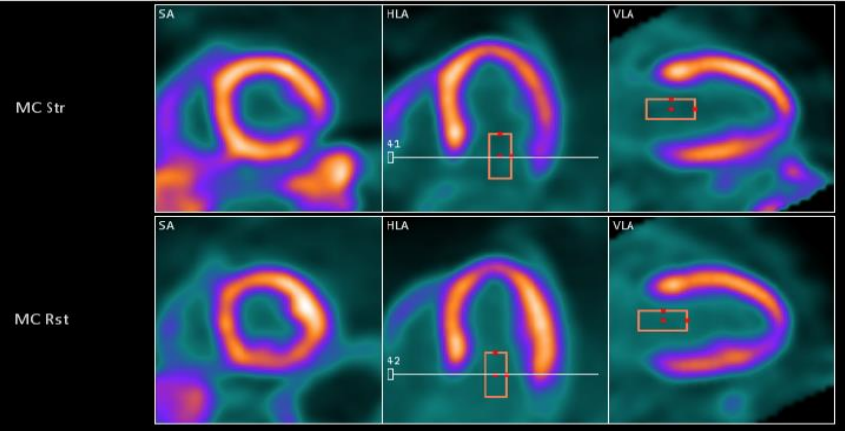

Global Results

Region	Mean MC Str	Mean MC Rst	Flow (ml/min/g) MC Str	Flow (ml/min/g) MC Rst	Flow (ml/min/g) Reserve
LAD	88 %	79 %	1.69	0.78	2.18
LCX	68 %	87 %	1.31	0.91	1.45
RCA	82 %	72 %	1.66	0.70	2.36
TOT	81 %	79 %	1.57	0.79	2.00

Algorithm (MC Str): INVIA N-13 ROI 1:1
Algorithm (MC Rst): INVIA N-13 ROI 1:1

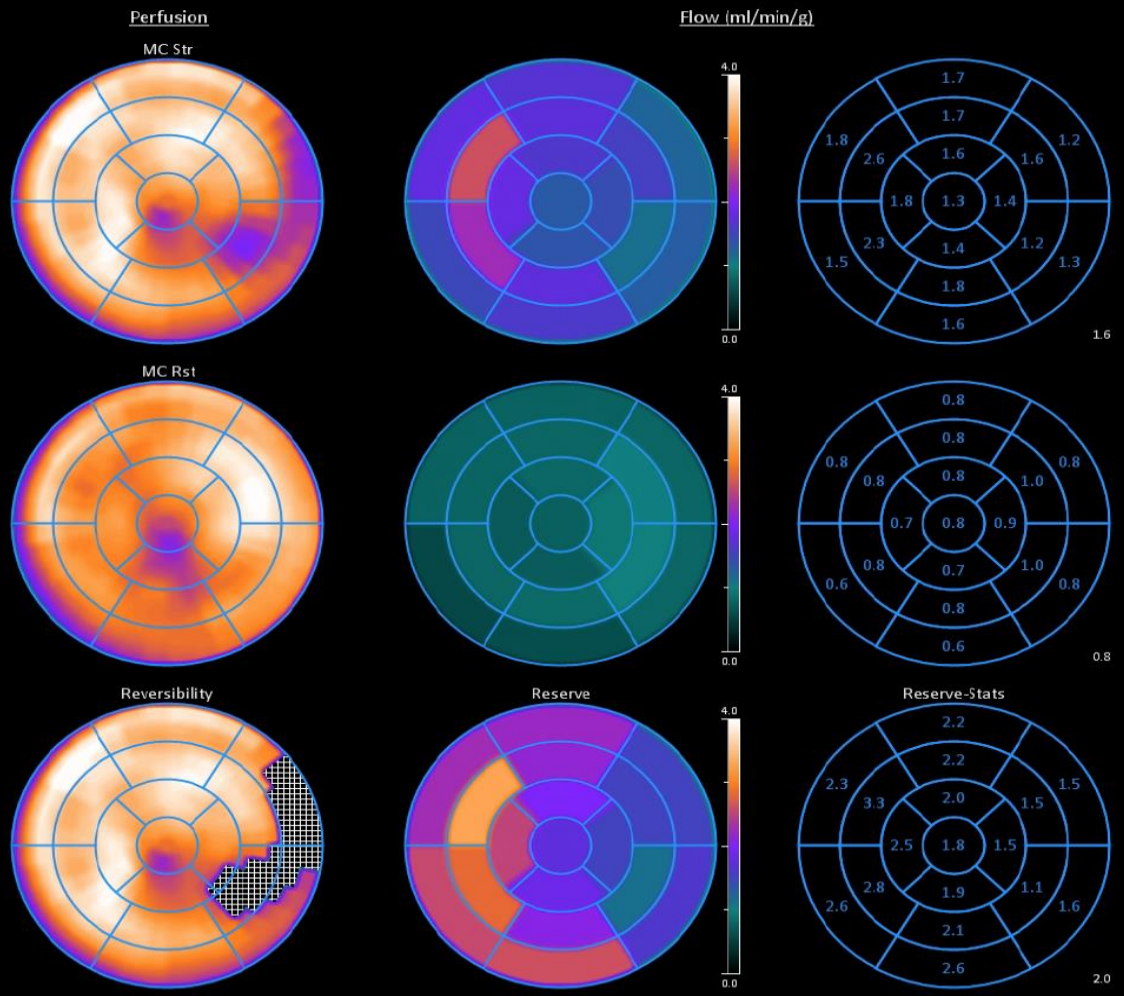

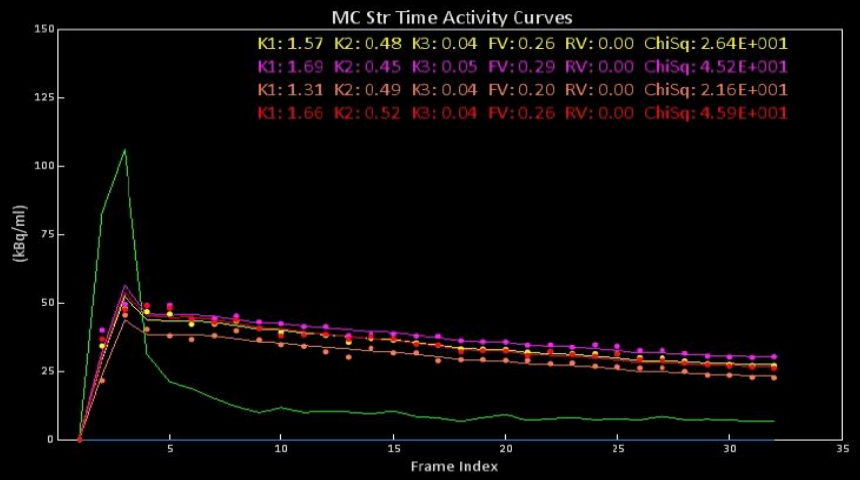

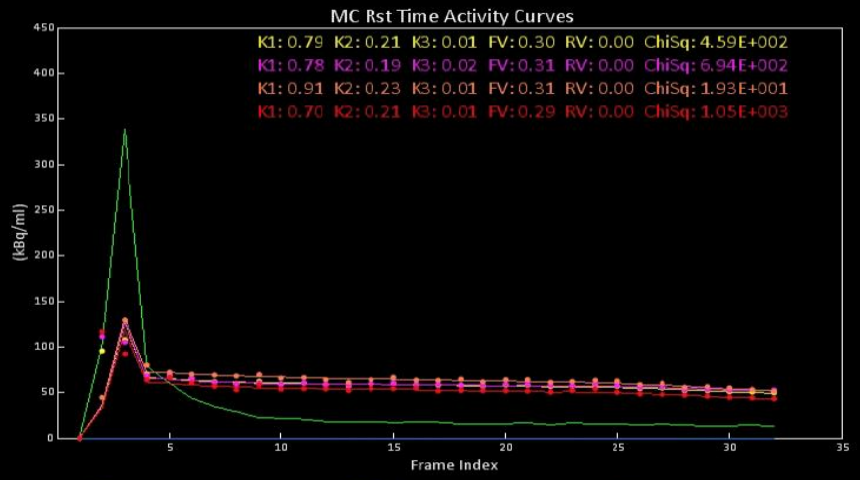

RESERVA DE FLUXO CORONARIANO - MFR

Global Results

	Mean		Flow (ml/min/g)		
Region	MC Str	MC Rst	MC Str	MC Rst	Reserve
LAD	88 %	79 %	1.69	0.78	2.18
LCX	68 %	87 %	1.31	0.91	1.45
RCA	82 %	72 %	1.66	0.70	2.36
TOT	81 %	79 %	1.57	0.79	2.00

Algorithm (MC Str): INVIA N-13 ROI 1:1

Algorithm (MC Rst): INVIA N-13 ROI 1:1

Why study the CFR?

An analysis of the relationship between MFR and cardiac mortality suggests an **excellent prognosis** for a **CFR of more than 2** and a steady **increase in cardiac mortality** for a **CFR of less than 2**

Murthy VL, Lee BC, Sitek A, et al. Comparison and prognostic validation of multiple methods of quantification of myocardial blood flow with ^{82}Rb PET. *J Nucl Med.* 2014;55:1952–1958.

Many studies have demonstrated that **as many as half of intermediate-risk subjects may be reclassified on the basis of CFR**, even after accounting for clinical characteristics, relative MPI interpretation, and left ventricular ejection fraction.

Di Carli MF, Murthy VL. Cardiac PET/CT for the evaluation of known or suspected coronary artery disease. *Radiographics.* 2011;31:1239–1254.

Myocardial Blood Flow & Coronary Flow Reserve

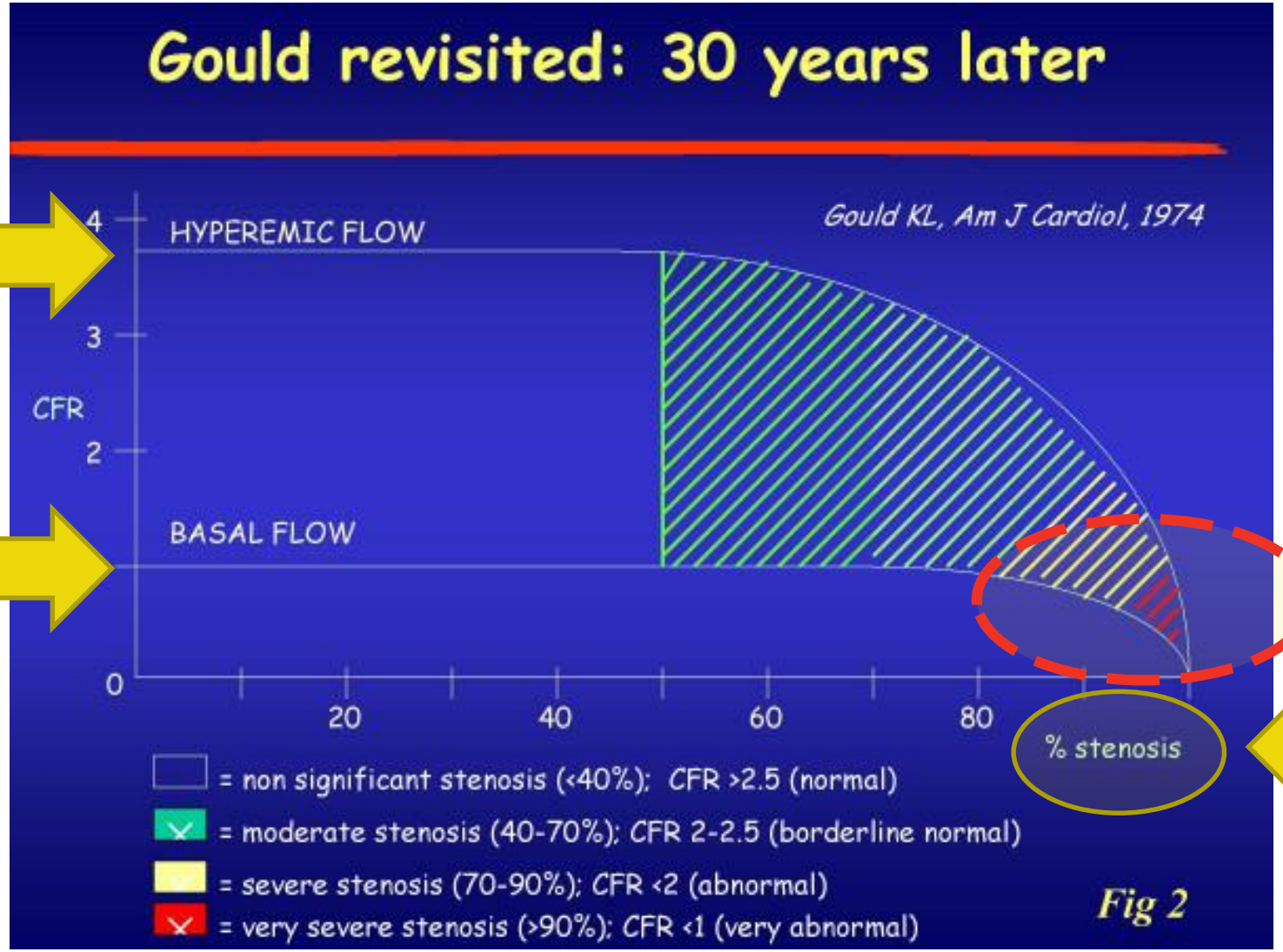

MBF @ Stress

MBF @ Rest

MBF – How much blood flows into the myocardium?

Units: ml (blood) / min / gr (gram of myocardium)

CFR – Ratio between Stress (hyperemic) and Rest (basal) flows.

No Units

Relationship between CFR and risk of cardiac death using different kinetic model

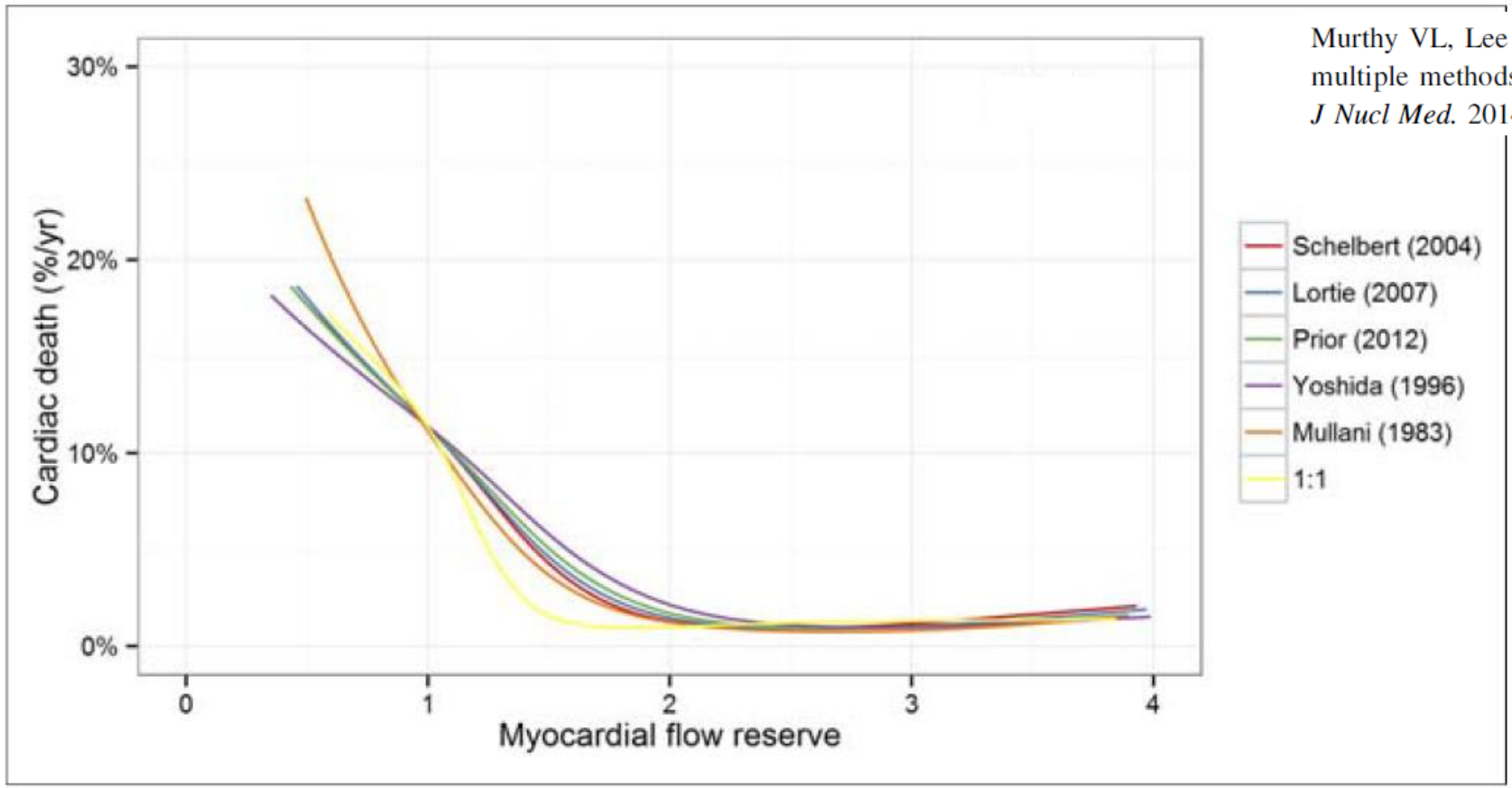

Murthy VL, Lee BC, Sitek A, et al. Comparison and prognostic validation of multiple methods of quantification of myocardial blood flow with ^{82}Rb PET. *J Nucl Med.* 2014;55:1952–1958.

Relationship between MFR and risk of cardiac death. Regardless of which ^{82}Rb tracer kinetic model is used, similar pattern of rising risk with MFR < 2 is seen. 1:1 indicates fictitious 100% extraction (MBF $= K_1$), which approximates assumptions for myocardial perfusion reserve index.

Growth of Myocardial Perfusion Imaging with Rubinium-82 PET in USA

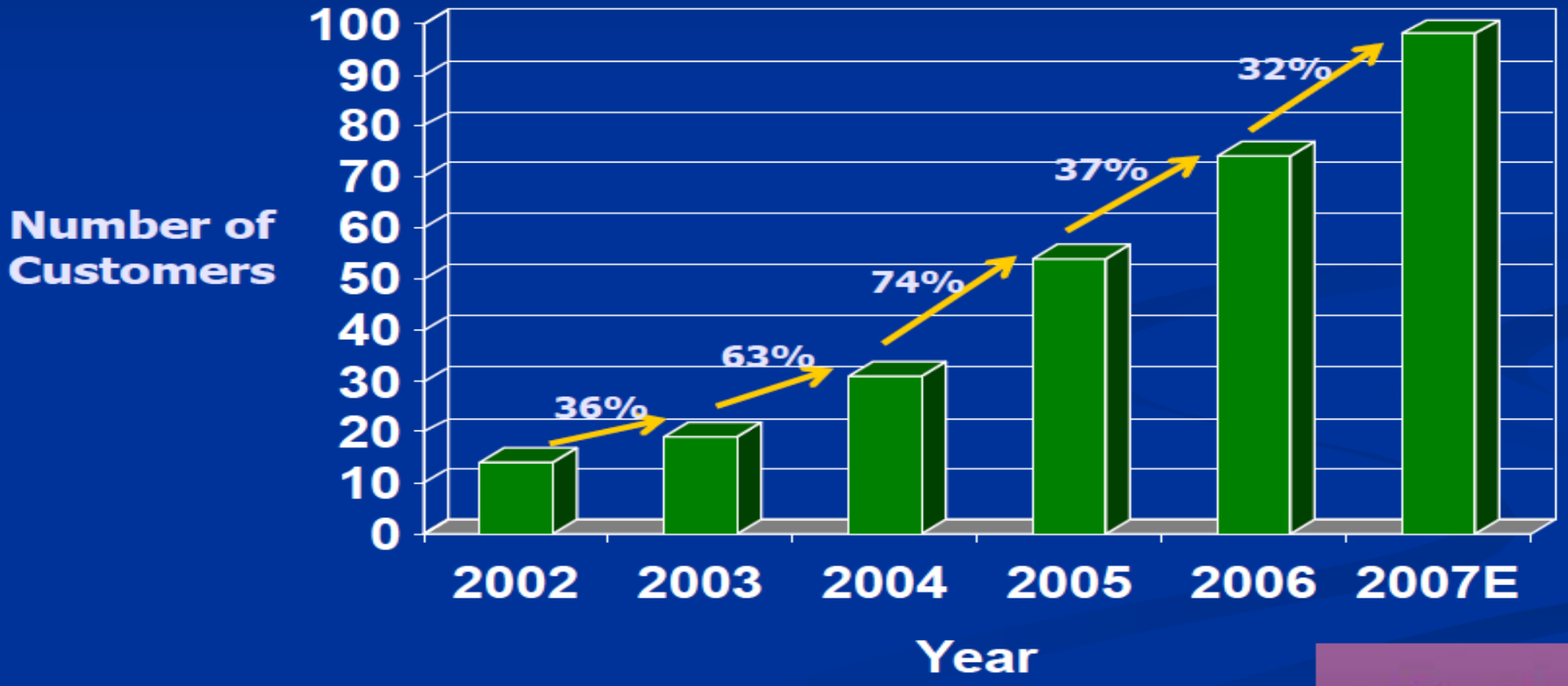

CARDIOGEN-82®
(RUBIDIUM RB 82 GENERATOR)

Cardiac Imaging UOHI

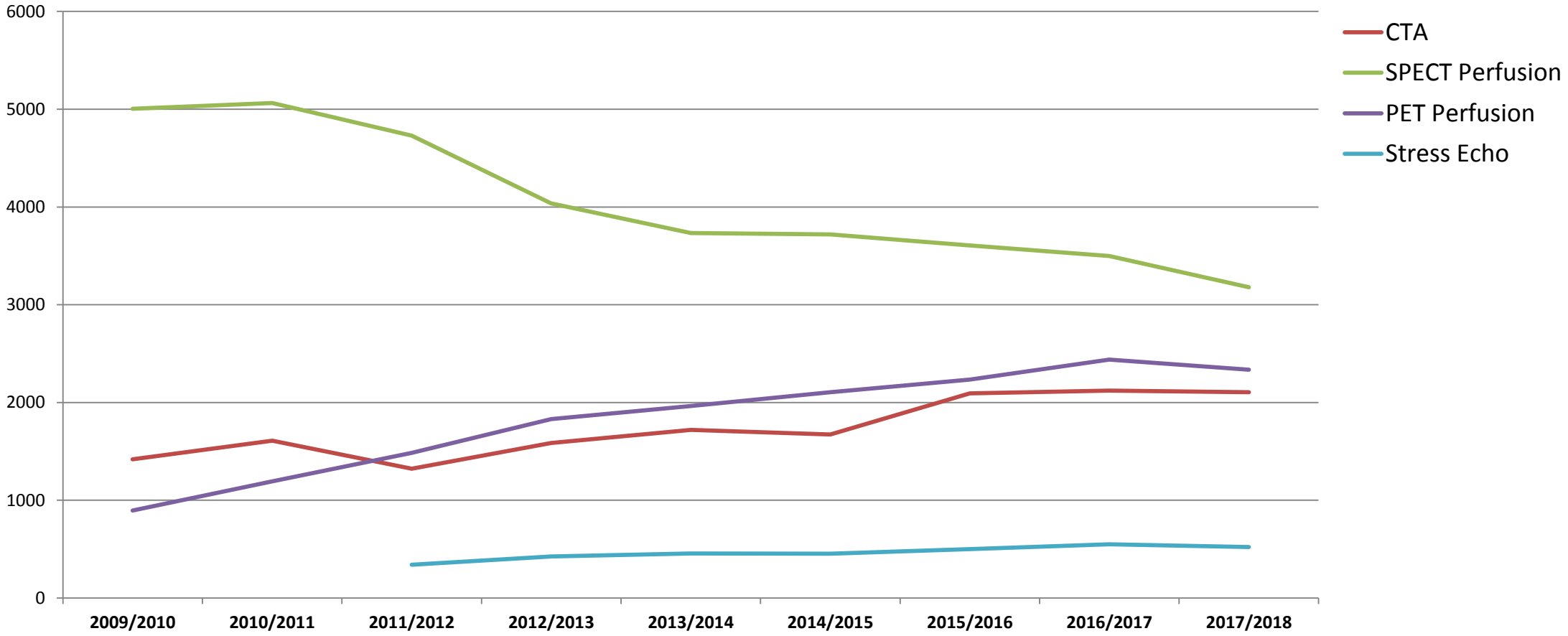

GE-BRESCIA DYNAMIC SPECT PROTOCOL

ACQUISITION – 99mTc Tetrofosmin

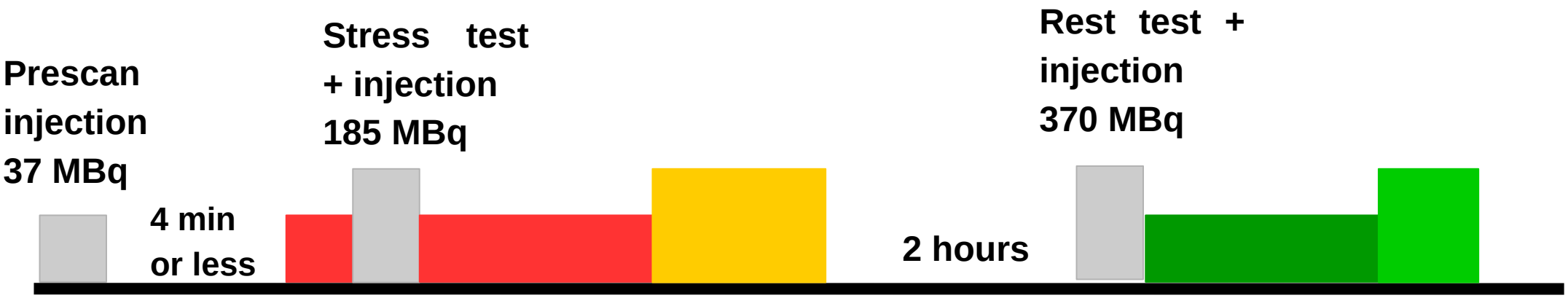


Discovery

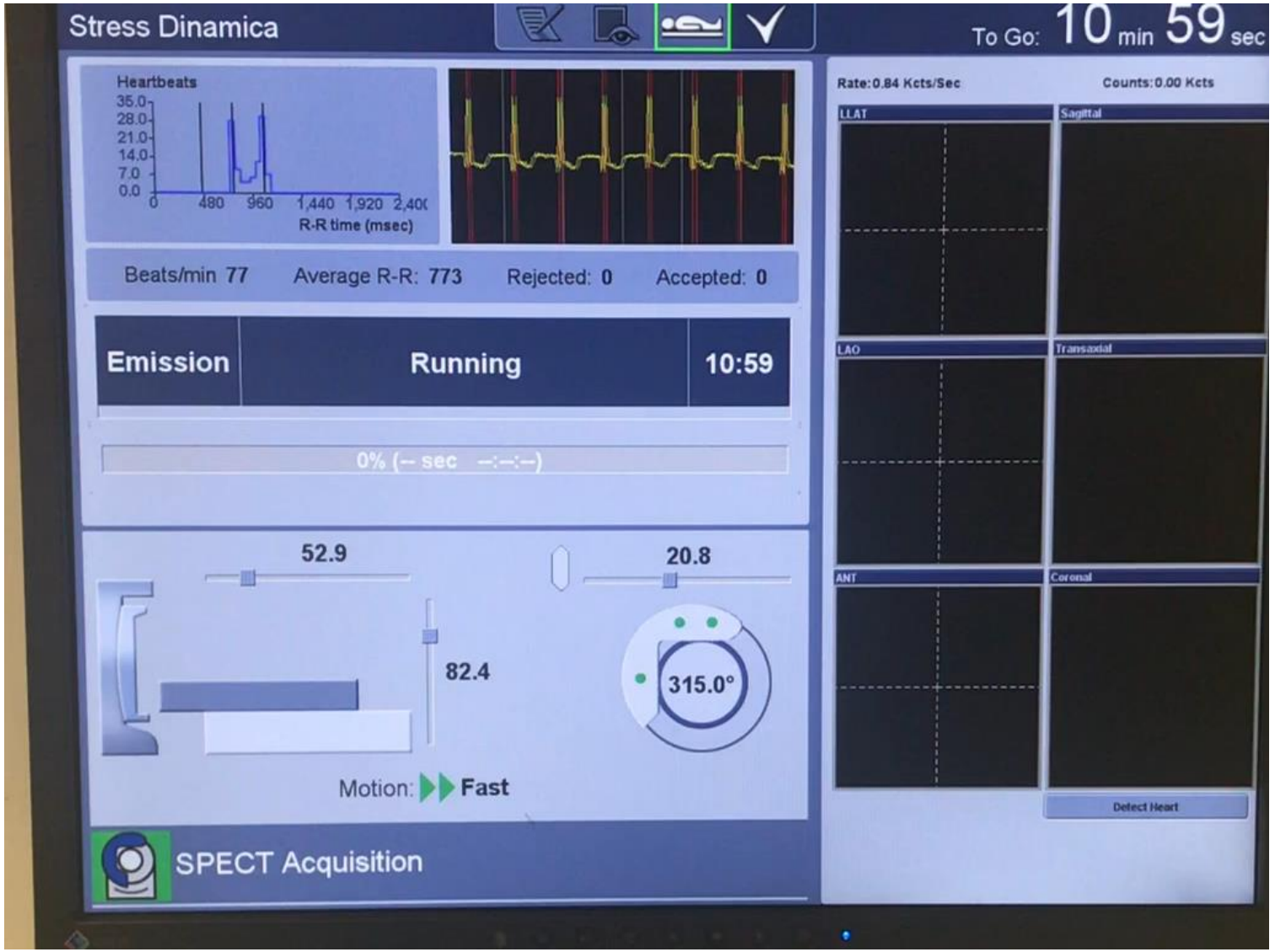
Stress Dinamica
To Go: 10 min 59 sec
Heartbeats
35.0
28.0
21.0
14.0
7.0
0.0
0
480
960
1,440
1,920
2,400
R-R time (msec)
Rate:0.84 Kcts/Sec
Counts:0.00 Kcts
LLAT
Sagittal
LAO
Transaxial
ANT
Coronal
Beats/min 77
Average R-R: 773
Rejected: 0
Accepted: 0
Emission
Running
10:59
0% (-- sec --:--:--)
52.9
20.8
82.4
315.0°
Motion: Fast
Detect Heart
SPECT Acquisition

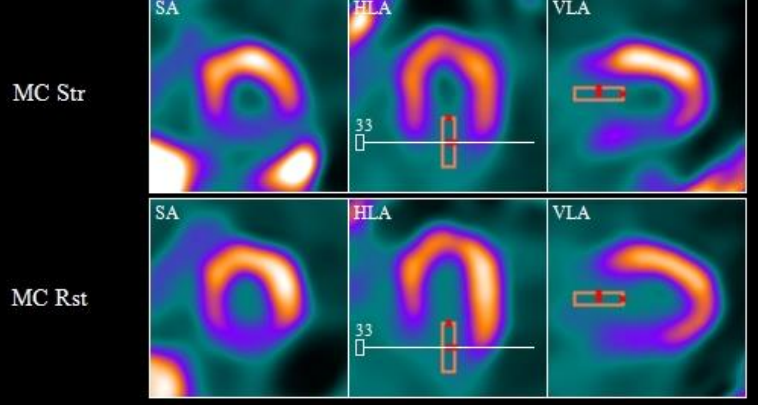

Global Results

Region	Mean MC Str	Mean MC Rst	Flow (ml/min/g) MC Str	Flow (ml/min/g) MC Rst	Reserve
LAD	85 %	82 %	1.18	0.65	1.80
LCX	70 %	87 %	0.68	0.66	1.02
RCA	53 %	58 %	0.52	0.29	1.81
TOT	73 %	77 %	0.83	0.52	1.57

Algorithm (MC Str): GE 530c Tc-99m ROI NetRet Leppo
Algorithm (MC Rst): GE 530c Tc-99m ROI NetRet Leppo

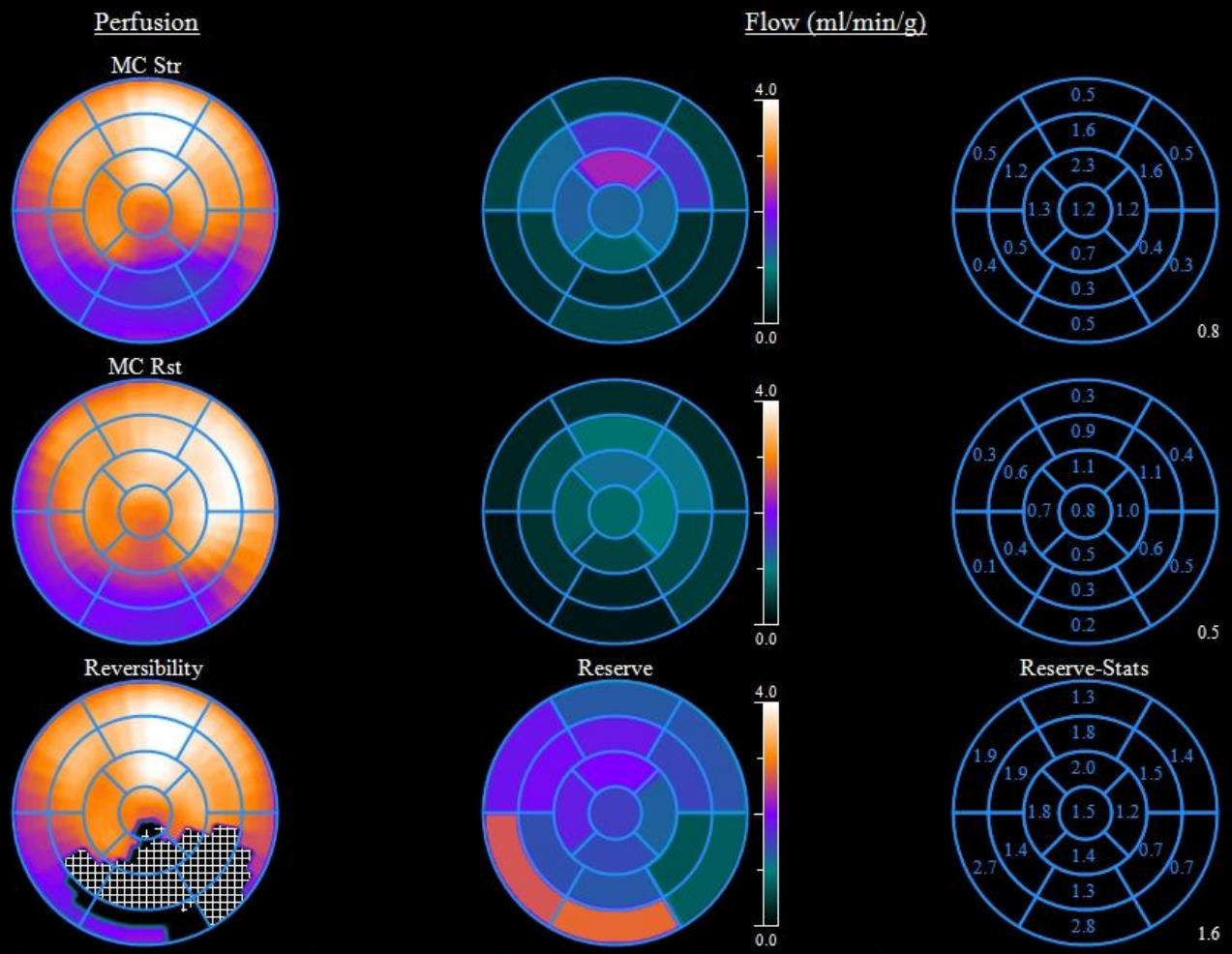

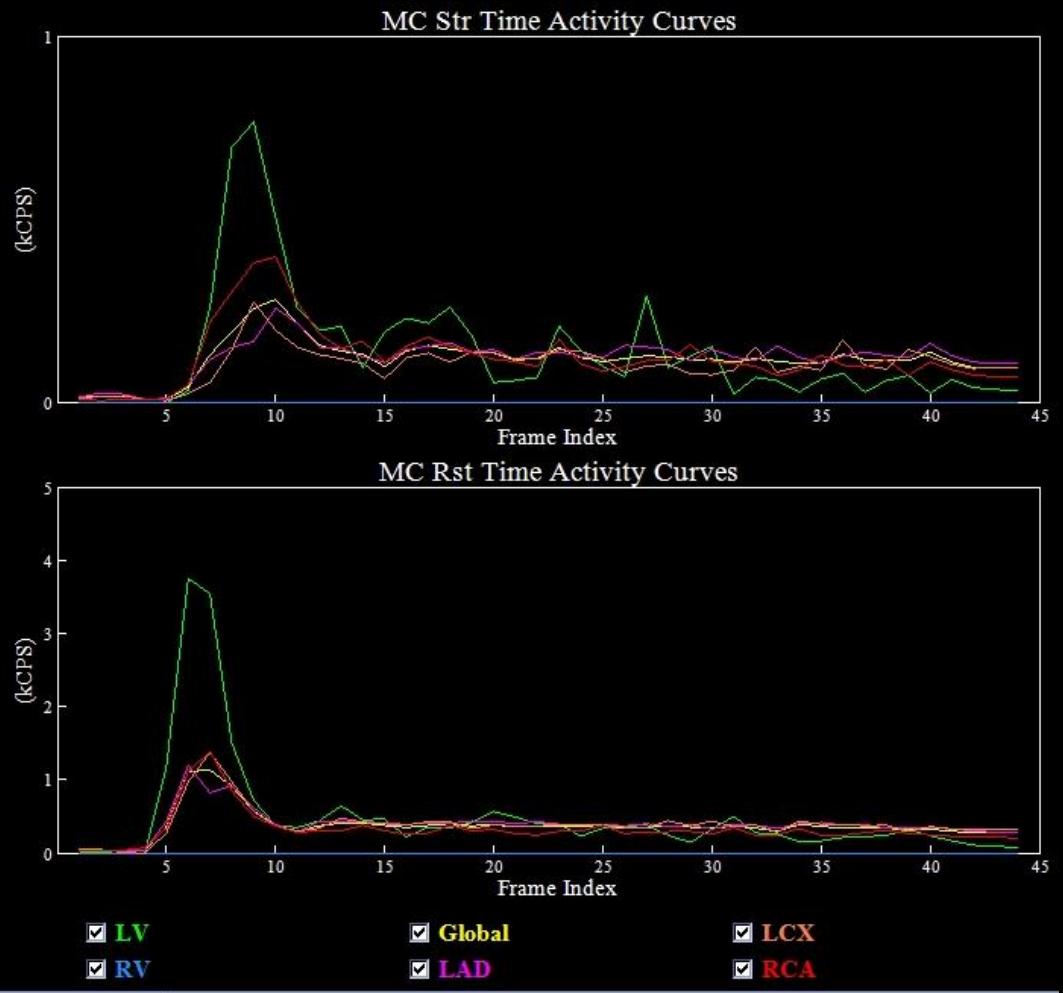

Auto | Sum | - | Ungated | Norm | Revers | - | None | -

PET – MFR

Global Results

Region	Mean Flow (ml/min/g) MC Str	MC Rst	MC Str	MC Rst	Reserve
LAD	88 %	79 %	1.69	0.78	2.18
LCX	68 %	87 %	1.31	0.91	1.45
RCA	82 %	72 %	1.66	0.70	2.36
TOT	81 %	79 %	1.57	0.79	2.00

Algorithm (MC Str): INVIA N-13 ROI 1:1
Algorithm (MC Rst): INVIA N-13 ROI 1:1

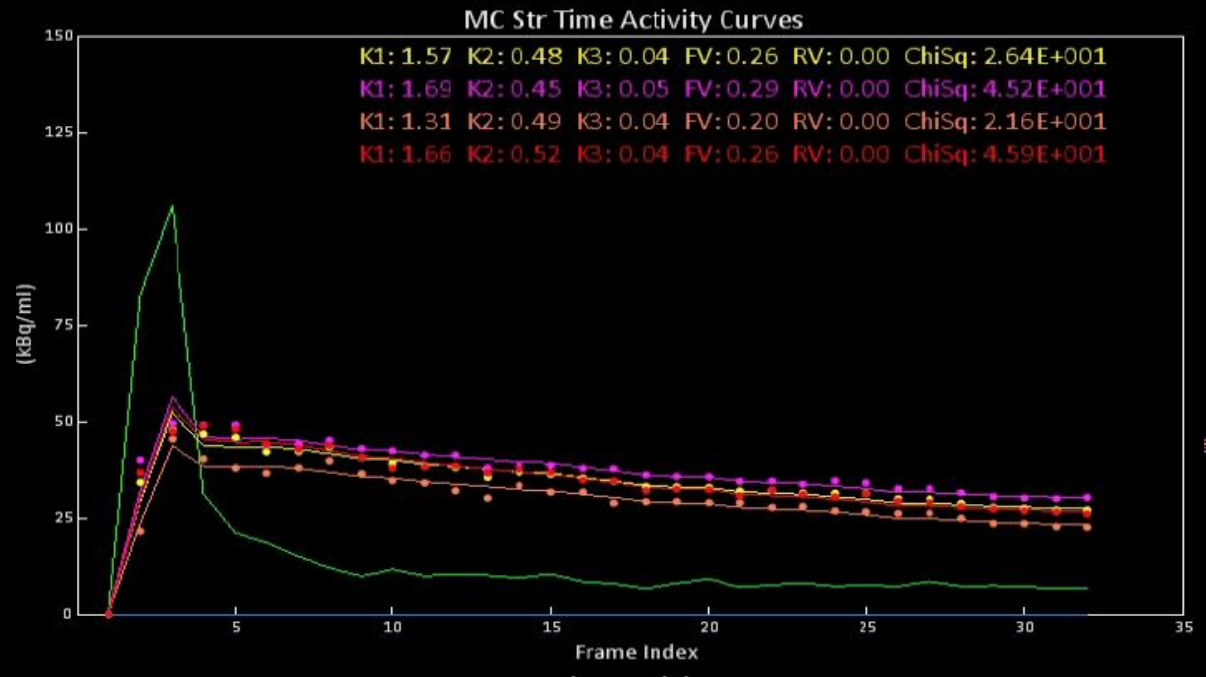

SPECT – MFR

Global Results

Mean Flow (ml/min/g) MC Str	MC Rst	MC Str	MC Rst	Reserve
85 %	82 %	1.18	0.65	1.80
70 %	87 %	0.68	0.66	1.02
53 %	58 %	0.52	0.29	1.81
73 %	77 %	0.83	0.52	1.57

lgorithm (MC Str): GE 530c Tc-99m ROI NetRet Leppo
lgorithm (MC Rst): GE 530c Tc-99m ROI NetRet Leppo

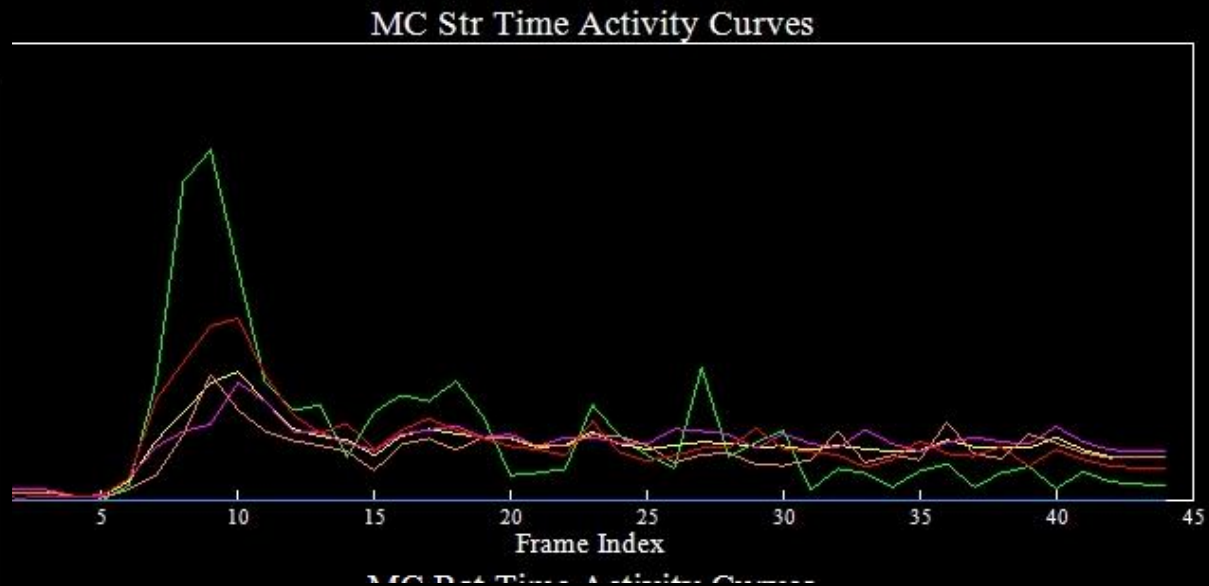

Agradecimento

Dra. Angelica Mazzoletti

Tecn Luca Camoni

Prof. Raffaele Giubbini

18F-Fluoride PET-CT and the progression of coronary calcification

Dr Mhairi Doris
Clinical Research Fellow
BHF Centre for Cardiovascular Science
University of Edinburgh, UK

ESC Congress Paris 2019
Together with World Congress of Cardiology

^{18}F-Fluoride

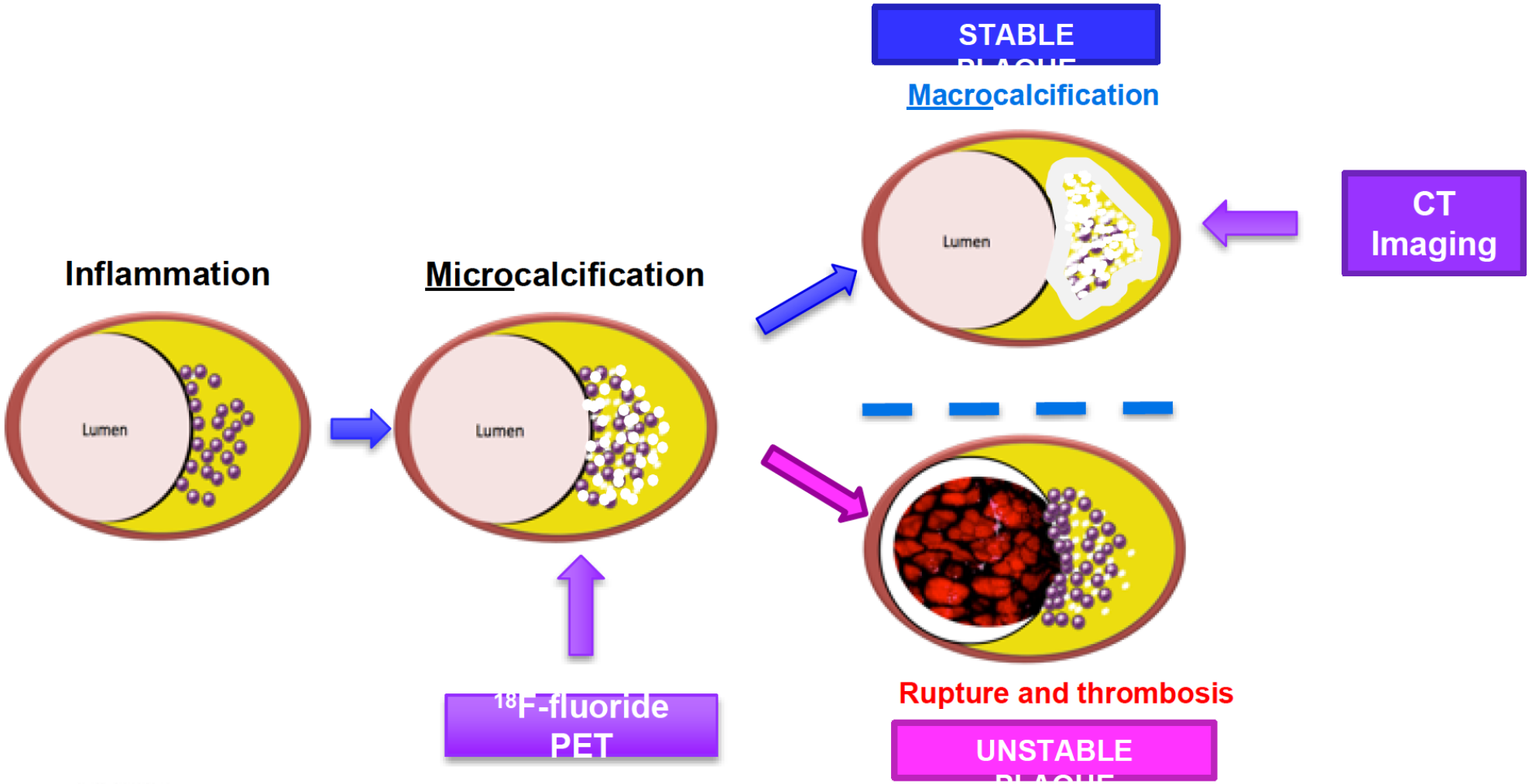

Adapted from: Adamson, et al. Cardiology clinics. 2016;34(1):179-86

^{18}F-Fluoride Identifies High Risk Coronary Plaque

Culprit plaque in acute myocardial infarction

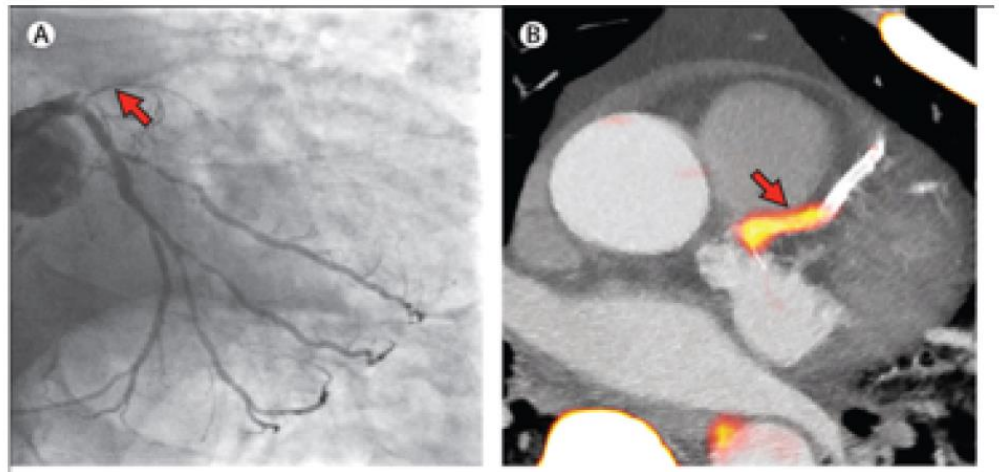

High risk plaque in clinically stable CAD

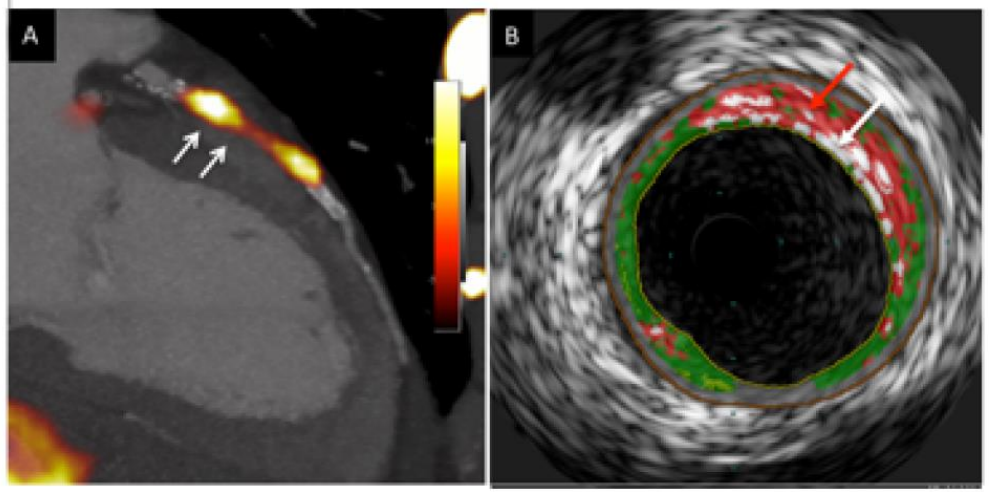

Joshi et al. Lancet 2014;383:705-713

Aims and hypotheses

- To investigate if coronary ^{18}F-fluoride activity will
  - Identify plaques more likely to demonstrate progressive calcification
  - Predict progression of total coronary calcium burden

Image Analysis

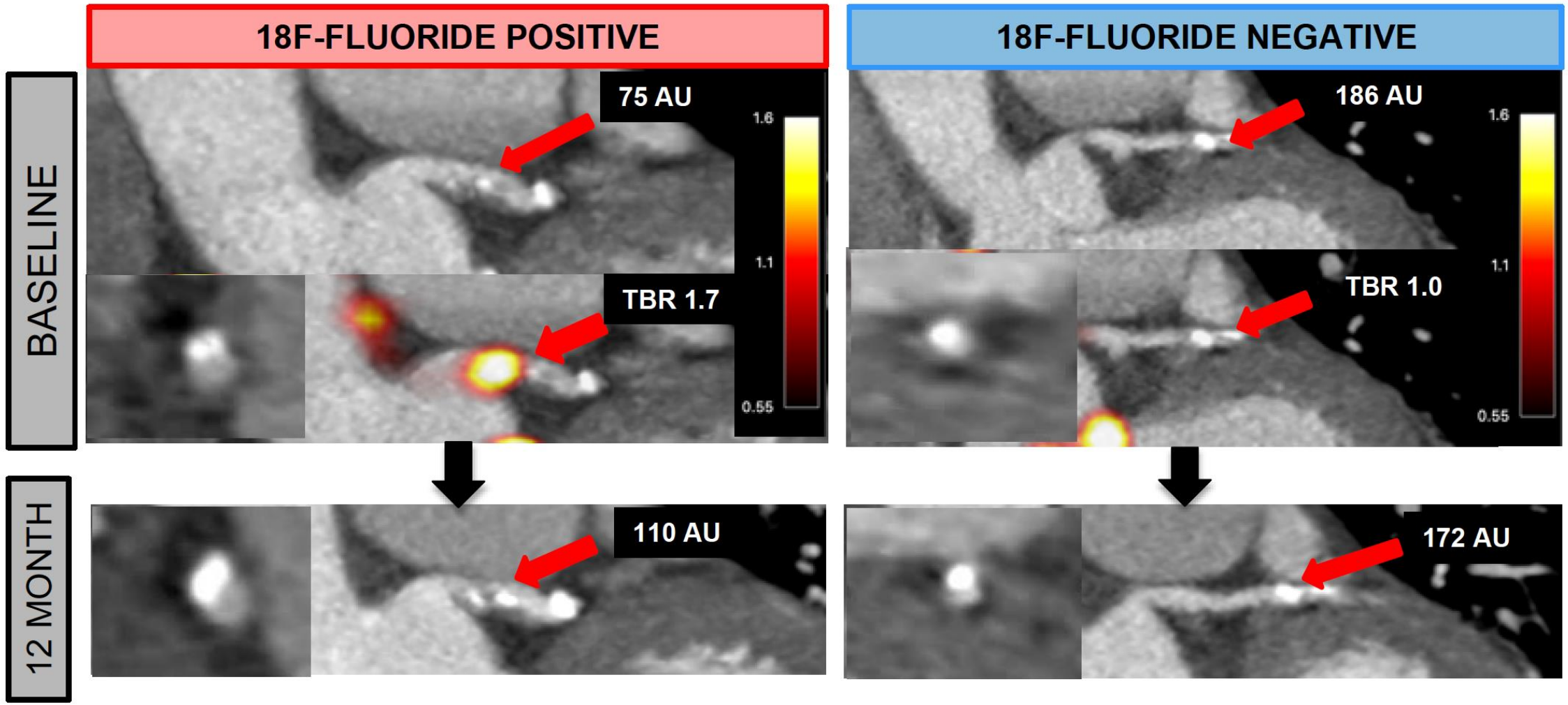

18F-Fluoride PET activity at baseline

PET-positive participants had a higher total calcium score, volume and mass at baseline

	PET POSITIVE (n=116)	PET NEGATIVE (N=67)	P value
Total Agatston Score (AU)	524 [242-1091]	136 [55-361]	p<0.001
Calcium Volume (mm^3)	491 [247-984]	131 [64-343]	p<0.001
Calcium Mass (mg)	99 [46-212]	24 [11-69]	p<0.001

Proportion of PET-positive participants increased with increasing baseline calcium score

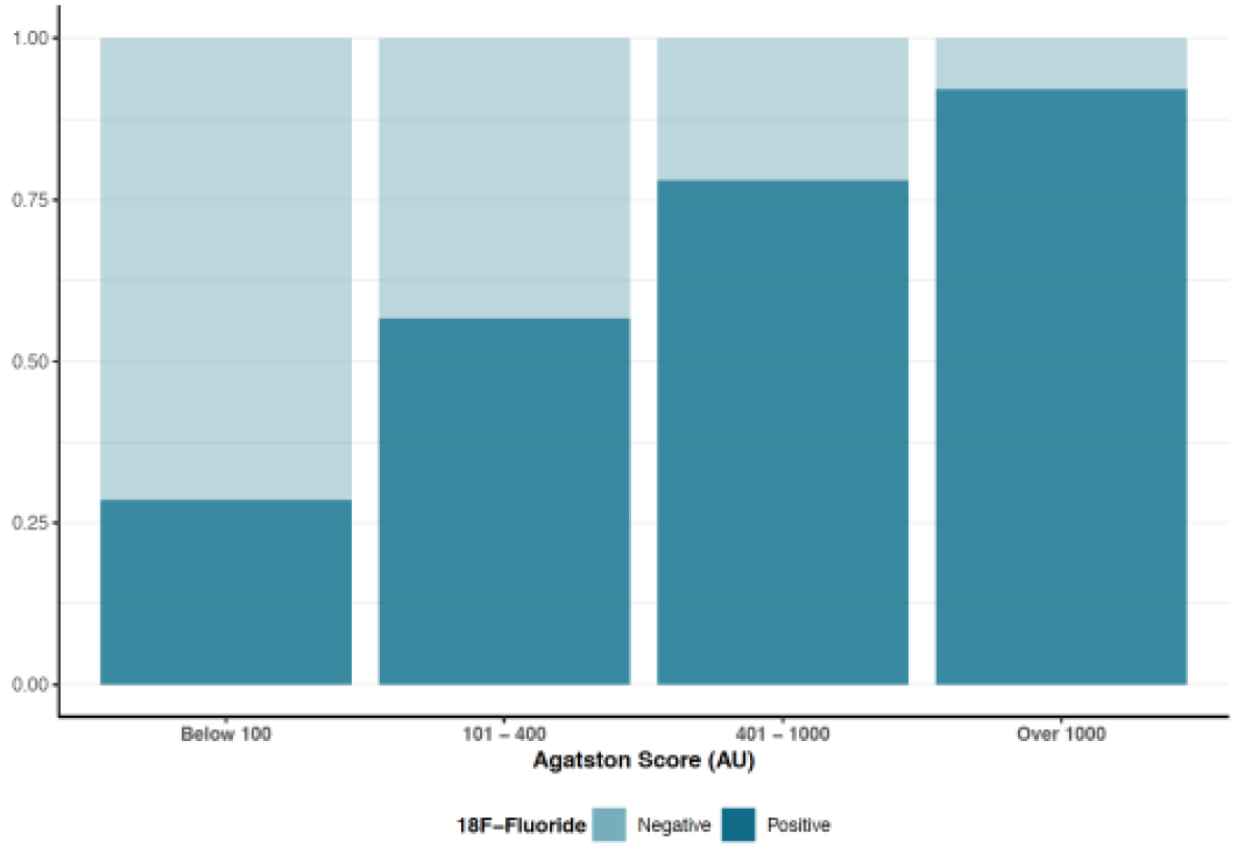

Calcium score at baseline vs follow-up

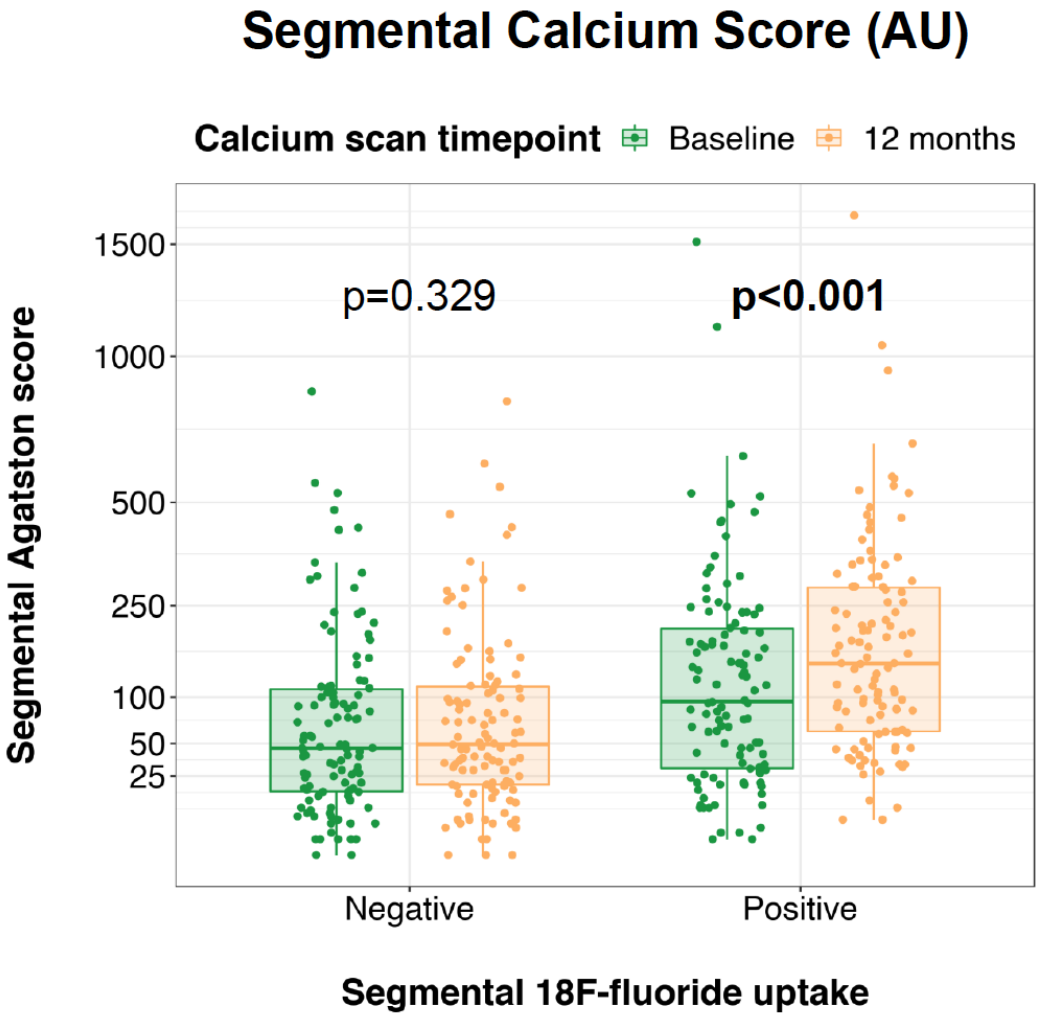

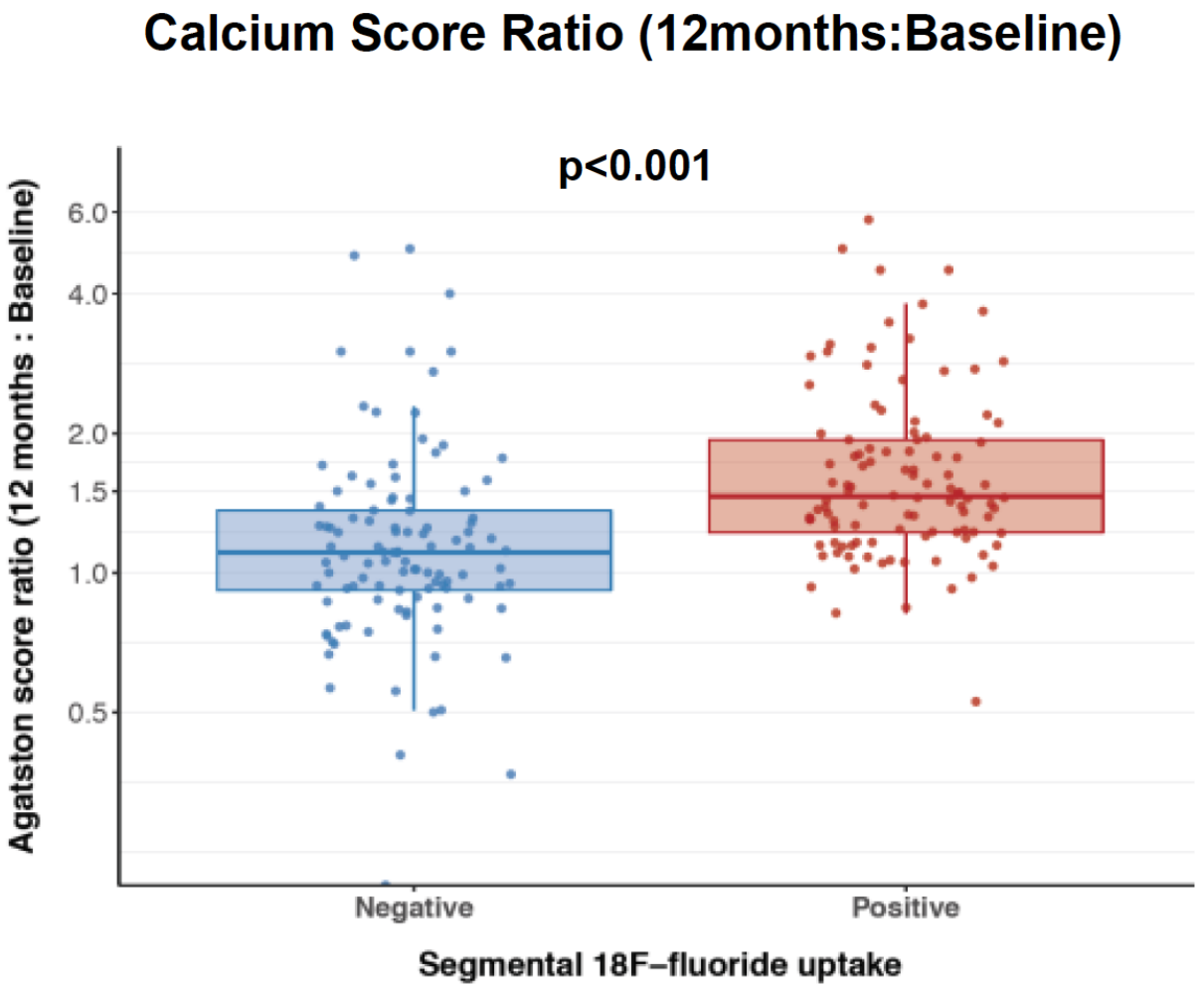

Relationship between baseline PET activity and calcification progression

		Change in total calcium burden (AU/year)	Change in total calcium volume (mm^3/year)	Change in total calcium mass (mg/year)
TBRmax	Correlation Coefficient	**0.37**	**0.38**	**0.46**
	P-value	**<0.001**	**<0.001**	**<0.001**
	N	183	183	183

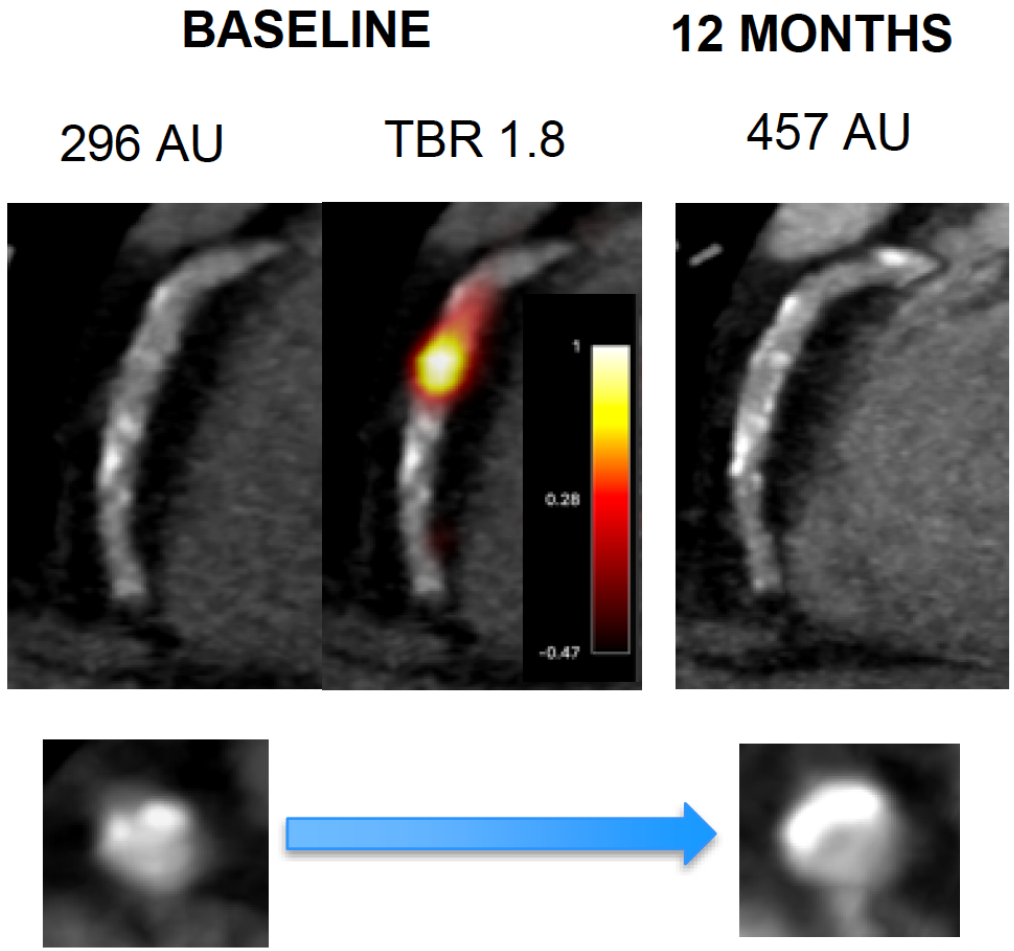

Conclusions

In patients with clinically stable, multivessel coronary artery disease, ^{18}F-fluoride PET-CT uptake:

- Is associated with more advanced coronary calcification at baseline
- Identifies plaques with more rapid progression of coronary calcification at one year
- Provides new insights into disease activity and progression of coronary atherosclerosis.

Table 1. Characteristics of an ideal PET perfusion tracer

Available as unit dose from a regional cyclotron (^{18}F-labeled)
High-extraction fraction
Ideal PET resolution (low positron range)
Possibility of rest-exercise imaging
Possibility of absolute quantification of myocardial blood flow

PET, Positron emission tomography.

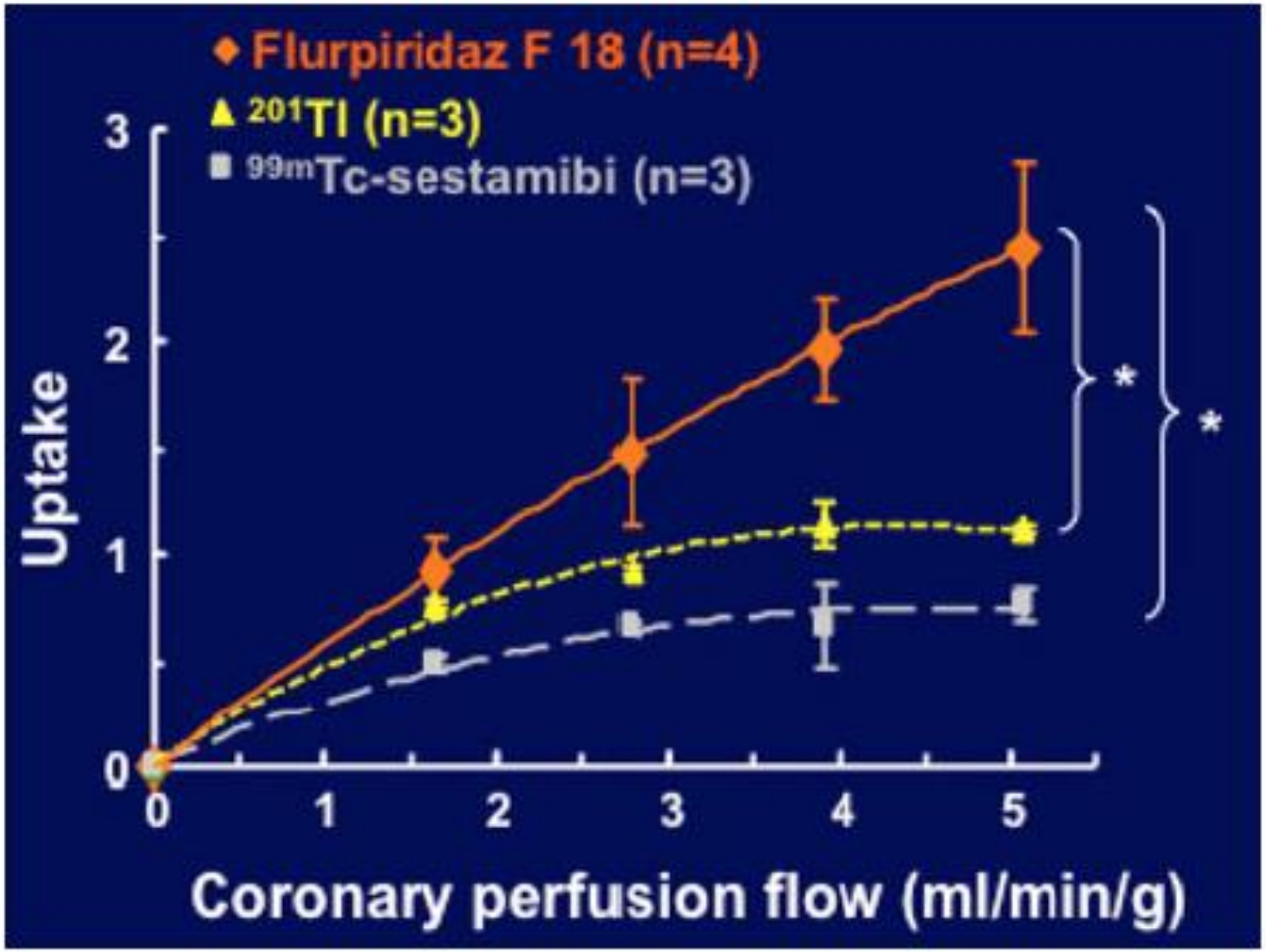

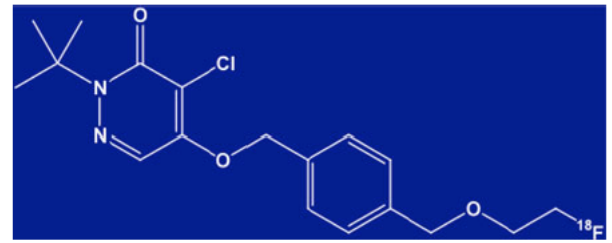

Figure 1. Chemical structure of flurpiridaz F 18. CAS name for flurpiridaz F 18 is: 2-*tert*-butyl-4-chloro-5-[4-(2-fluoro-ethoxymethyl)-benzyloxy]-2H-pyridazin-3-one. Other common name is BMS-747158-02.

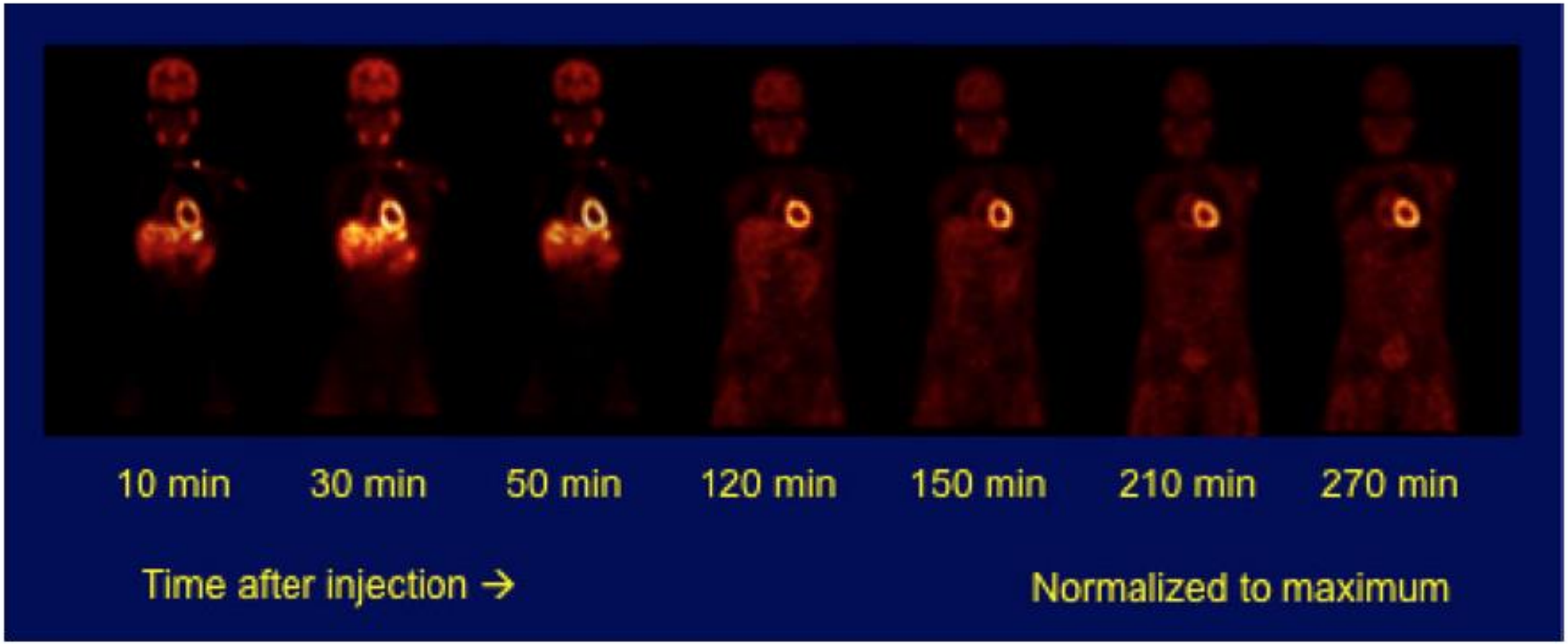

Figure 4. Sequential whole-body images acquired at specified times following injection of flurpiridaz F 18. Used with permission of the Journal of Nuclear Medicine.

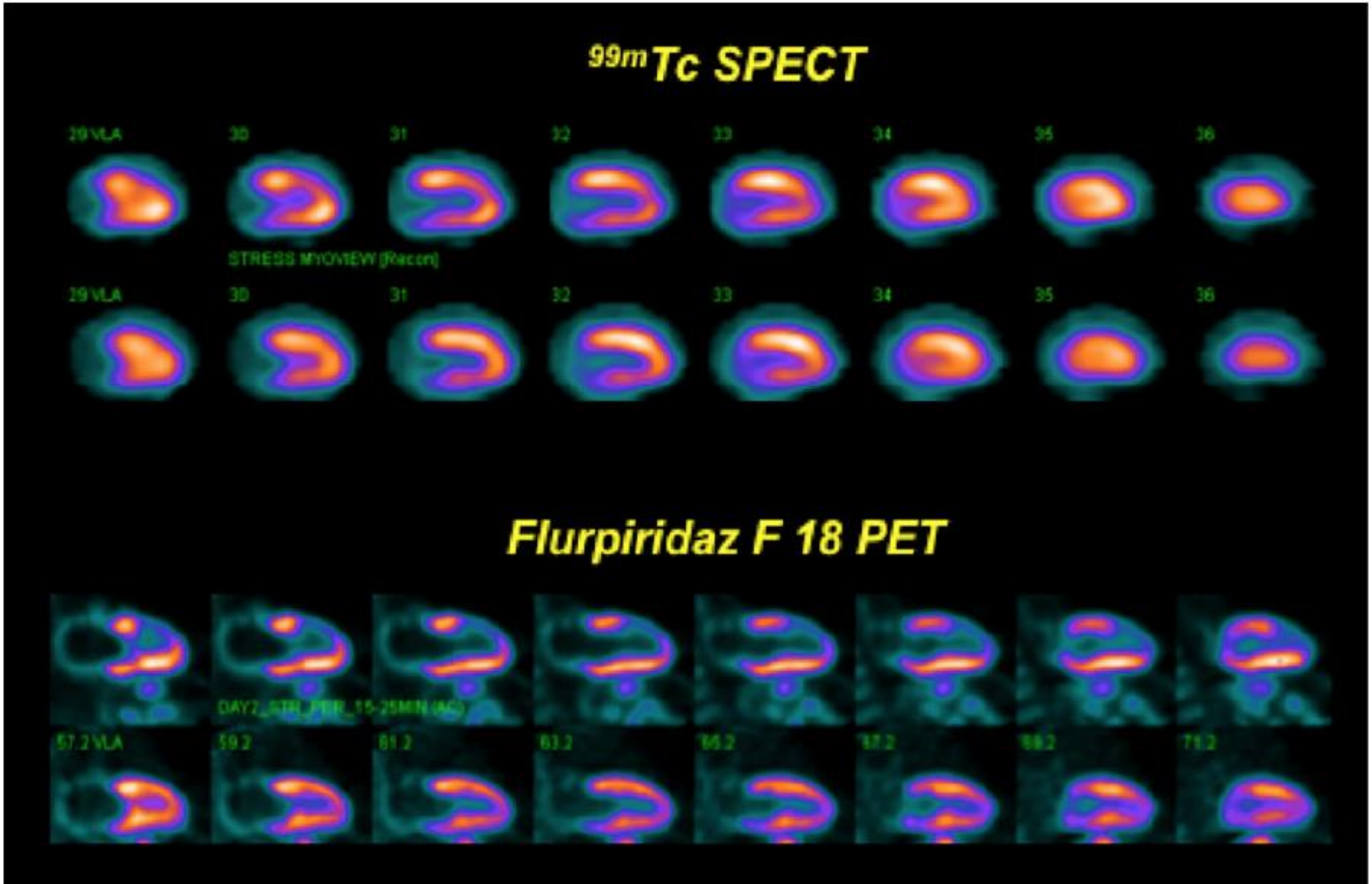
99m Tc SPECT
29 VLA
30
31
32
33
34
35
36
STRESS MYOVIEW (Racon)
29 VLA
30
31
32
33
34
35
36
Flurpiridaz F 18 PET
57.2 VLA
59.2
61.2
63.2
65.2
67.2
69.2
71.2

Caso Clínico 2

- O.R.F 75a, masculino, branco
- Admitido neste hospital devido à insuficiência cardíaca congestiva descompensada por provável síndrome infecciosa em CF IV (NYHA).
- Nega HAS, DM, dislipidemia.

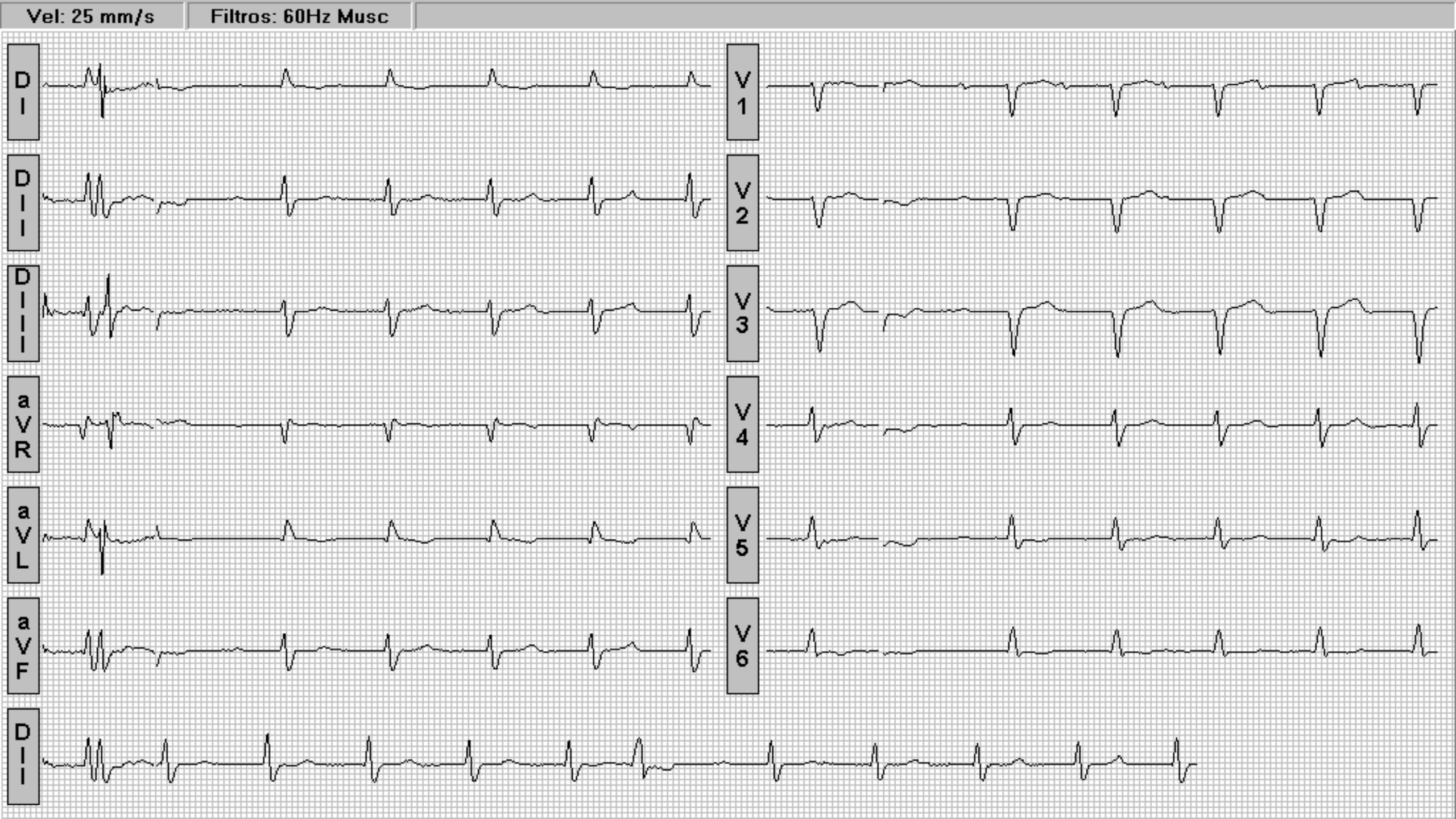
Vel: 25 mm/s
Filtros: 60Hz Musc
DI
DII
DIII
aVR
aVL
aVF
DII
V1
V2
V3
V4
V5
V6

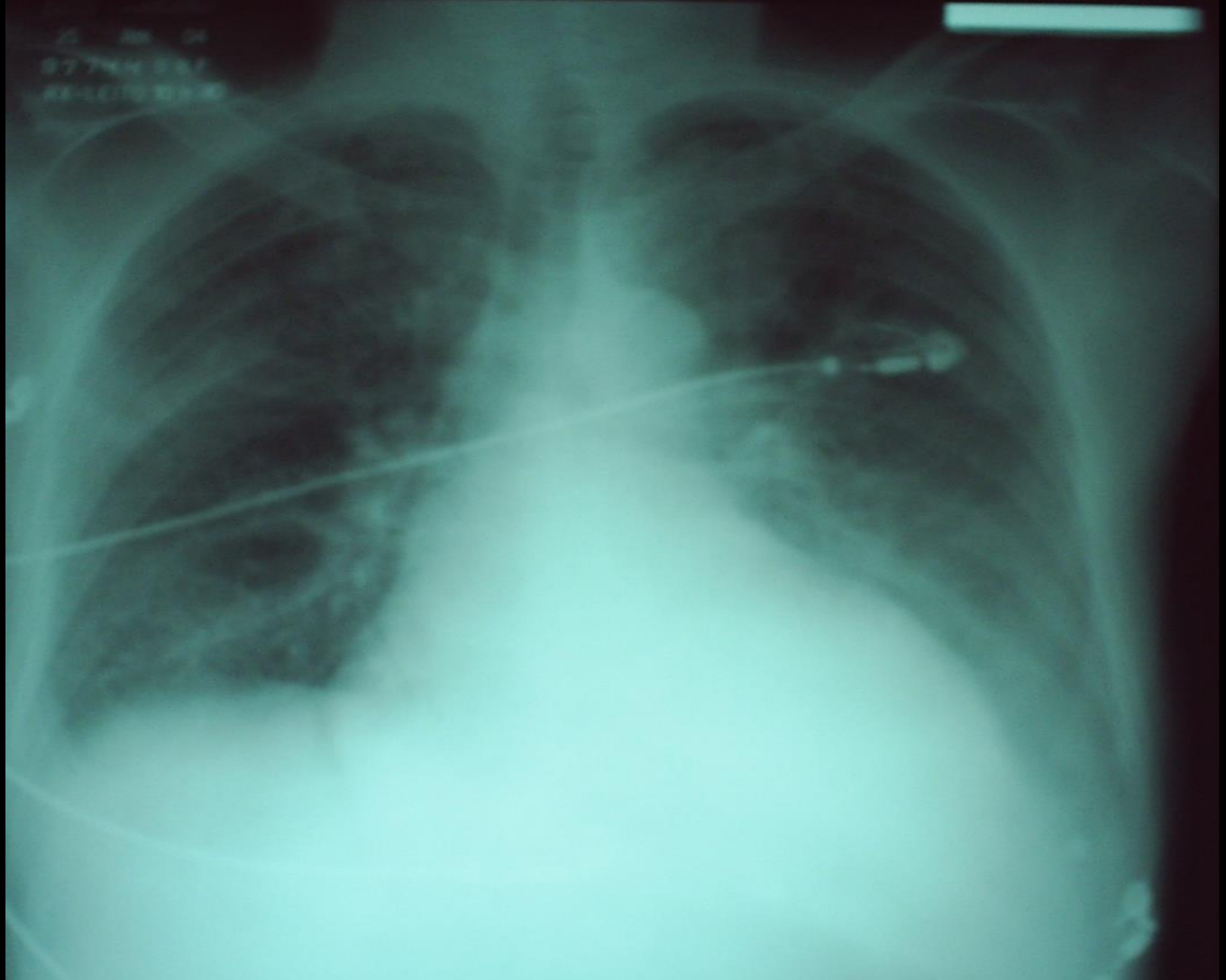

Ecocardiograma

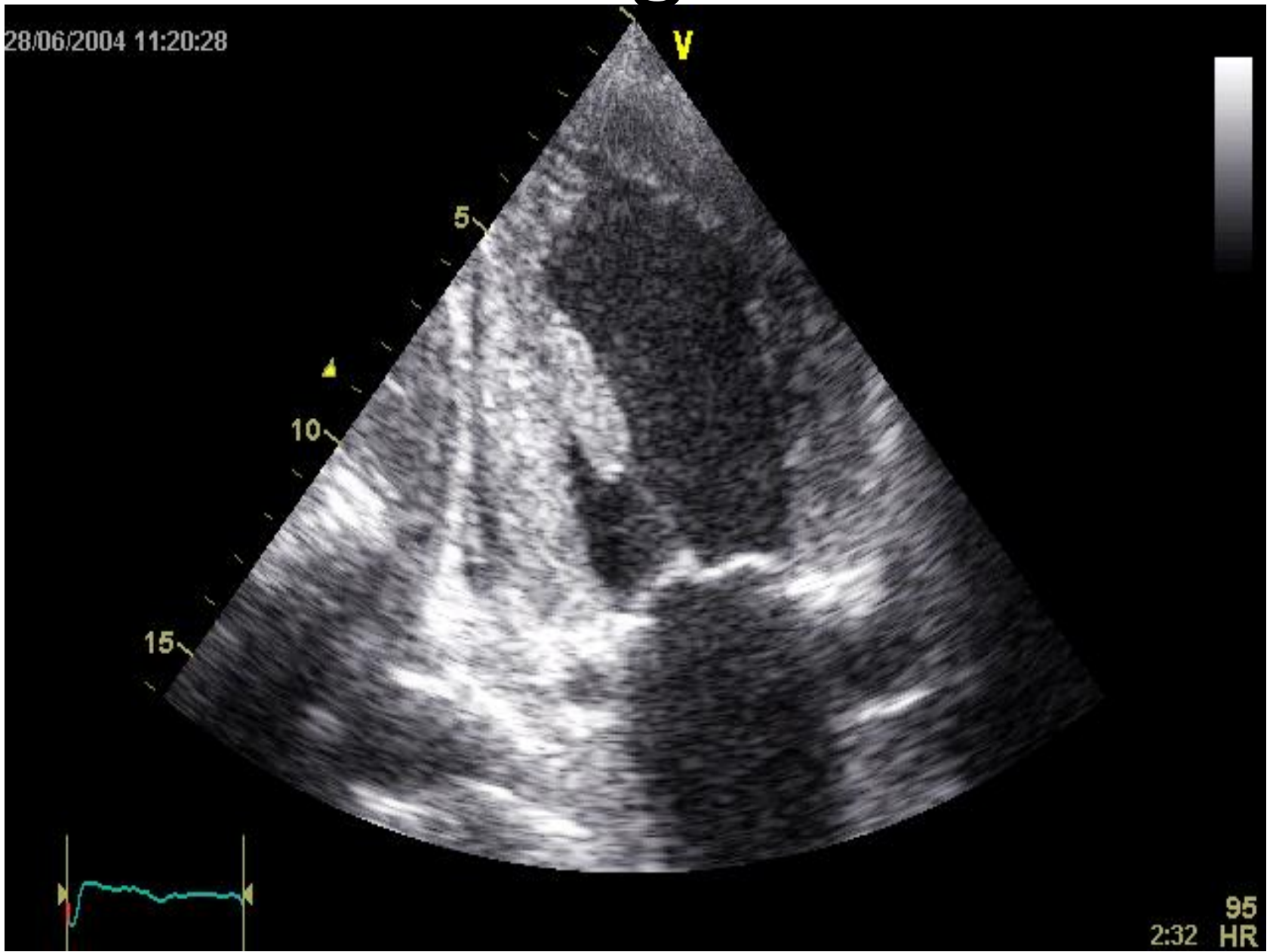

Ecocardiograma

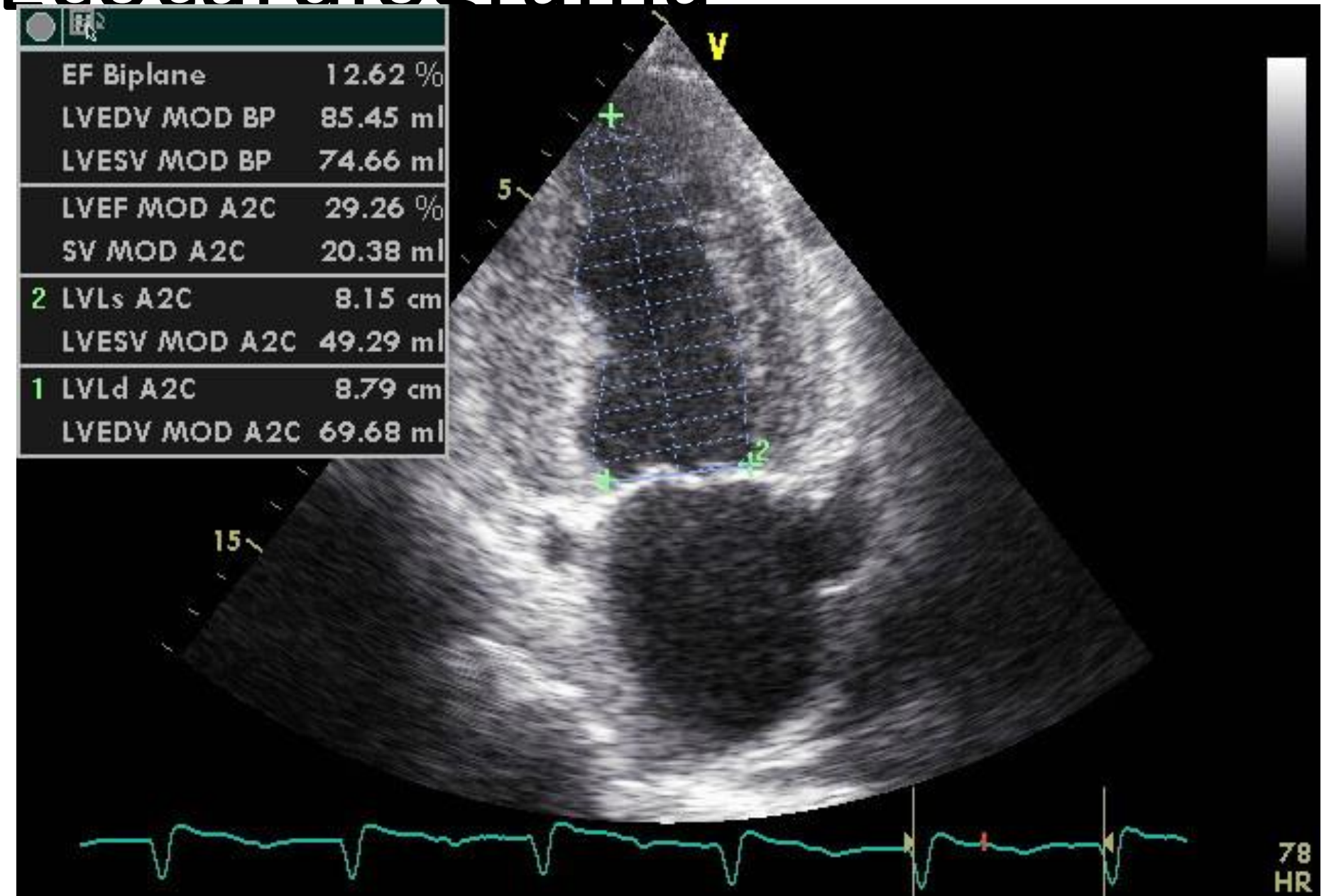

Ventriculografia Radionuclídica

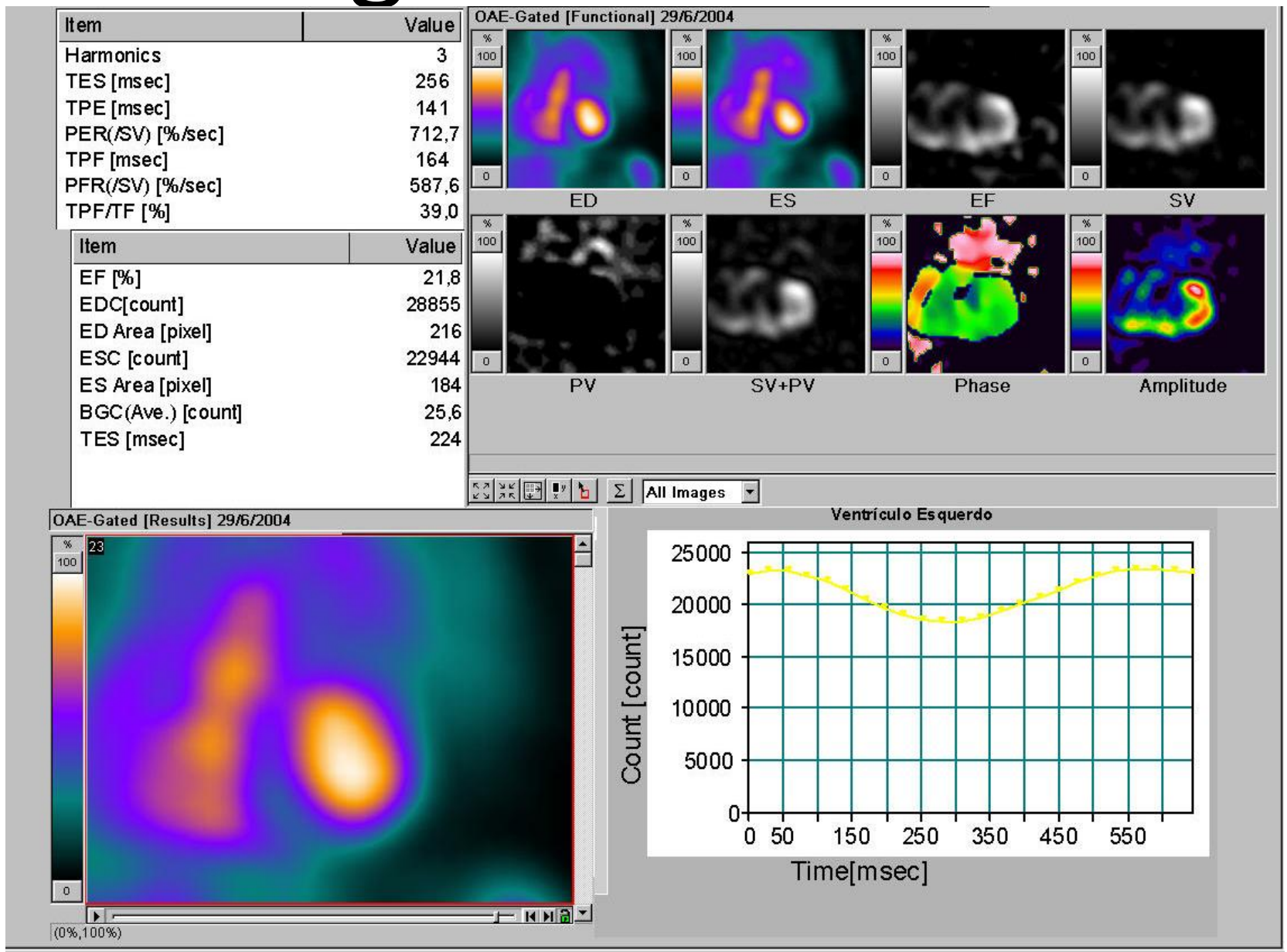

Cintilografia com Pirofosfato

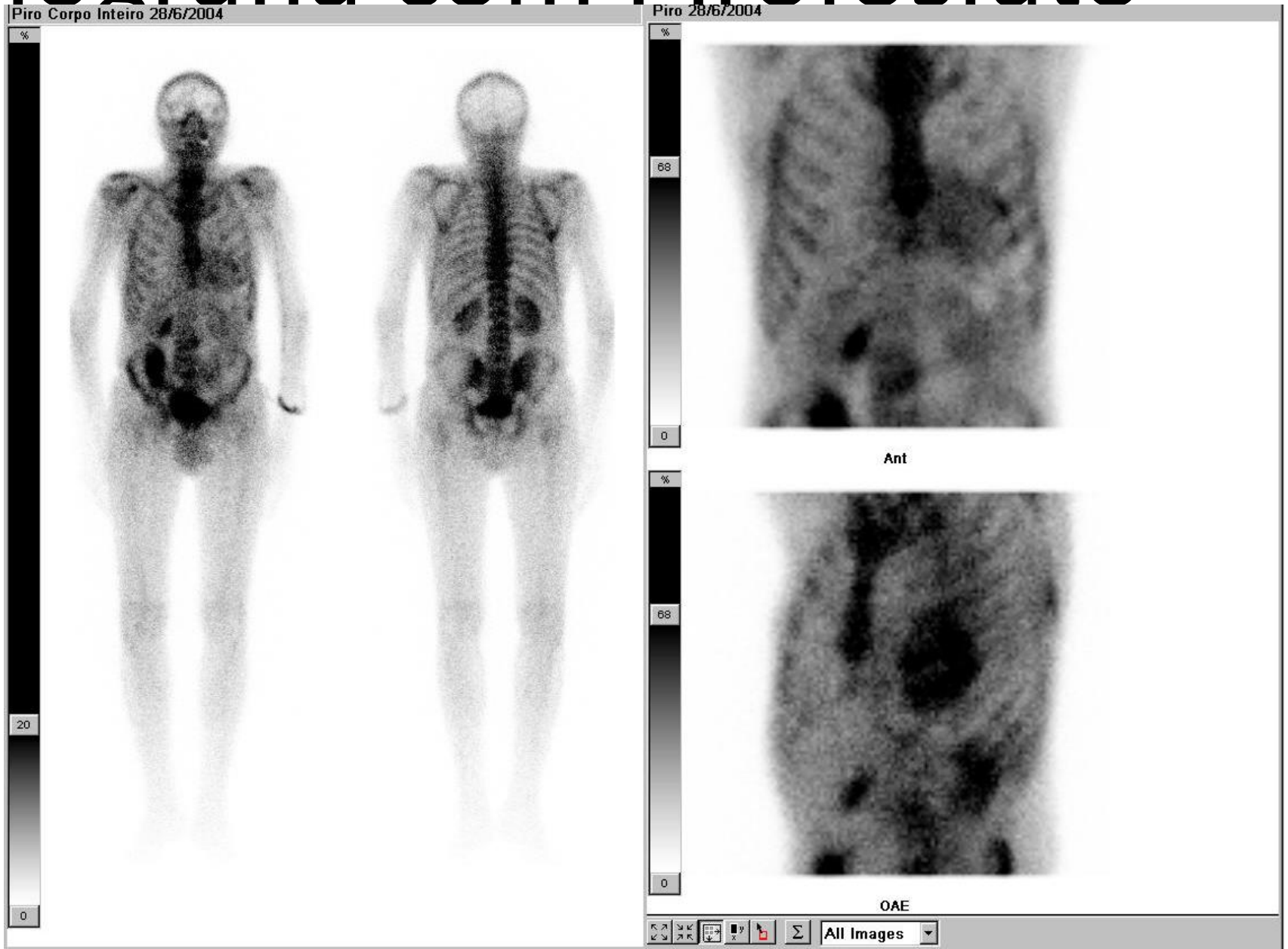

Cintilografia com Pirofosfato - SPECT

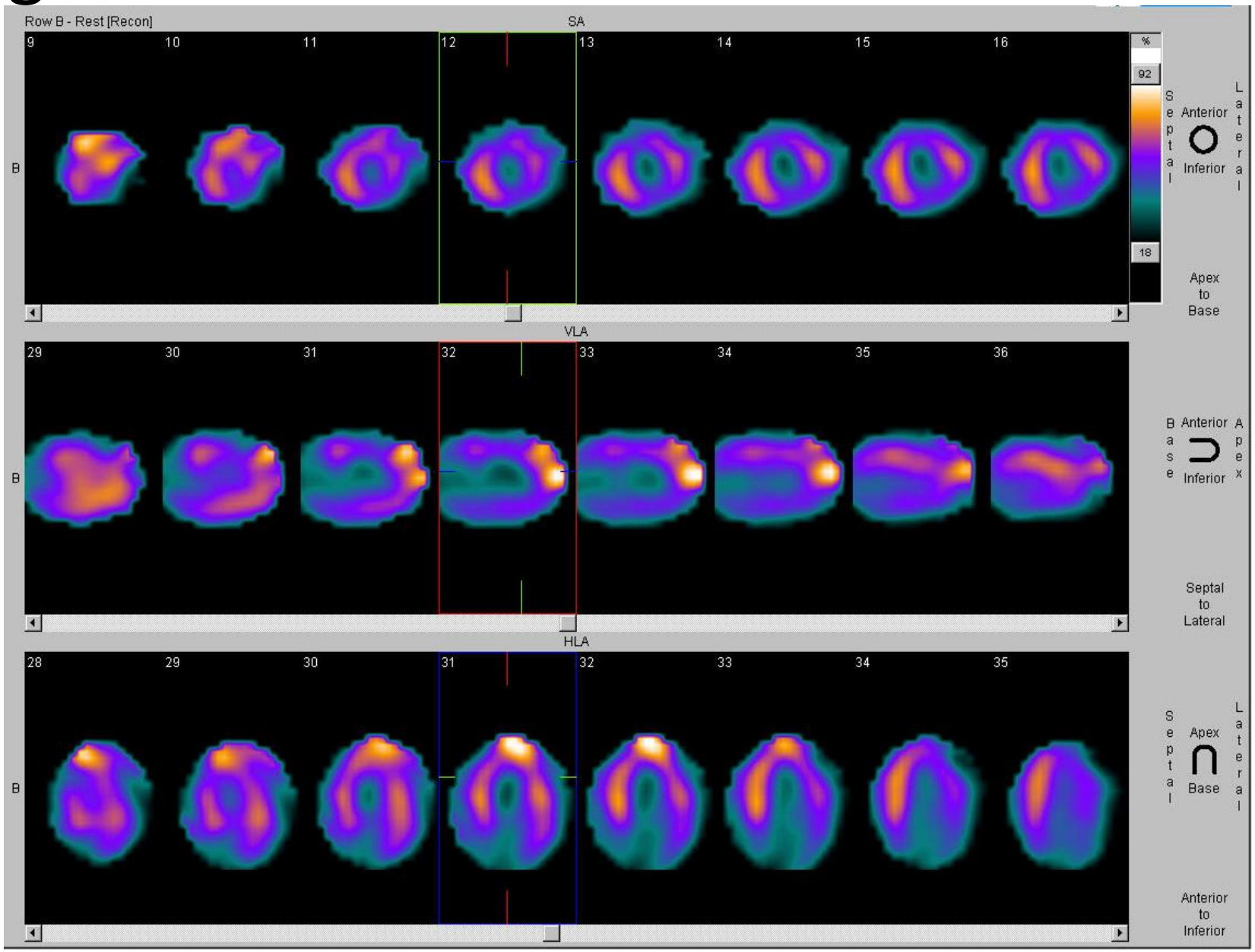

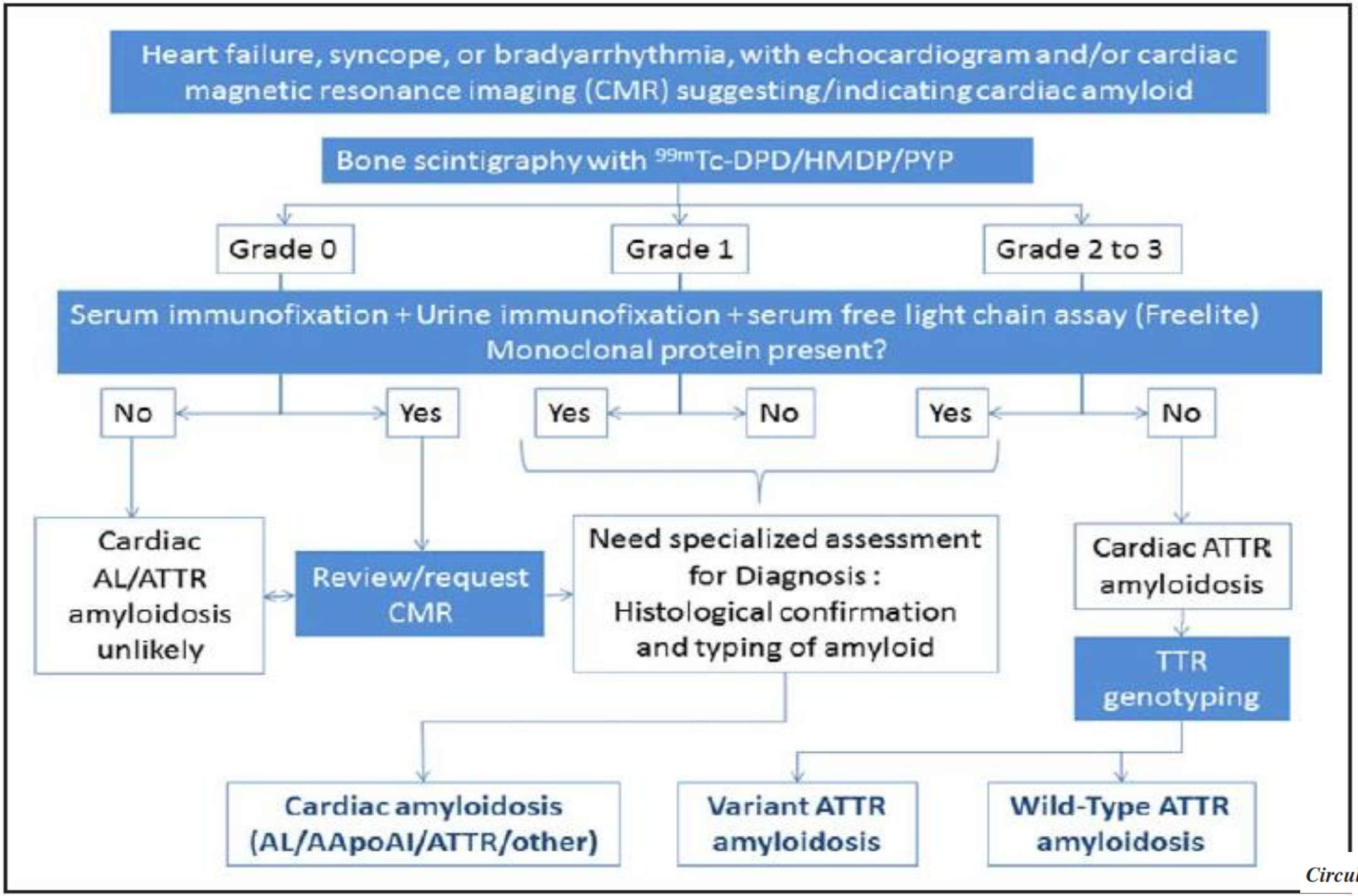
Heart failure, syncope, or bradyarrhythmia, with echocardiogram and/or cardiac magnetic resonance imaging (CMR) suggesting/indicating cardiac amyloid
Bone scintigraphy with 99mTc-DPD/HMDP/PYP
Grade 0
Grade 1
Grade 2 to 3
Serum immunofixation + Urine immunofixation + serum free light chain assay (Freelite) Monoclonal protein present?
No
Yes
Yes
No
Yes
No
Cardiac AL/ATTR amyloidosis unlikely
Review/request CMR
Need specialized assessment for Diagnosis : Histological confirmation and typing of amyloid
Cardiac ATTR amyloidosis
TTR genotyping
Cardiac amyloidosis (AL/AApoAI/ATTR/other)
Variant ATTR amyloidosis
Wild-Type ATTR amyloidosis

Nonbiopsy Diagnosis of Cardiac Transthyretin Amyloidosis

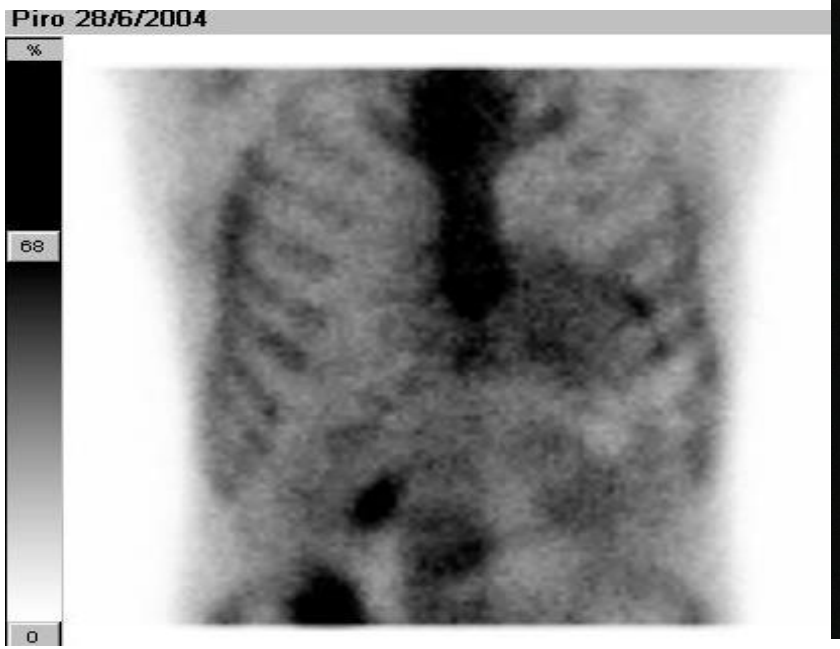

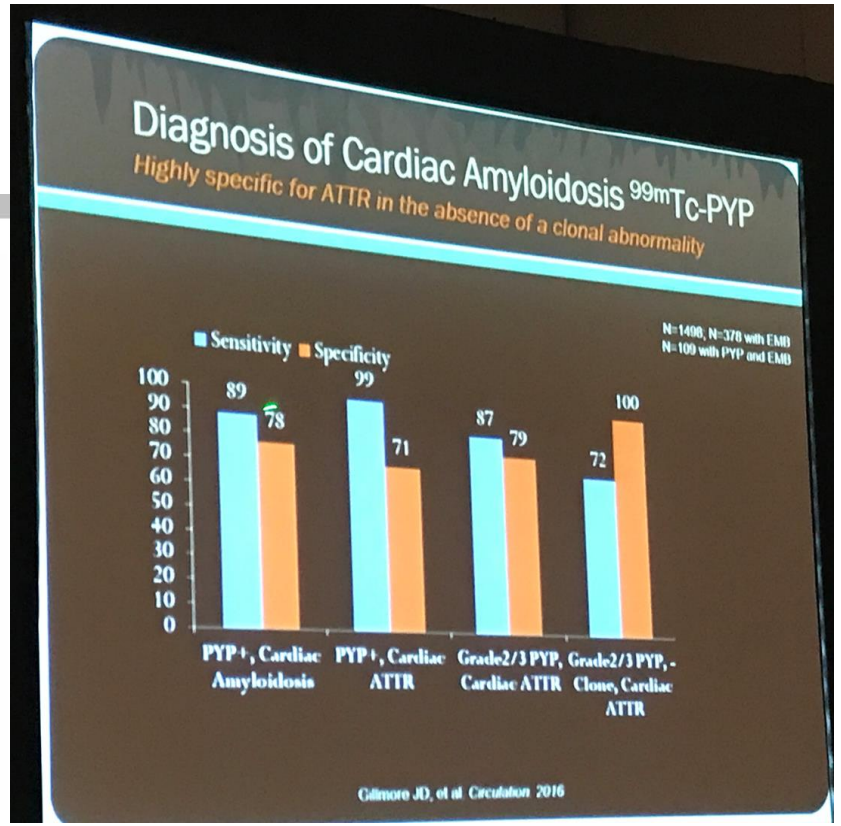

Conclusions—Bone scintigraphy enables the diagnosis of cardiac ATTR amyloidosis to be made reliably without the need for histology in patients who do not have a monoclonal gammopathy. We propose noninvasive diagnostic criteria for cardiac ATTR amyloidosis that are applicable to the majority of patients with this disease. (***Circulation*. 2016;133:2404-2412. DOI: 10.1161/CIRCULATIONAHA.116.021612.)**

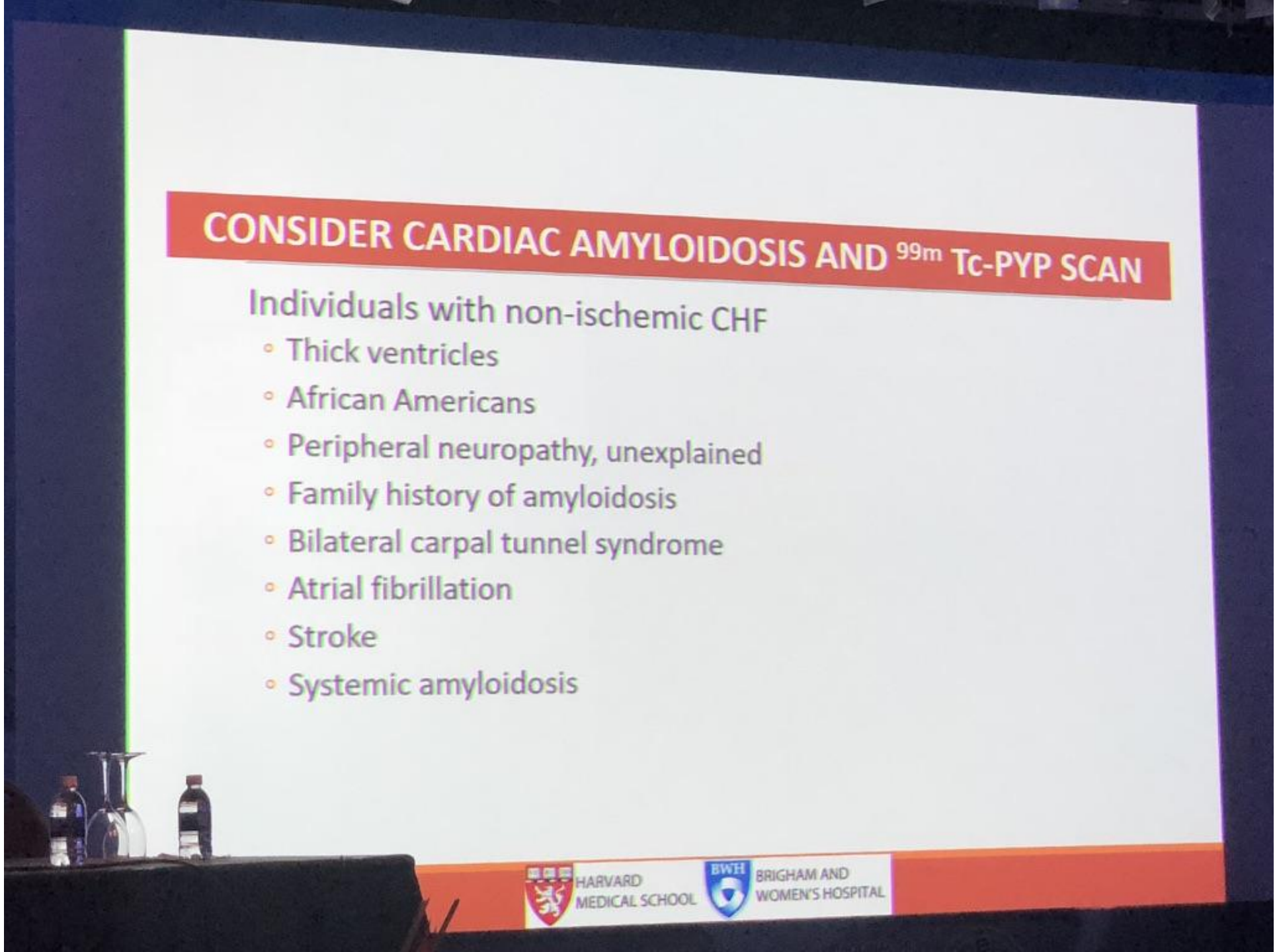
CONSIDER CARDIAC AMYLOIDOSIS AND 99m Tc-PYP SCAN
Individuals with non-ischemic CHF
Thick ventricles
African Americans
Peripheral neuropathy, unexplained
Family history of amyloidosis
Bilateral carpal tunnel syndrome
Atrial fibrillation
Stroke
Systemic amyloidosis
HARVARD MEDICAL SCHOOL
BWH
BRIGHAM AND WOMEN'S HOSPITAL

Table 1. Red Flags and Caveats in Cardiac Amyloidosis

A high index of suspicion is mandatory for the recognition of CA (ie, if you don't think of it, you won't diagnose it).
Cardiac amyloid should be suspected in any patient with heart failure, unexplained increased LV wall thickness, and a nondilated LV.
In a patient with a suspicion for HCM, look for the infiltrative features that suggest amyloid such as pericardial effusion, AV block, interatrial septal and valvular thickening, and apical sparring.
A distinctive sign of CA is the abnormal ratio between LV thickness and QRS voltages rather than low QRS voltages alone. The absence of low QRS voltages does not rule out a CA and up to 20% of subjects with CA can have electrocardiographic evidence of LV hypertrophy.
In an elderly man with unexplained symmetrical LV hypertrophy, especially in the absence of hypertension, always consider the possibility of ATTRwt-CA.
CA in an elderly patient with a monoclonal gammopathy is not necessarily attributable to AL: consider the possibility of ATTRwt and MGUS.
Longitudinal LV function can be severely depressed despite a normal LVEF, and the myocardial contraction fraction is often low, suggesting reduced global myocardial shortening.
Myocardial deformation is reduced in cardiac amyloidosis, but the apex is generally spared.
On cardiac MRI, both T1 signal abnormalities and marked extracellular volume expansion in patients with LV hypertrophy are strongly suggestive of CA. LGE distribution is heterogeneous, and subendocardial enhancement is not the only pattern.
A history of bilateral carpal tunnel syndrome in a man with HCM-like phenotype on echocardiography is highly suggestive of ATTRwt-CA.

Circulation. 2017;135:1357–1377. DOI: 10.1161/CIRCULATIONAHA.116.024438

Table 2. Semi-quantitative Visual Grading of Myocardial ^{99m}Tc-PYP Uptake by Comparison to Bone(rib) Uptake

Grade	Myocardial ^{99m}Tc-PYP Uptake
Grade 0	no uptake and normal bone uptake
Grade 1	uptake less than rib uptake
Grade 2	uptake equal to rib uptake
Grade 3	uptake greater than rib uptake with mild/ absent rib uptake

Figure 2. Grading ^{99m}Tc-PYP Uptake on Planar and SPECT Images

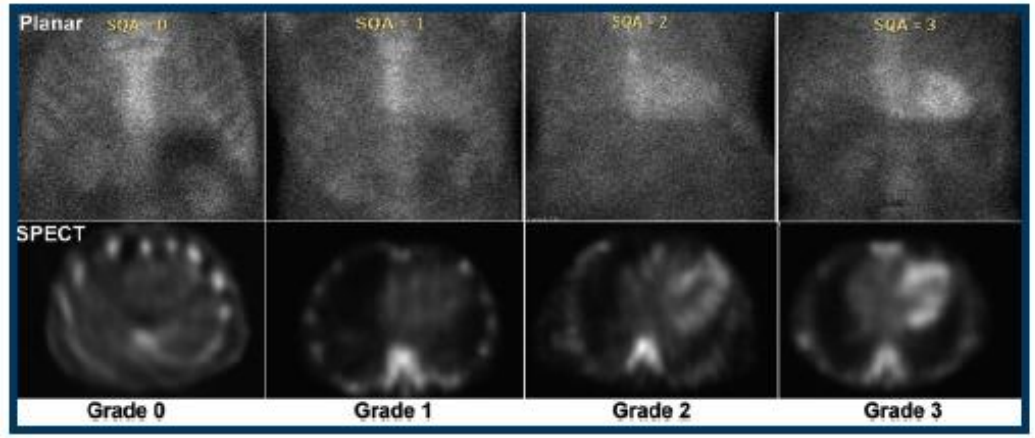

Figure 1. Quantitation of Cardiac ^{99m}Tc-PYP Uptake Using Heart to Contralateral Lung (H/CL) Ratio

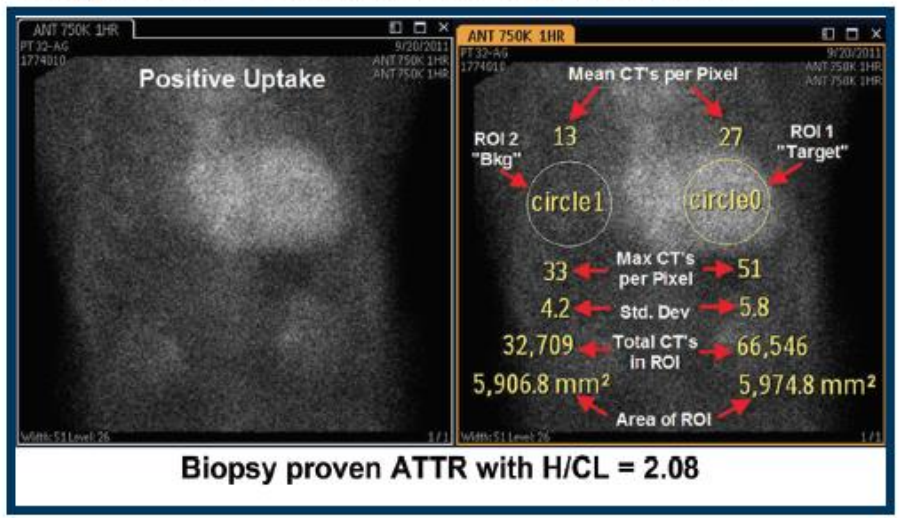

State-of-the-art radionuclide imaging in cardiac transthyretin amyloidosis

Vasvi Singh, MD,[a] Rodney Falk, MD,[b] Marcelo F. Di Carli, MD,[a] Marie Kijewski, PhD,[a] Claudio Rapezzi, MD,[c] and Sharmila Dorbala, MD[a,b,d]

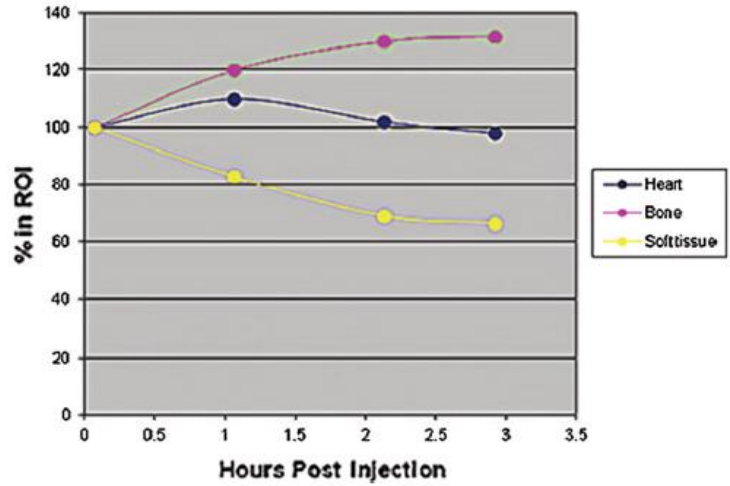

Table 1. Accuracy of Tc-pyrophosphate scan for detecting ATTR Cardiac amyloidosis based on semiquantitative and quantitative assessments

	Sensitivity (%)	Specificity (%)	AUC (95% CI)
Semiquantitative visual Score			
1-hour delay positive scan ≥ 2	95	79	0.938 (0.873-0.984)
3-hour delay positive scan ≥ 2	58	100	0.980 (0.932-1.000)
Combined analysis	88	88	0.945 (0.901-0.977)
Quantitative H/CL ratio			
1-hour delay positive scan ≥ 1.5	92	97	0.971 (0.949-0.992)
3-hour delay positive scan ≥ 1.3	88	86	0.935 (0.848-0.988)
Combined analysis	91	92	0.960 (0.930-0.981)

Tc-PYP, Tc pyrophosphate; *ATTR*, transthyretin amyloidosis; *AUC*, area under the curve; *CI*, confidence interval; *H/CL*, ratio = heart-to-contralateral lung ratio. Adapted from Castano et al.[25]

Journal of Nuclear Cardiology®
Volume 26, Number 1;158–73

Diagnosis of TTR cardiac amyloidosis

^{99m}Tc-PYP & EMB

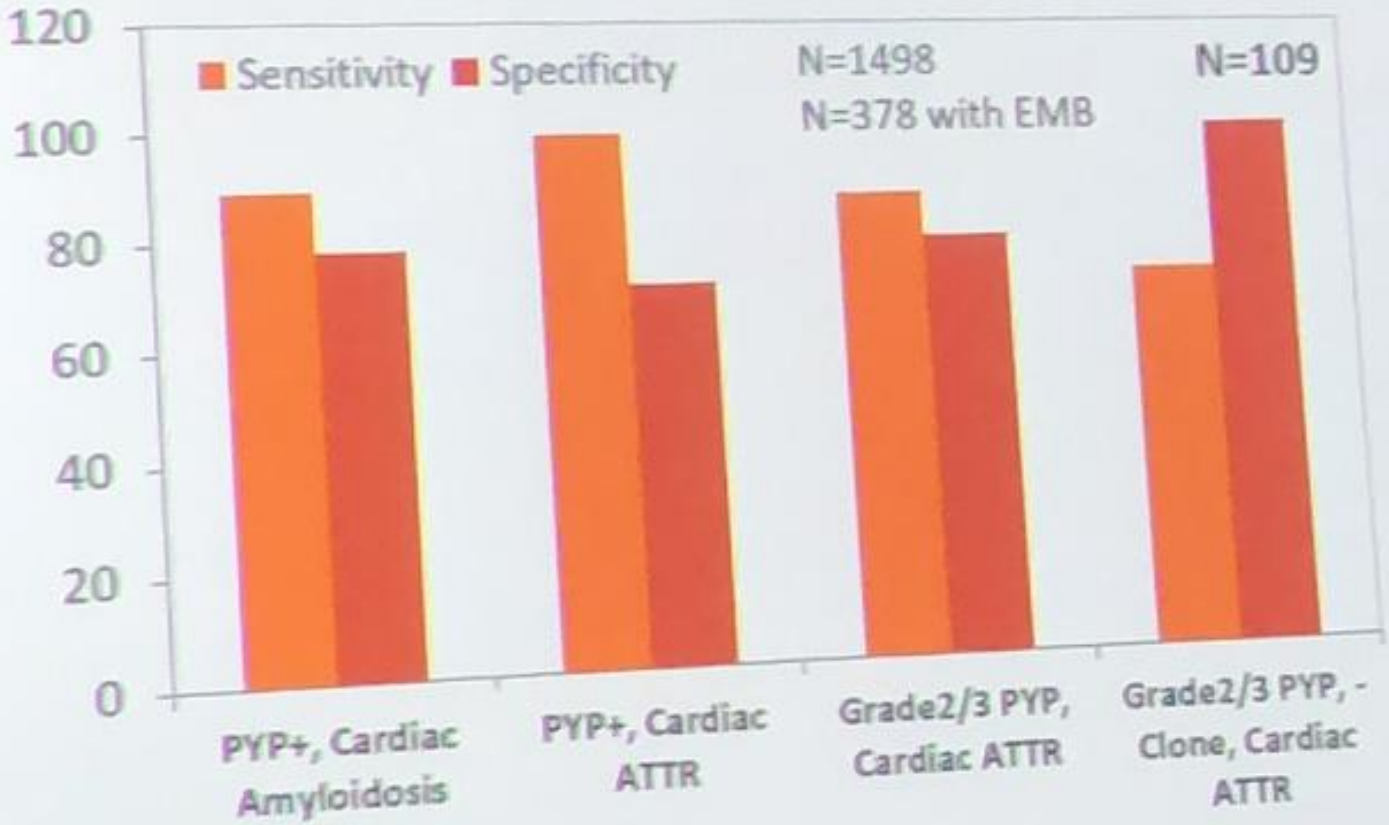

, Maurer MS, Falk RH, et al. *Circulation*. 2016

HARVARD MEDICAL SCHOOL

BWH BRIGHAM AND WOMEN'S HOSPITAL

Contents lists available at ScienceDirect

International Journal of Cardiology

journal homepage: www.elsevier.com/locate/ijcard

Correspondence

Role of ^{99m}Tc-DPD scintigraphy on discrimination of familial cardiac amyloidosis

Suzane Garcia Ferreira [a,b,*], Alexandre Marins Rocha [a], Osvaldo José Moreira do Nascimento [a], Claudio Tinoco Mesquita [a,b]

[a] Antonio Pedro University Hospital, Fluminense Federal University, Niterói, Rio de Janeiro, Brazil
[b] Pró-Cardíaco Hospital, Rio de Janeiro, Brazil

http://dx.doi.org/10.1016/j.ijcard.2015.11.002

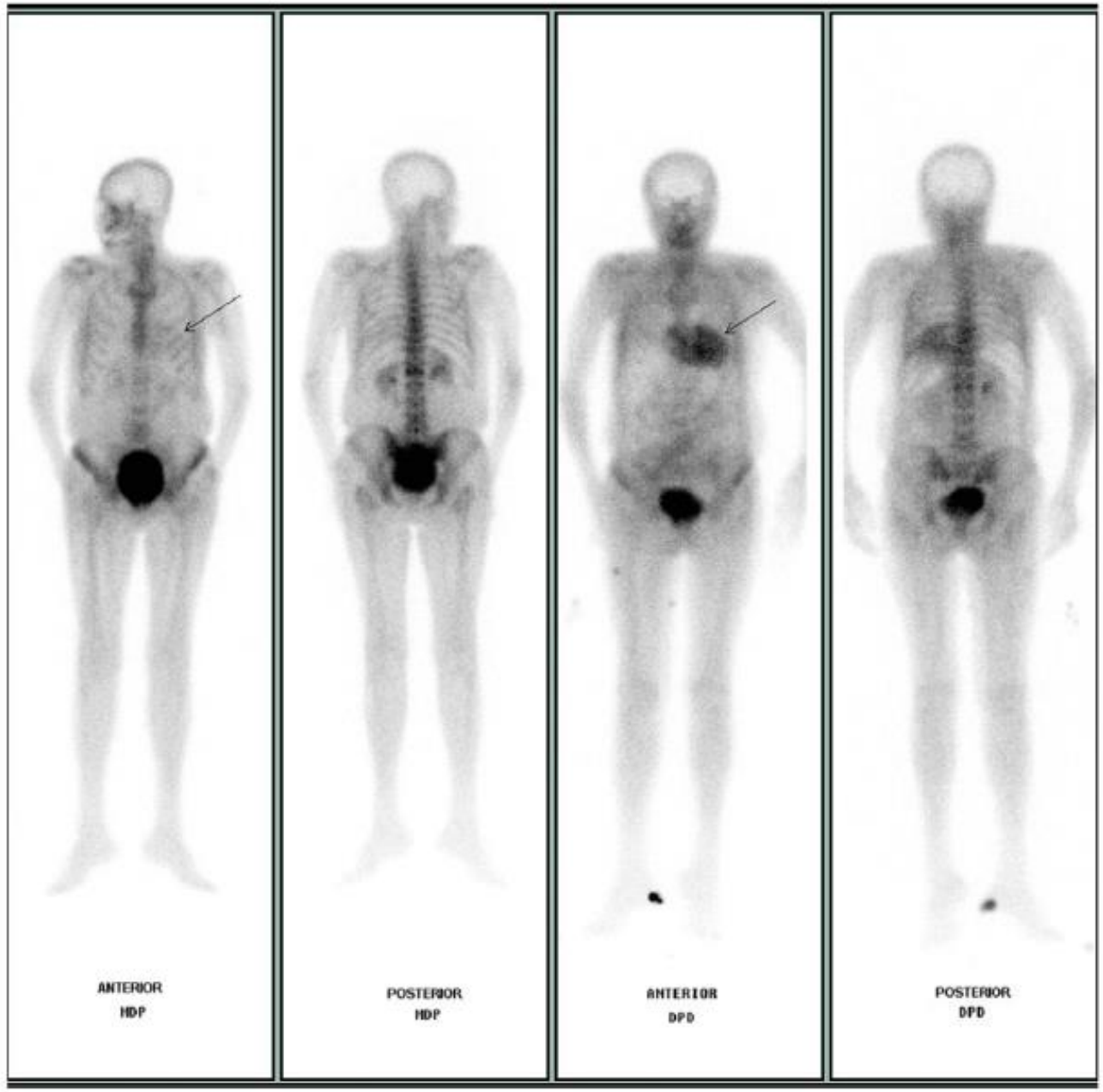

Table 1
Demography and imaging findings in subjects studied.

Patient	Sex	Age	Echo positive	Mutation	Score ^{99m}Tc-MDP	Score ^{99m}Tc-DPD
1	F	41	N	val122Ile	0	0
2	F	64	LVH	val30met	1	3
3	M	31	N	val30met	0	0
4	F	33	LVH	val30met	0	0
5	M	54	AST	val30met	1	2
6	F	31	N	val30met	0	0
7	M	60	N	val30met	0	0
8	F	56	N	NA	0	0
9	F	21	N	NA	0	0
10	M	38	N	val30met	0	0
11	F	36	N	val30met	0	0
12	M	39	AST	val30met	0	0
13	M	45	N	val30met	0	0
14	F	22	N	val30met	0	0
15	F	59	AST	val30met	–	0
16	M	52	AST	NA	0	0
17	F	25	N	NA	0	0
18	F	31	N	val30met	0	0
19	M	35	N	val30met	0	0

Uptake intensity was graded according to a visual scale ranging from 0 to 3 points, in which the absence of uptake was assigned a value of 0 points: uptake less than that observed in bone (referred to as the adjacent rib), 1 point; uptake similar to that of bone, 2 points; and uptake greater than that of bone, 3 points.

http://dx.doi.org/10.1016/j.ijcard.2015.11.002

Fig. 1. Comparison of ^{99m}Tc-DPD and ^{99m}Tc-MDP scintigraphy in a cardiac amyloidosis confirmed patient. There is abnormal uptake in cardiac region more intense in DPD image.

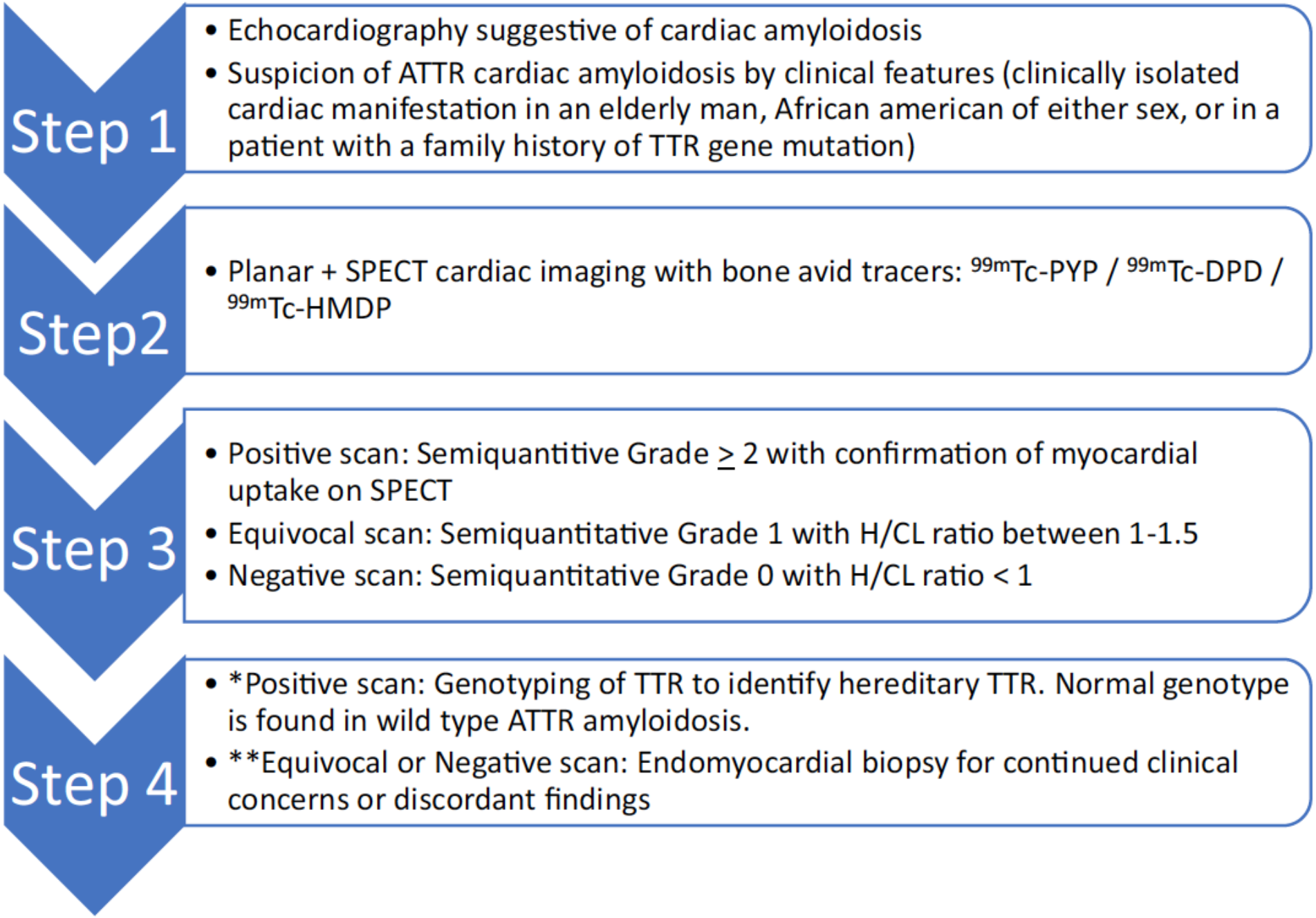

Journal of Nuclear Cardiology®
Volume 26, Number 1;158–73

Amiloidose TTR - mutação genética

- A proteína transtiretina, sintetizada primariamente no fígado, quando sofre mutação, resulta em depósitos fibrilares proteicos
- Doença autossômica dominante é que uma proteína mutante (a transtirretina) produz fibrilas amilóides, a partir da vida adulta. – valina na posição 30 Met é a mais comum
- ATTR varia de apresentação dependendo da mutação
- Dç renal é menos frequente e não cursa com macroglossia.

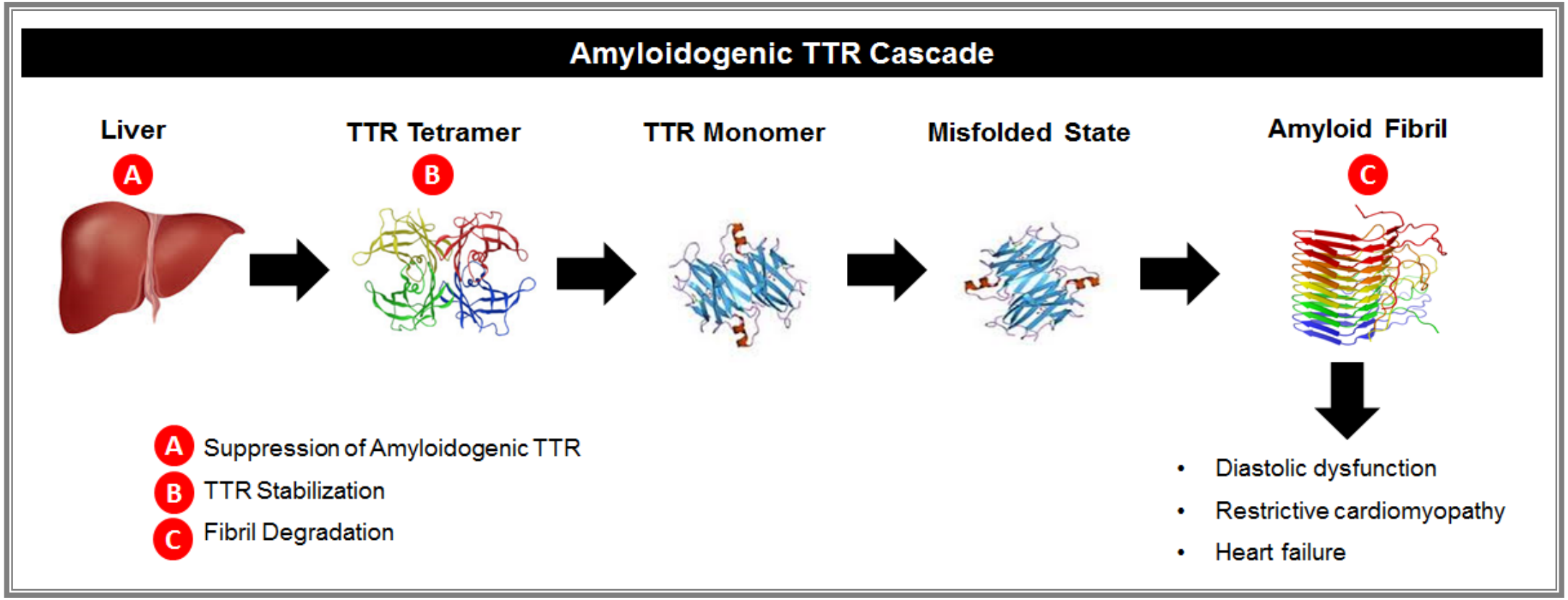

The NEW ENGLAND JOURNAL of MEDICINE

ORIGINAL ARTICLE

Tafamidis Treatment for Patients with Transthyretin Amyloid Cardiomyopathy

Mathew S. Maurer, M.D., Jeffrey H. Schwartz, Ph.D., Balarama Gundapaneni, M.S., Perry M. Elliott, M.D., Giampaolo Merlini, M.D., Ph.D., Marcia Waddington-Cruz, M.D., Arnt V. Kristen, M.D., Martha Grogan, M.D., Ronald Witteles, M.D., Thibaud Damy, M.D., Ph.D., Brian M. Drachman, M.D., Sanjiv J. Shah, M.D., Mazen Hanna, M.D., Daniel P. Judge, M.D., Alexandra I. Barsdorf, Ph.D., Peter Huber, R.Ph., Terrell A. Patterson, Ph.D., Steven Riley, Pharm.D., Ph.D., Jennifer Schumacher, Ph.D., Michelle Stewart, Ph.D., Marla B. Sultan, M.D., M.B.A., and Claudio Rapezzi, M.D., for the ATTR-ACT Study Investigators*

This article was published on August 27, 2018, at NEJM.org.

Figure 2. Primary Analysis and Components.

Panel A shows the results of the primary analysis as determined with the use of the Finkelstein–Schoenfeld method. Panel B shows an analysis of all-cause mortality for pooled tafamidis and for placebo, a secondary end point. Panel C shows the frequency of cardiovascular-related hospitalizations, also a secondary end point.

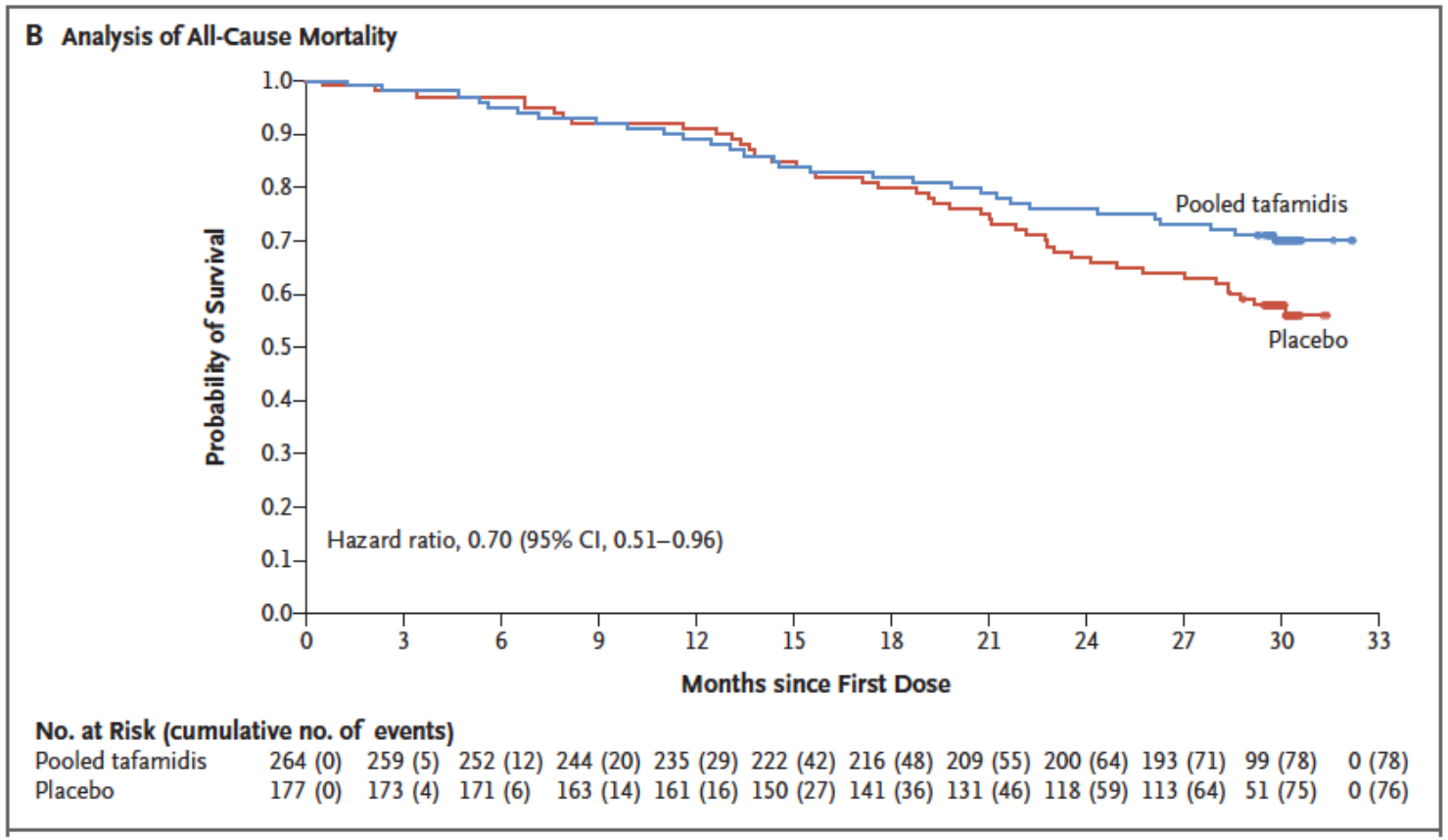

Intelligence is the ability to adapt to change.

- Stephen Hawking

claudiotinocomesquita@id.uff.br

Goalcast